

# Etude aéroacoustique d'un canal avec obstacle(s) - Application à la production de fricatives

## Yō FUJISO

*GIPSA-lab, Département Parole & Cognition*

*Equipe GAMA (Gestes phonatoires, Analyse & Modélisation Acoustique)*

Supervisor: Annemie VAN HIRTUM

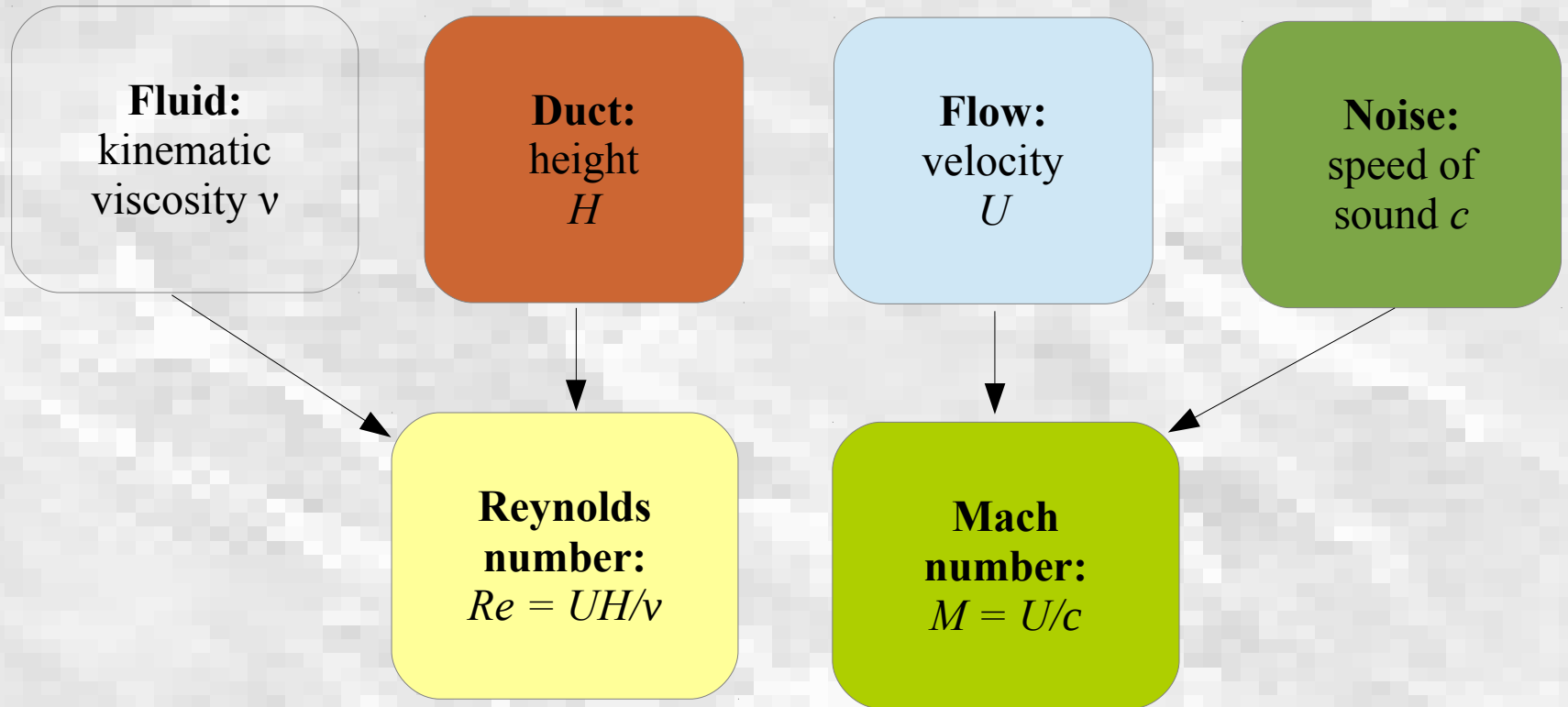
February 14th, 2014



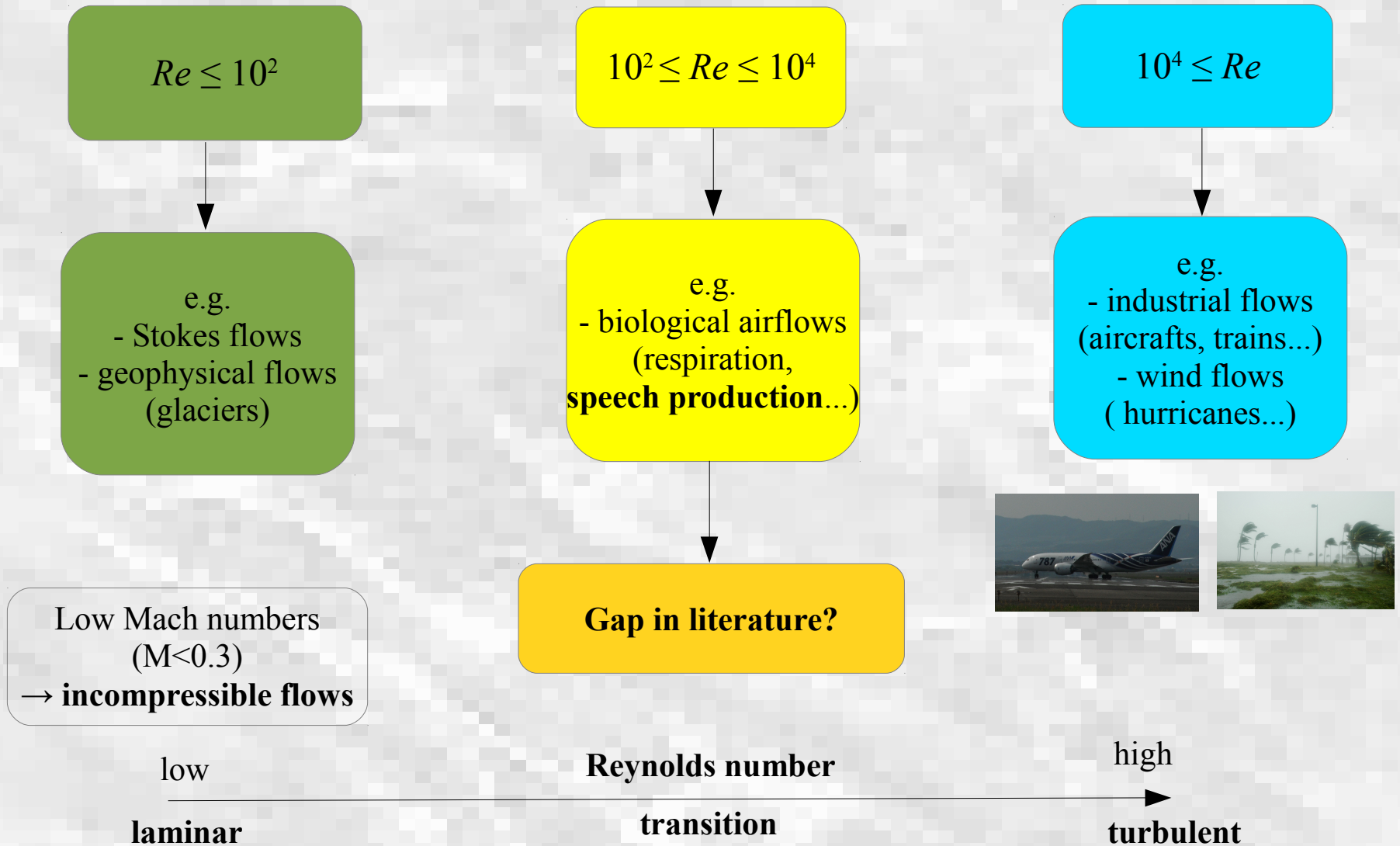
Rhône-Alpes Région

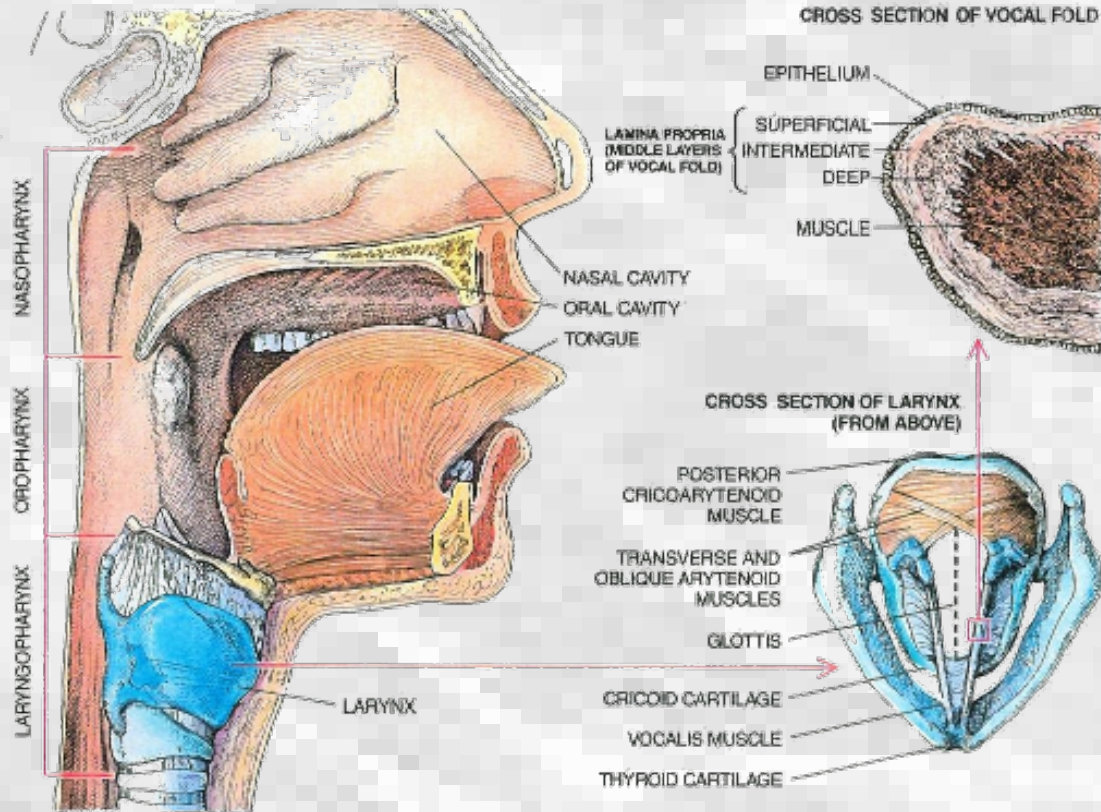


Duct aeroacoustics?



## Flow classification according to Reynolds number





Upper airways, vocal tract [Sataloff 1992]

## Human speech production:

**Airflow**  $\rightarrow Re=O(10^4)$  &  $M<0.3$   
(from *in-vivo* observations)

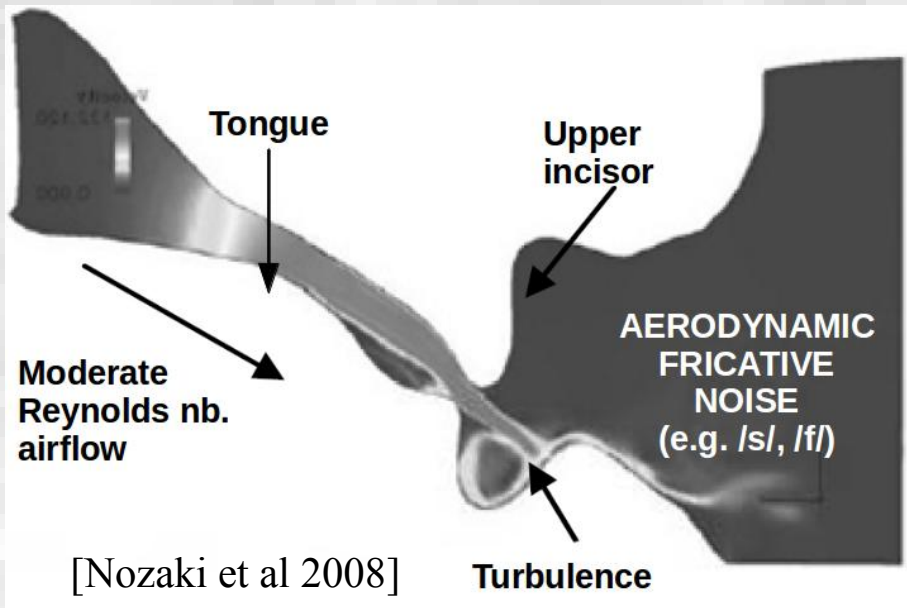
## Various speech sounds:

\* **Voiced sounds** e.g. vowels  $\rightarrow$   
vibration of vocal folds

\* **Unvoiced (or voiceless) sounds** e.g. unv. stops, unv. fricatives

$\rightarrow$  no vibration of vocal folds

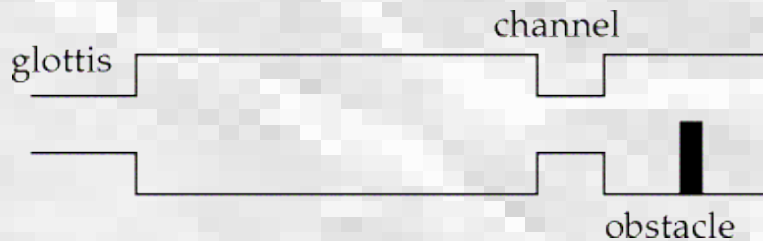
$\rightarrow$  various sound sources



**Unvoiced fricative consonants:**  
/f/ ('fanfare'), /s/ ('scie'), /ʃ/ ('chat')

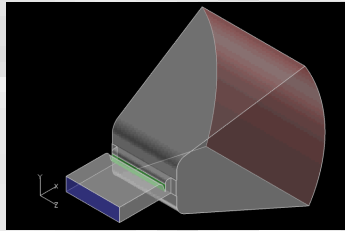
**System:** upstream duct + downstream obstacle

**Source:** turbulent jet interacting with surface/obstacle



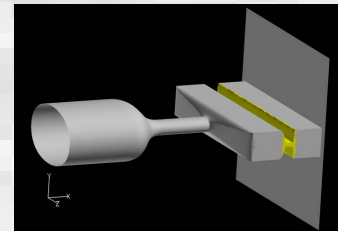
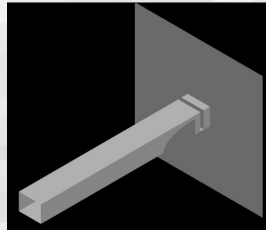
[Shadle 1985-1991; Ramsay 2006]

**Approach:**  
→ *In-vitro*  
geometries



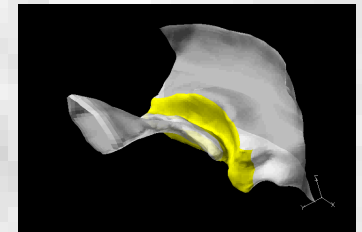
Incisor & free field  
[Cisonni et al 2013]

Tongue & incisor  
[Van Hirtum et al 2011]



Tongue & incisor  
[Van Hirtum et al 2009]

Human oral cavity  
[Nozaki 2010]

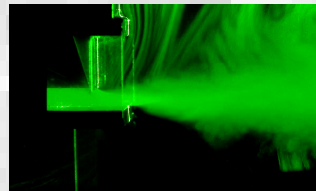


Re=4000, uniform inlet velocity profile



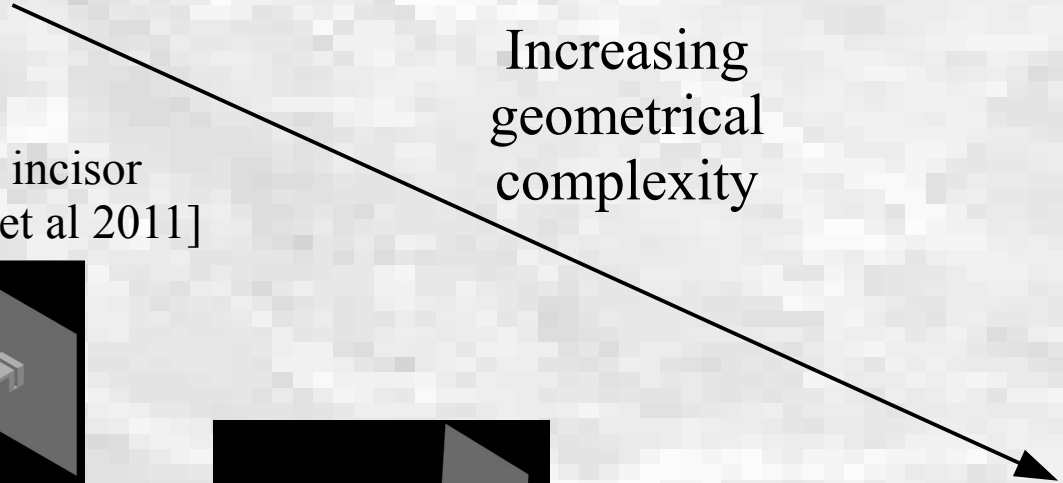
Cisonni et al 2013

≠



Grandchamp 2009

Increasing geometrical complexity



→ Influence of **initial conditions?** (IC)

### Previous studies:

- \* Reynolds number  $Re = 4000$  (exp.+sim.)
- \* Constriction degree (exp.+sim.)
- \* Uniform inlet velocity profile (sim.)

### This thesis

**Unvoiced  
fricative  
production**

Flow initial  
conditions?

Reynolds  
numbers  $Re$ ?

Obstacle(s)  
geometry?

**Aeroacoustic  
analysis**

- \* Experiments
- \* Simulations

## I. Introduction

## II. Theory

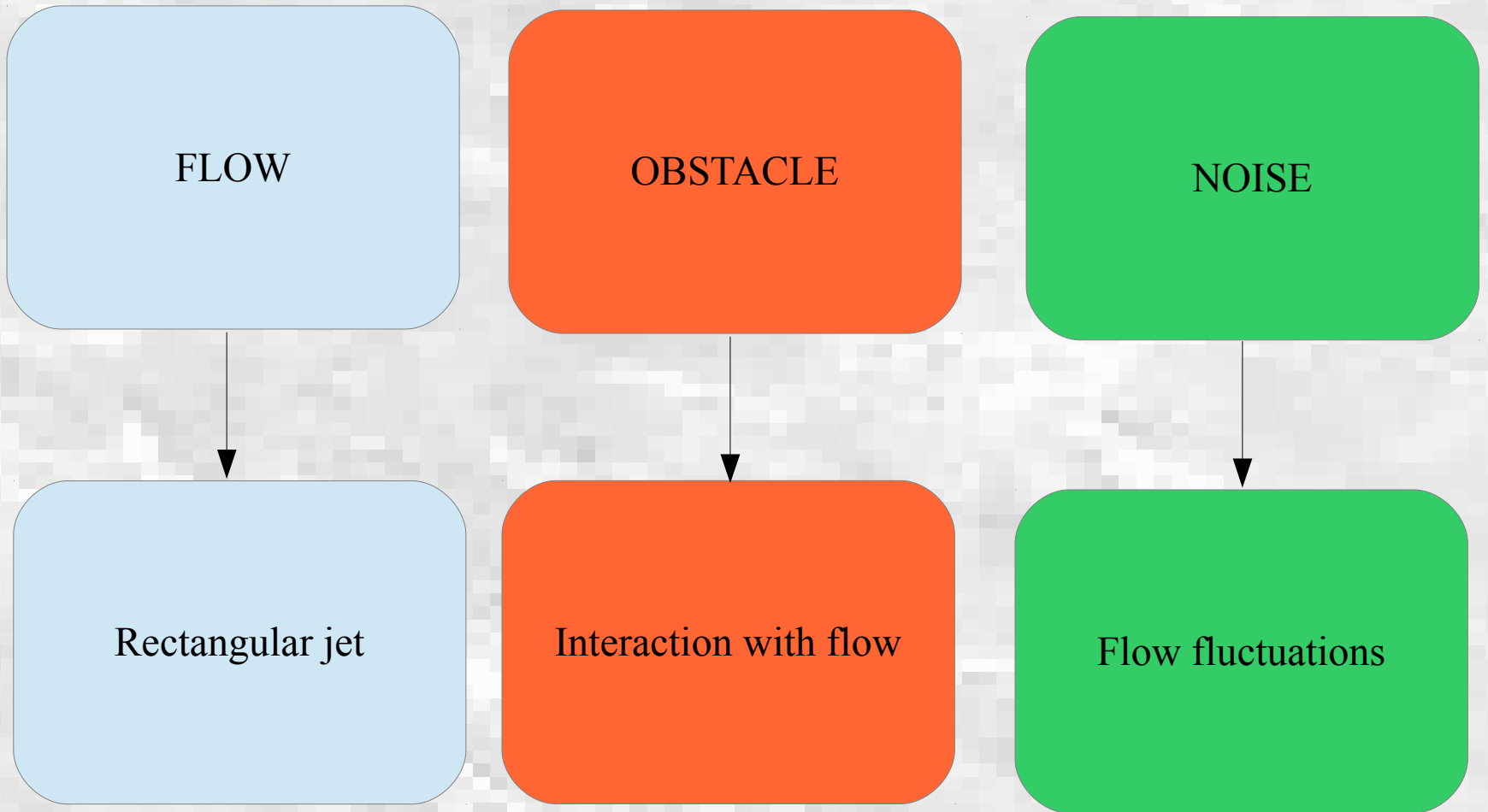
- Jet
- Obstacle
- Noise

## III. Method

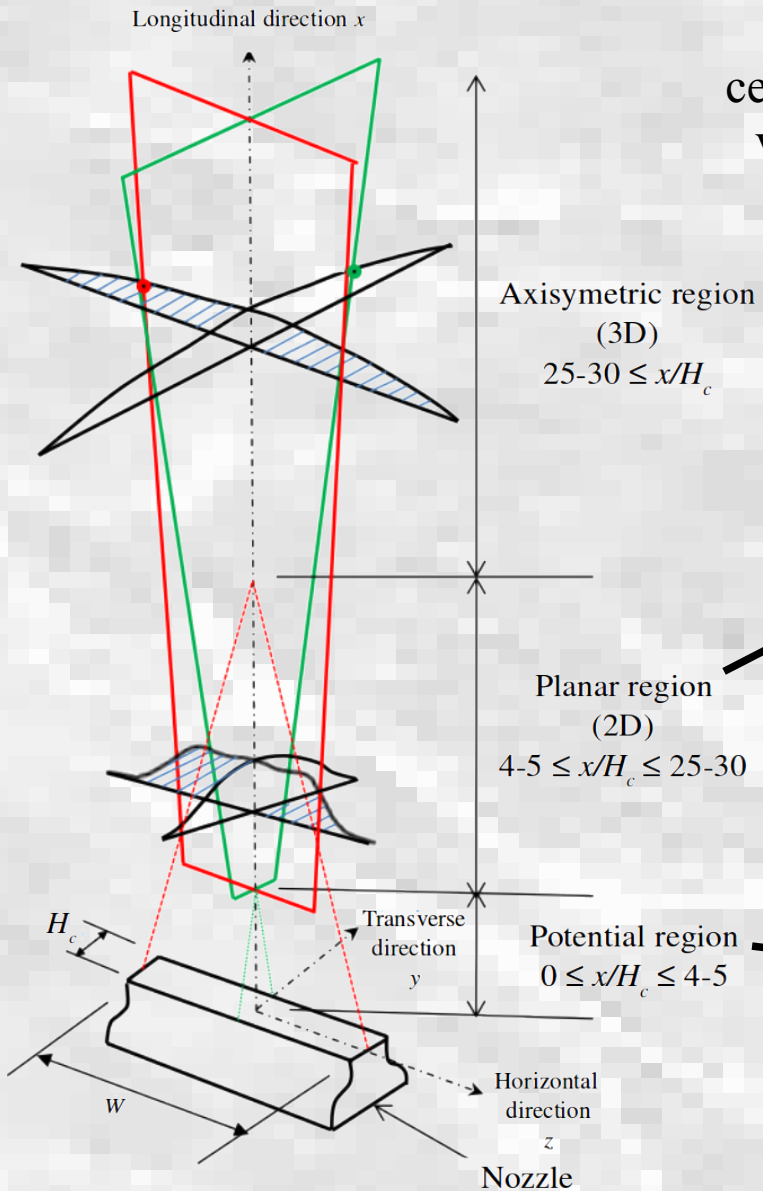
## IV. Results

## V. Conclusion





# Theory Rectangular jets



center bulk velocity

center bulk velocity at  $x=0$

**'Square' decay law**

$$\left( \frac{U_{dc}}{U_c} \right)^2 = K_u \left( \frac{x}{H_c} + \frac{x_{01}}{H_c} \right)$$

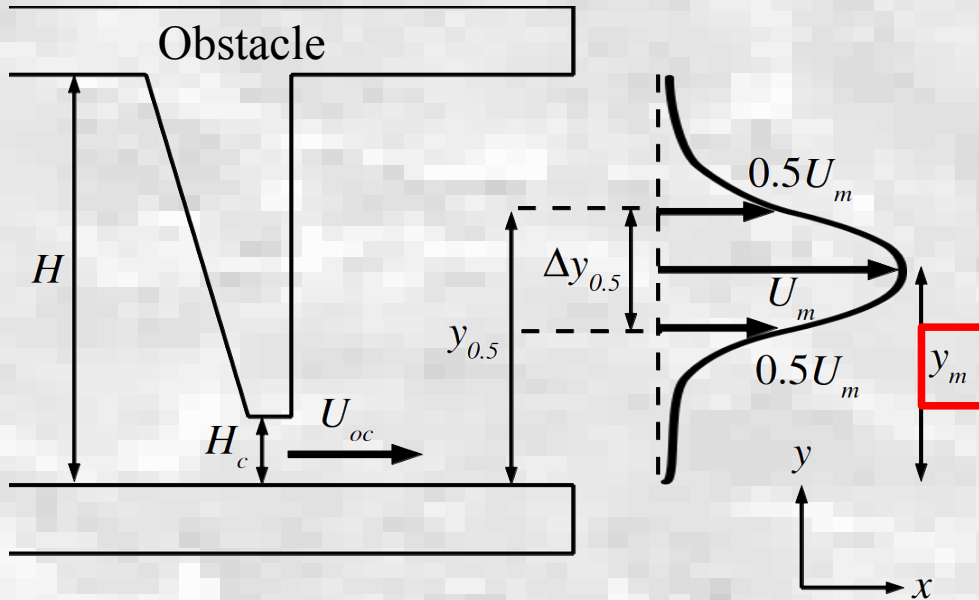
**Strouhal number**

$$St = \frac{f H_c}{U_{dc}}$$

**Vortex shedding**  
 $St \sim 0.3$  (typically)

**Potential core length**

$$x_{pc} = x \Big|_{U_c = 0.95 U_0}$$



**Reynolds decomposition for velocity field:**

$$u(t) = \bar{U} + \tilde{u}(t)$$

Mean velocity

Fluctuating velocity

**Turbulence intensity**

$$Tu = \frac{u'}{\bar{U}}$$

RMS velocity (2<sup>nd</sup> order moment)

**Bulk Reynolds number**

$$Re_d = \frac{U_d h}{\nu} = \frac{Q}{W\nu} \quad (h \in \{H; H_c\})$$

Width of rect. duct

**Constriction degree**

$$\frac{H_c}{H}$$

**Aspect ratio**

$$AR = \frac{W}{H_c}$$

Conservation of momentum  $\rightarrow$  **Navier-Stokes equation**

$$\rho \left( \frac{\partial \vec{u}}{\partial t} + (\vec{u} \cdot \nabla) \vec{u} \right) = -\nabla P + \nabla \cdot \bar{\bar{\tau}} + \vec{f}$$

Diagram illustrating the Navier-Stokes equation with labels and arrows pointing to terms:

- $\rho$ : unsteadiness
- $\frac{\partial \vec{u}}{\partial t}$ : unsteadiness
- $(\vec{u} \cdot \nabla) \vec{u}$ : convection
- $-\nabla P$ : pressure-driven
- $\nabla \cdot \bar{\bar{\tau}}$ : stress tensor
- $\vec{f}$ : body forces

## Turbulent flow 3D modeling by LES

filtered pressure  $p = \bar{p} + \tilde{p}$

$$\frac{\partial \bar{u}_i}{\partial t} (\bar{u}_i \bar{u}_j) = -\frac{1}{\rho_0} \frac{\partial \bar{p}}{\partial x_i} + \nu \frac{\partial}{\partial x_j} \left( \frac{\partial \bar{u}_i}{\partial x_j} + \frac{\partial \bar{u}_j}{\partial x_i} \right) - \frac{\partial \tau_{ij}}{\partial x_j}$$

**filtered momentum equation**

filtered velocity  
 $u_i = \bar{u}_i + \tilde{u}_i$

$$\frac{\partial \bar{u}_i}{\partial x_i} = 0, \quad i = 1, 2, 3$$

**filtered continuity equation**

**resolvable part**

**subgrid-scale (SGS) part → modeled by dynamic Smagorinsky model**

$C_s$ : Smagorinsky constant

$$\tau_{ij} = \bar{u}_i \bar{u}_j - \overline{u_i u_j} \quad \bar{S}_{ij} = \frac{1}{2} \left( \frac{\partial \bar{u}_i}{\partial x_j} + \frac{\partial \bar{u}_j}{\partial x_i} \right)$$

**Subgrid-scale eddy viscosity**

$$\tau_{ij} - \frac{1}{3} \tau_{kk} \delta_{ij} = -2\mu_t \bar{S}_{ij}$$

$$\mu_t = \rho (C_s \Delta)^2 \sqrt{2\bar{S}_{ij} \bar{S}_{ij}}$$

**Lighthill's equation  
(1952):**

$$\frac{\partial^2 \rho}{\partial t^2} - c^2 \Delta \rho = \frac{\partial^2 T_{ij}}{\partial x_i \partial x_j}$$

Lighthill's  
tensor

viscous  
stress tensor

$$T_{ij} = \rho u_i u_j + (p - c^2 \rho) \delta_{ij} - \tau_{ij}$$

Incompressible  
isentropic flow

$$T_{ij} \approx \rho_0 u_i u_j$$

**Solution of Lighthill's equation in time domain:**

$$p(\vec{x}, t) = c^2 \rho(\vec{x}, t) = \iiint_V \int_{\tau} T_{ij} \frac{\partial^2 G}{\partial y_i \partial y_j} d\tau dV$$

↑  
radiated jet-induced  
acoustic pressure

↑  
quadrupole noise source

**G:** Green  
function  
in free field



De Havilland Comet (1949): 1<sup>st</sup>  
**turbojet** civil aircraft  
→ much louder than  
propeller-aircrafts, WHY?

**No solid  
boundaries!**

**Approximate solution in free field:**

$$p(\vec{x}, t) = \frac{1}{4\pi} \frac{\partial^2}{\partial x_i \partial x_j} \iiint_V \frac{1}{d} T_{ij}(\vec{y}, t) d\vec{y}$$

volume of source region

$$d = |\vec{x} - \vec{y}|$$

position  
of receiver  
point

position  
of source  
point

After some mathematical manipulations, and by taking the **Fourier transform (F.T.)** of  $T_{ij}$ , one can obtain an **approximate solution in frequency domain**:

F.T. of  
pressure  
 $p$

$$P_\omega(\vec{x}) = -\frac{\omega^2}{4\pi c^2} \iiint_V \frac{d_i d_j}{d^3} e^{\frac{-i\omega d}{c}} \hat{T}_{ij}(\vec{y}, \omega) dV$$

F.T. of  $T_{ij}$

**Aeroacoustic analogy of Powell (1964):**

$$\left( \frac{1}{c^2} \frac{\partial^2}{\partial t^2} - \nabla^2 \right) p = \rho \nabla \cdot (\vec{\omega} \times \vec{u}) + \nabla^2 \left( \frac{1}{2} \rho \vec{u}^2 \right)$$

**Vorticity**  
 $\vec{\omega} = \overrightarrow{rot} \vec{u}$

**Lamb vector**

$$\vec{\mathcal{L}} = \vec{u} \times \vec{\omega}$$

**Estimation of dipole noise source:**

$$\Phi_D = \frac{1}{S_D} \int_D |\nabla \vec{\mathcal{L}}| dS$$

**surface of  
source region**

**Lamb vector divergence**



I. Introduction

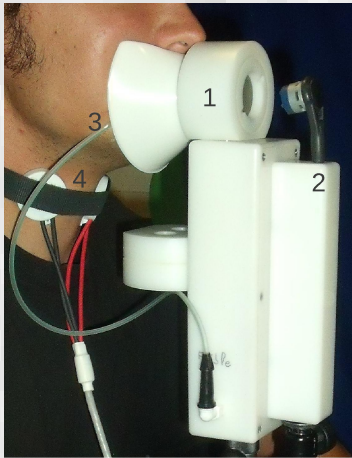
II. Theory

III. Method

- Experiments
- Simulations

IV. Results

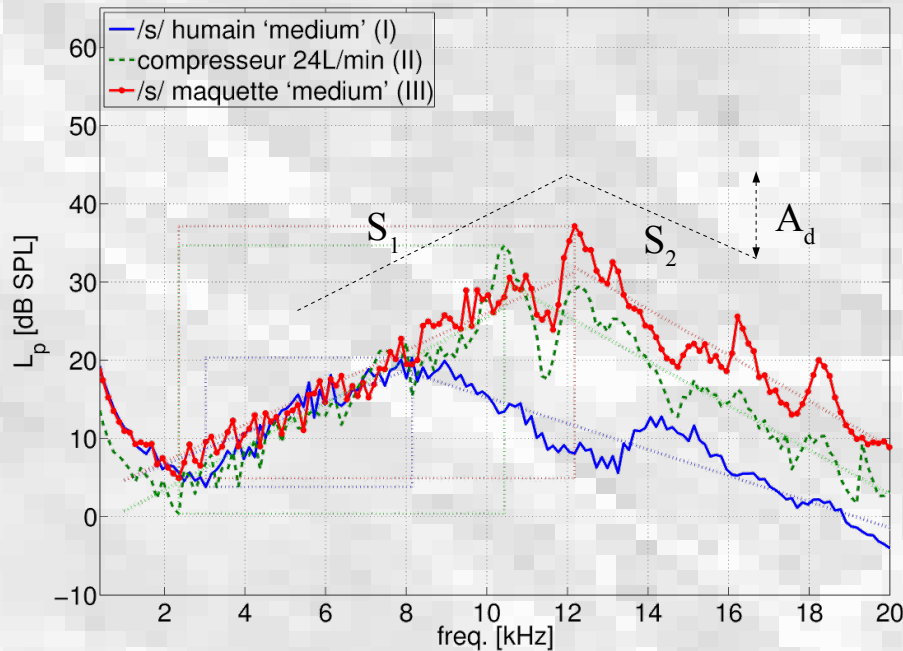
V. Conclusion



## EVA\* meas. station Gipsa-lab Stendhal Univ.

- 1: oral airflowmeter
- 2: microphone
- 3: intra-oral pressure probe
- 4: electroglottograph (EGG)

\**Evaluation Vocale Assistée*



## *In-vivo* experiments:

\* **Subjects:** two healthy adult males ('YF' & 'KN')

\* **Task:** produced repeated sustained unvoiced /s/ & /f/ utterances

\* **Three intensity levels:** 'soft'; 'medium'; 'loud'

## Objective:

→ Obtain some reference *in-vivo* aerodyn. data & spectral parameters

$10 \leq Q \leq 300 \text{ L/min}$

$100 \leq Re \leq 3000$

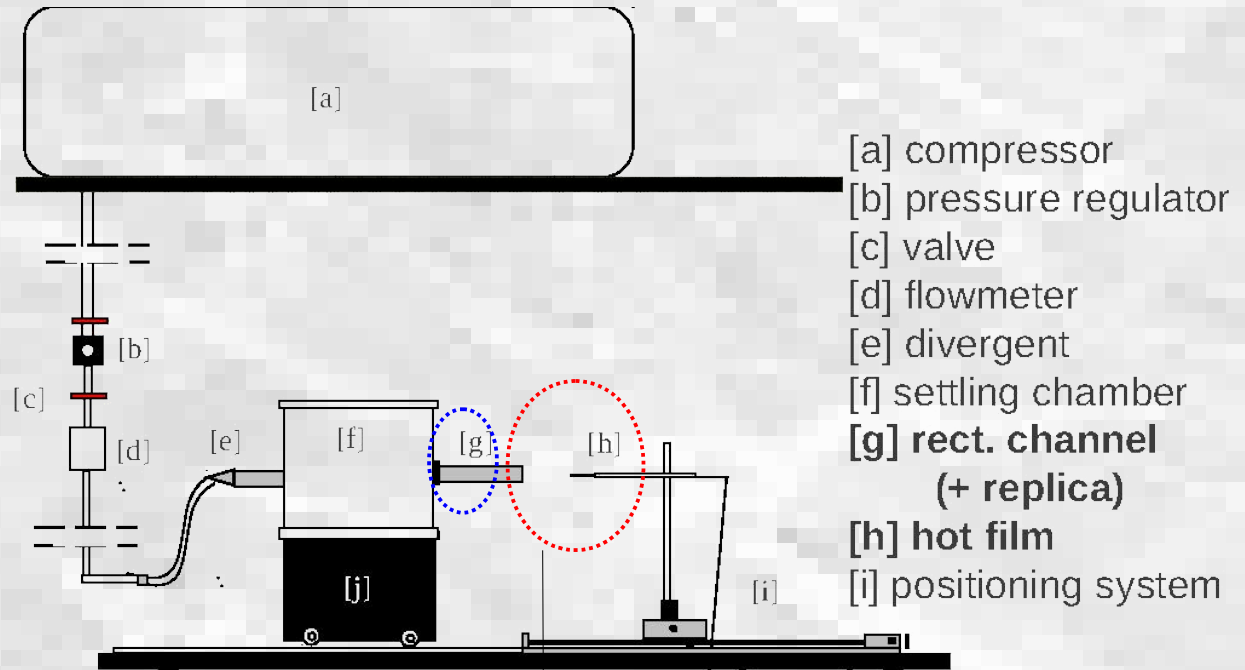
Variable  
volume  
flow rate  $Q$

## Objective:

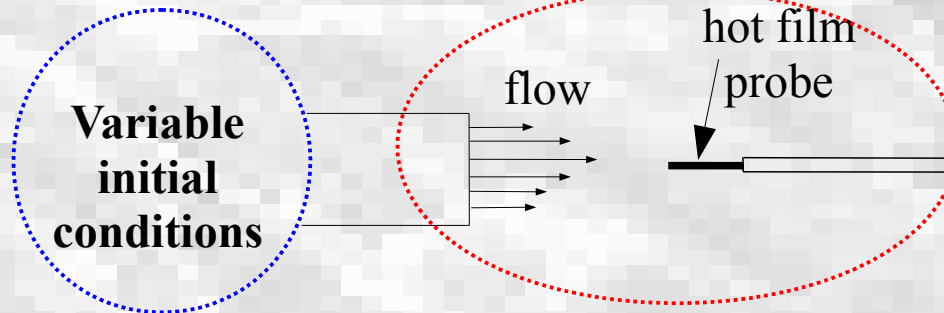
→ Meas. of flow velocity field issued from a replica

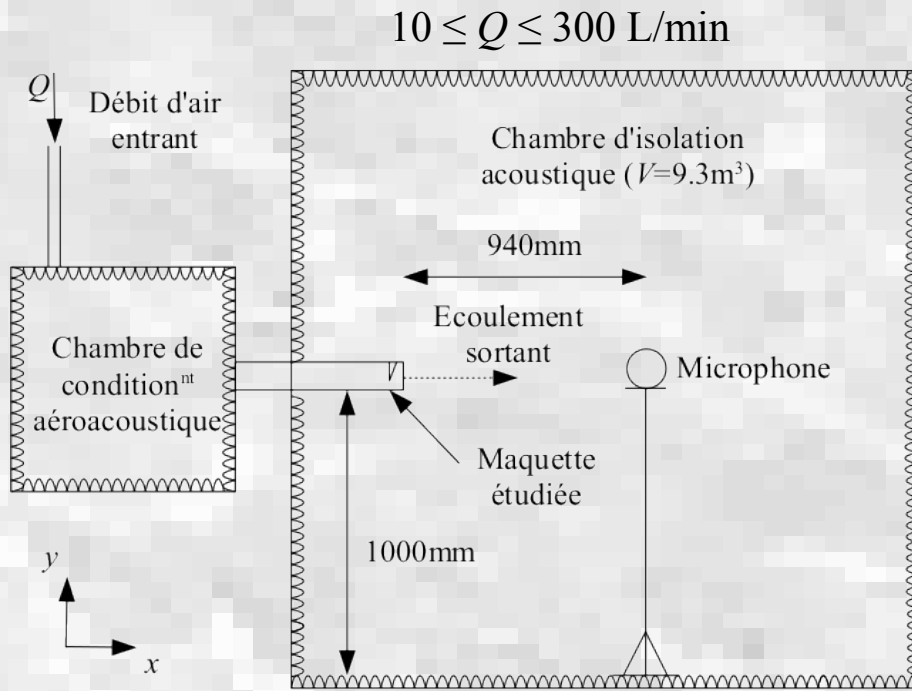
→ Variation of initial conditions & geometry

## Hot film meas. setup



- [a] compressor
- [b] pressure regulator
- [c] valve
- [d] flowmeter
- [e] divergent
- [f] settling chamber
- [g] rect. channel (+ replica)
- [h] hot film
- [i] positioning system





Meas. of acoustic pressure

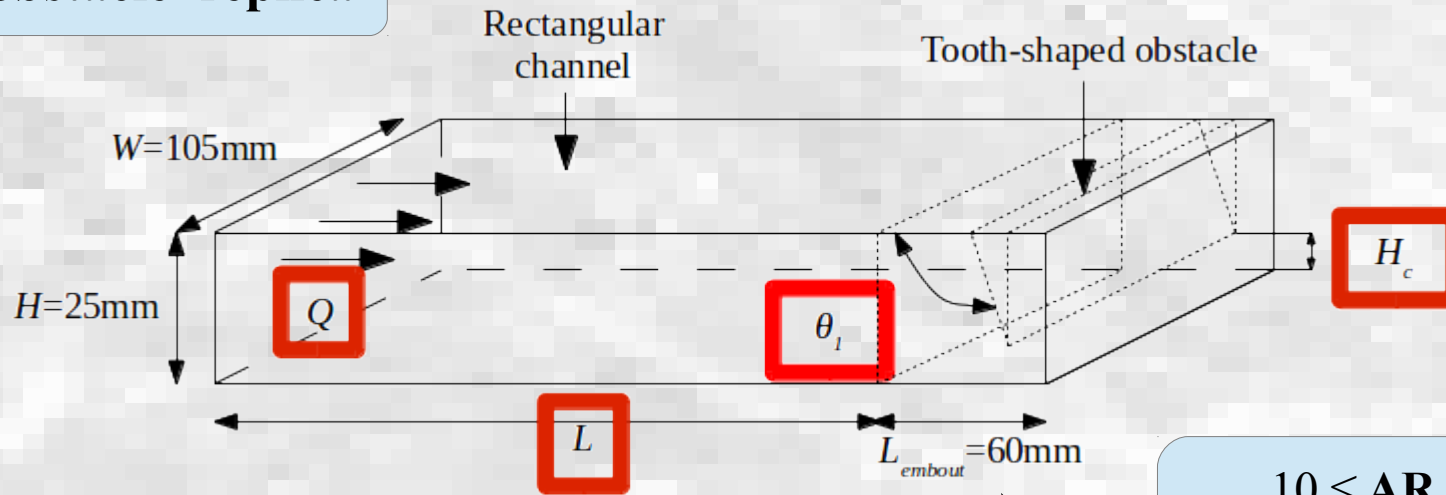


Meas. of acoustic directivity

## Objective:

- Meas. of flow noise issued from a replica
- Variation of initial conditions & geometry
- Meas. of noise directivity

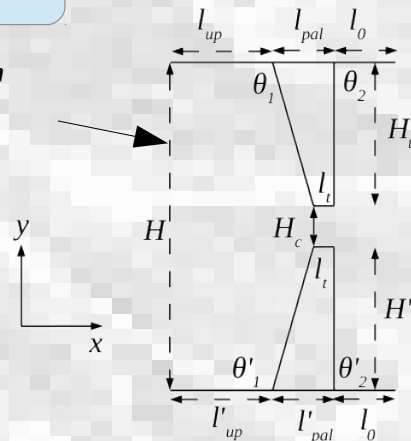
'Single obstacle' replica



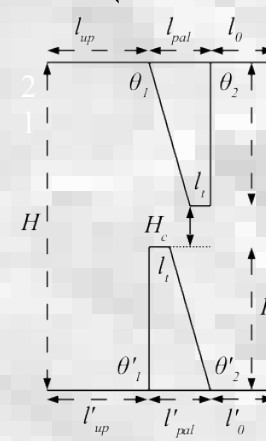
$10 \leq AR \leq 200$   
 $H_c/H: 2.4; 10; 30; 100\%$

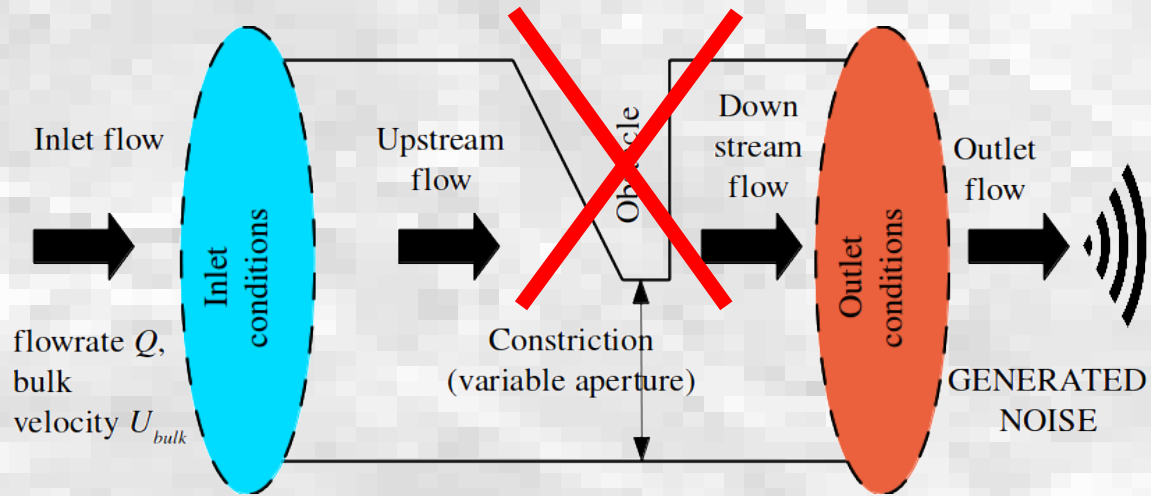
'Dual obstacle' replica

'Symmetric' config.

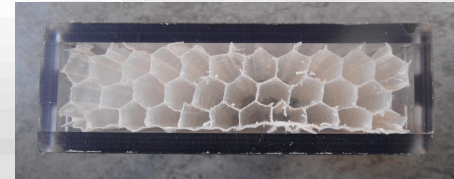
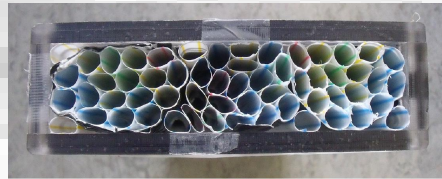
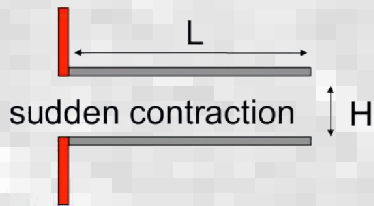


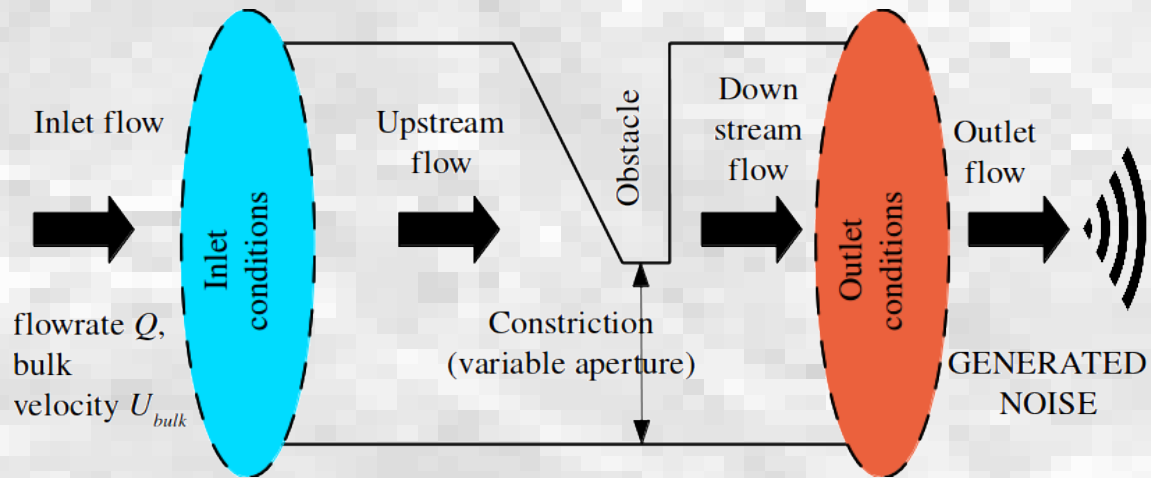
'Asymmetric' config.



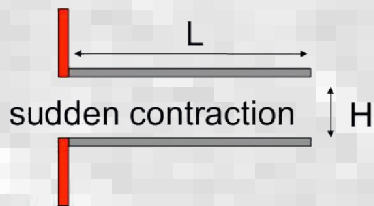


Inlet conditions

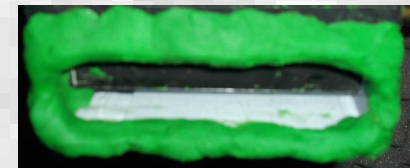
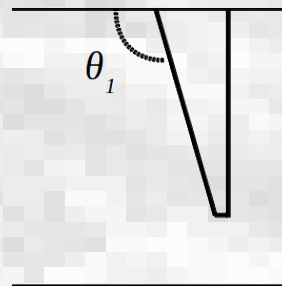
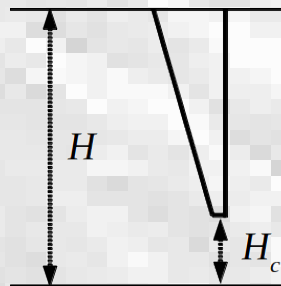




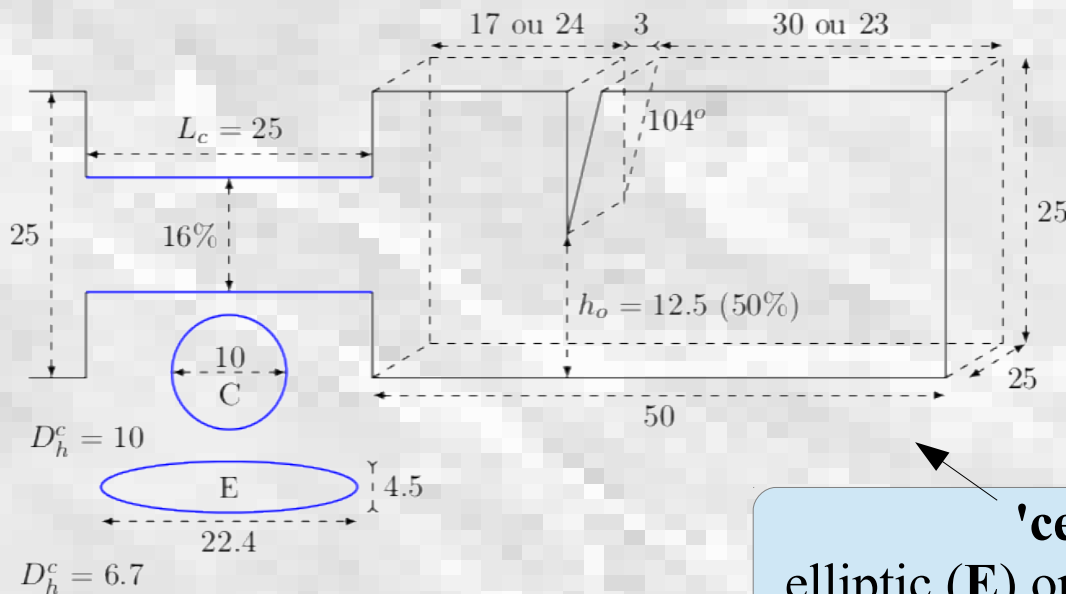
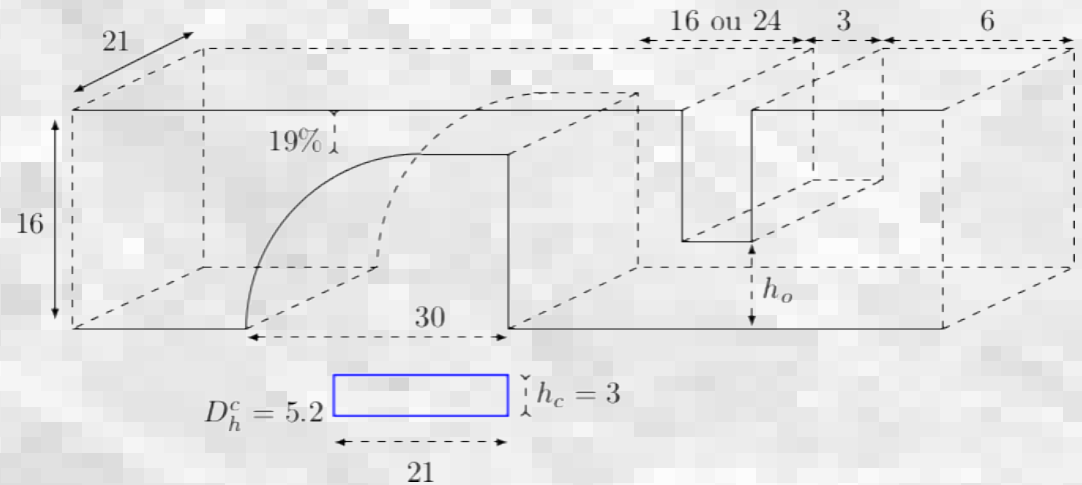
Inlet conditions



Outlet conditions



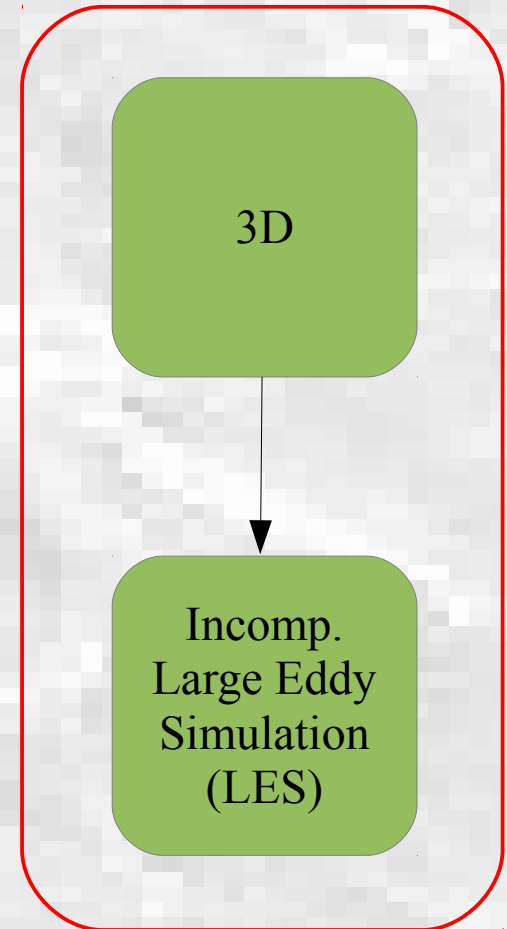
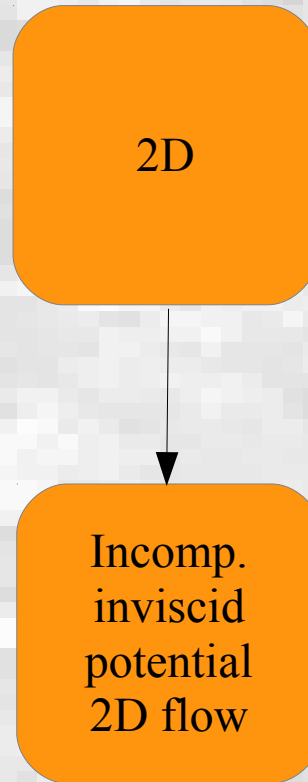
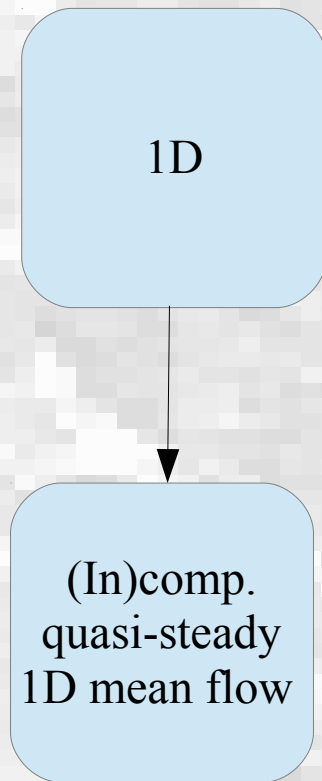
'offset' replica



'centred' replica:  
elliptic (E) or circular (C) cross-section



## Flow simulations: 3 approaches considered



## 3D turbulent incomp. flow model: Large Eddy Simulation (LES)

→ Dynamic Smagorinsky model

\* **Simulated durations:**

$$0.018s \leq T_{sim} \leq 0.54s$$

\* **Reynolds numbers:**

$$Re = 402; 1079; 2084$$

\* **Constriction degrees:**

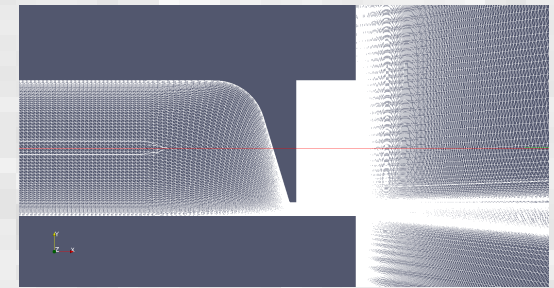
$$H_c/H = 2.4; 10; 30\%$$

Boundary conditions:

- \* **Variable inlet velocity profile**
- \* No-slip cond. on duct walls
- \* No backflow at outlet
- \* 0Pa-static pressure at free field bound.

**LES code:**  
FrontFlow Blue v6.1

**Postprocessing:**  
ParaView



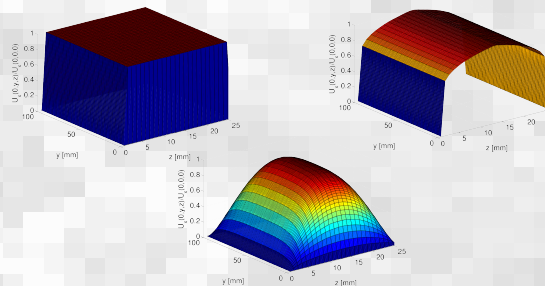
'Single obstacle' mesh:

≈7 millions hexahedral elements

$$2.2 \cdot 10^{-5} < \Delta x < 6.7 \cdot 10^{-5} \text{m}$$

$$9.5 \cdot 10^{-6} < \Delta y < 2.7 \cdot 10^{-5} \text{m}$$

**Supercomputer:**  
NEC SX9 (Osaka Univ.)



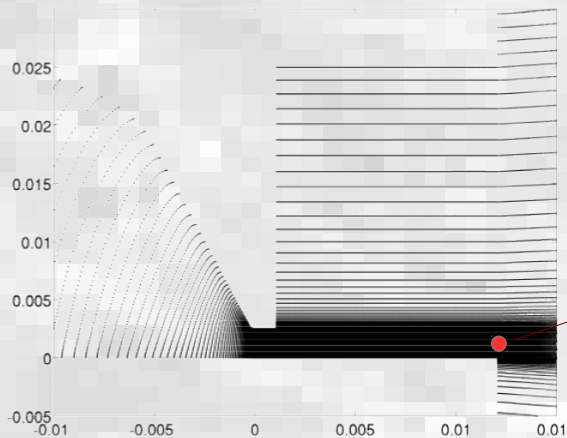
## **PROBLEM: TURB. JET NOISE PREDICTION**

→ How to obtain enough time steps for a **large bandwidth acoustic prediction & for several geometries?** (up to **20kHz**)

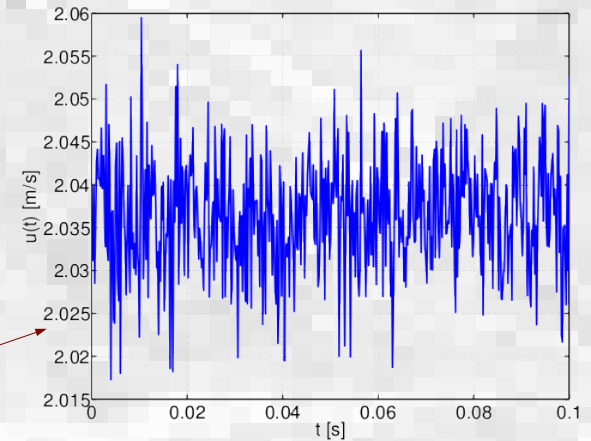
## **METHOD**

→ **Synthetic turbulence**

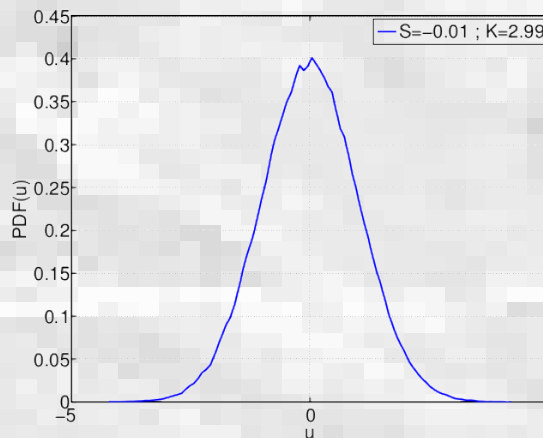
→ **Gaussian regeneration** of all time steps using **LES mean & RMS vel. fields**



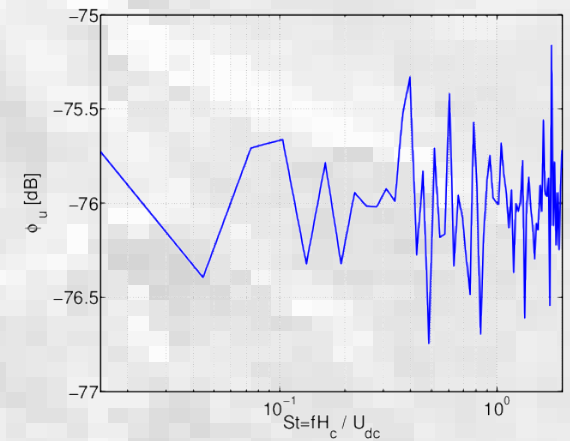
(a) Emplacement du point considéré (en rouge)



(b) Signal temporel de la vitesse longitudinale régénérée au niveau du point

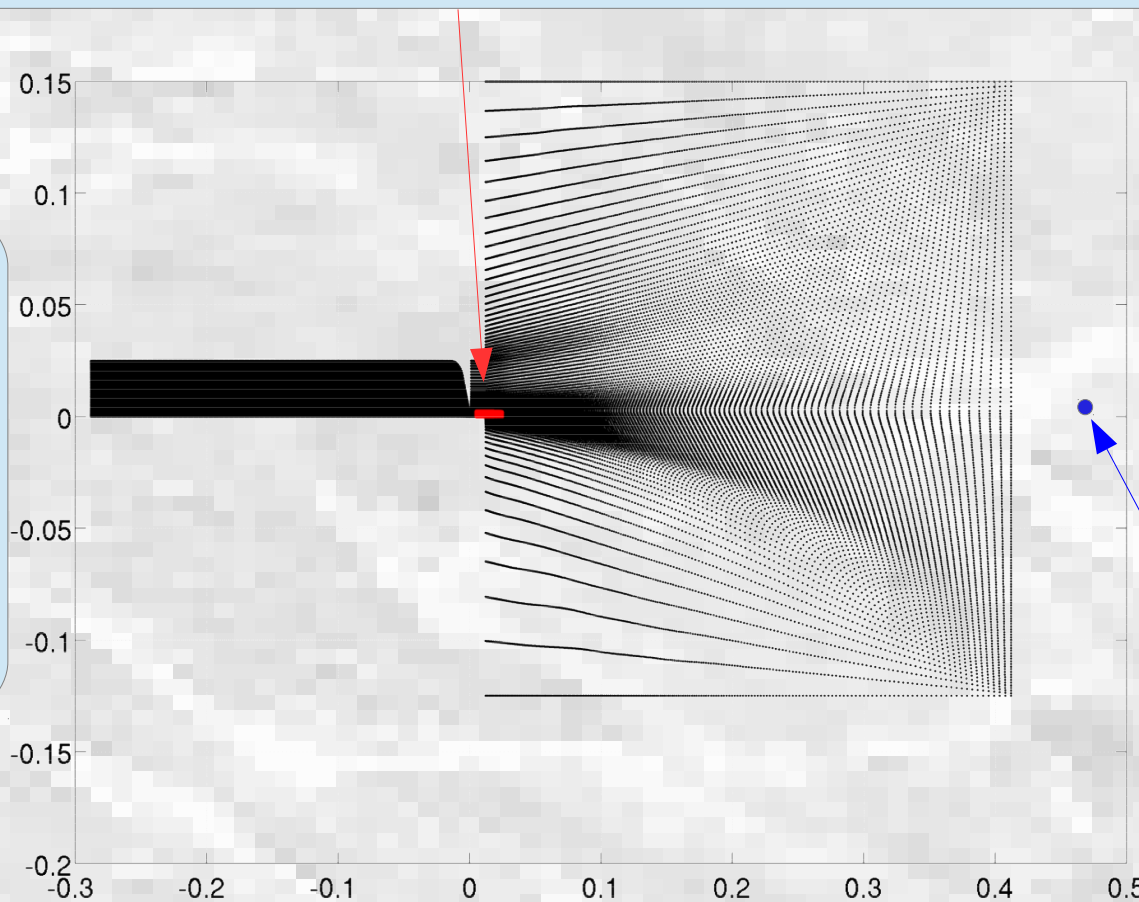


(c) Fonction de densité de probabilité correspondante



(d) Densité spectrale de puissance correspondante

**Noise source region used for acoustic predictions using Lighthill's equation approx. solution in freq. domain**



**1cm-thick 'buffer' layer around source region:**

→ Smooth transition to surrounding flow field

Combined use of **LES mean & RMS flow data** + **synthetic turbulence time steps**

**Receiver point** (virtual microphone, 0.94m from outlet)

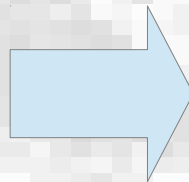
I. Introduction

II. Theory

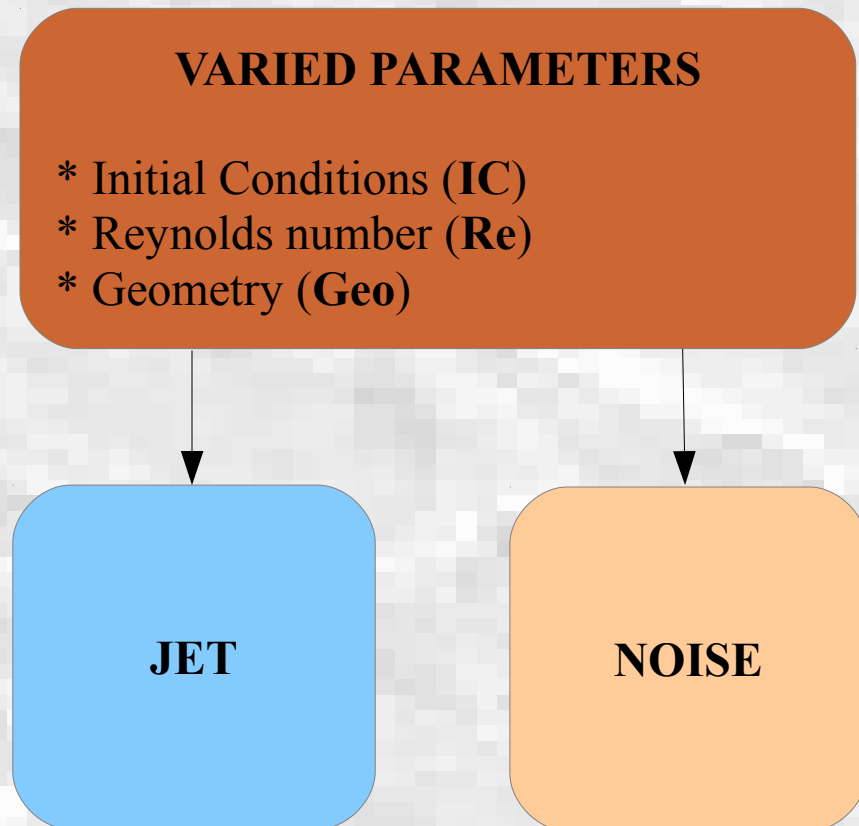
III. Method

IV. Results

- Experiments
- Simulations

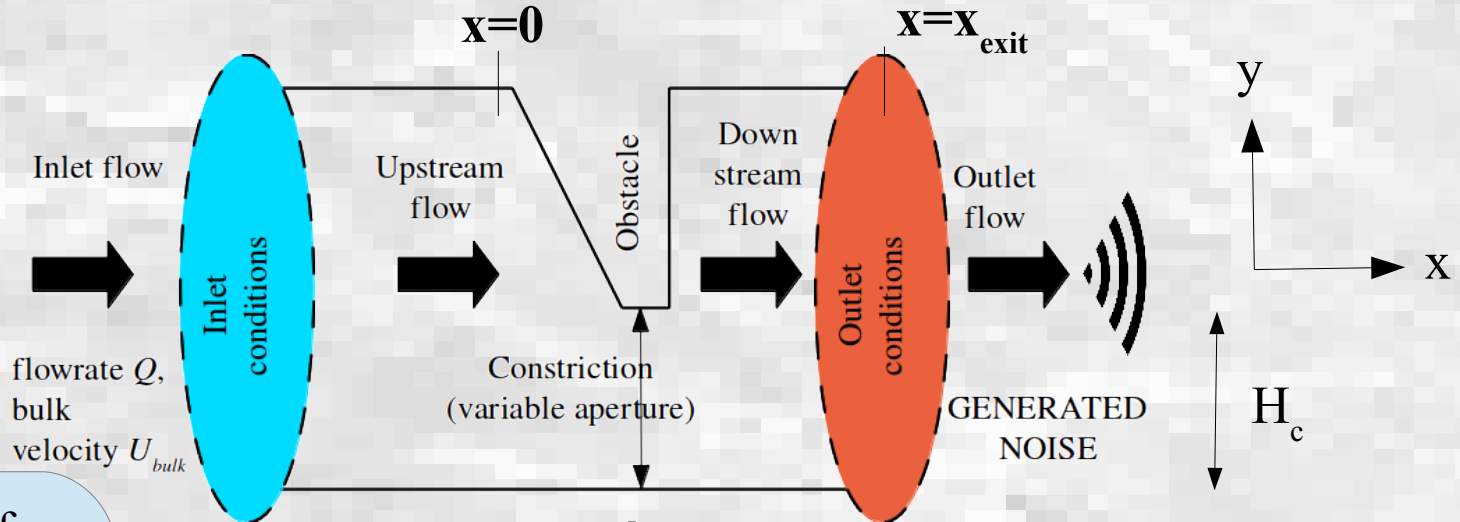


V. Conclusion



Shape of jet:  
rectangular or  
rather 'hybrid'?

## Single tooth-shaped obstacle replica



Influence of

IC  
&  
Geo  
&  
Re

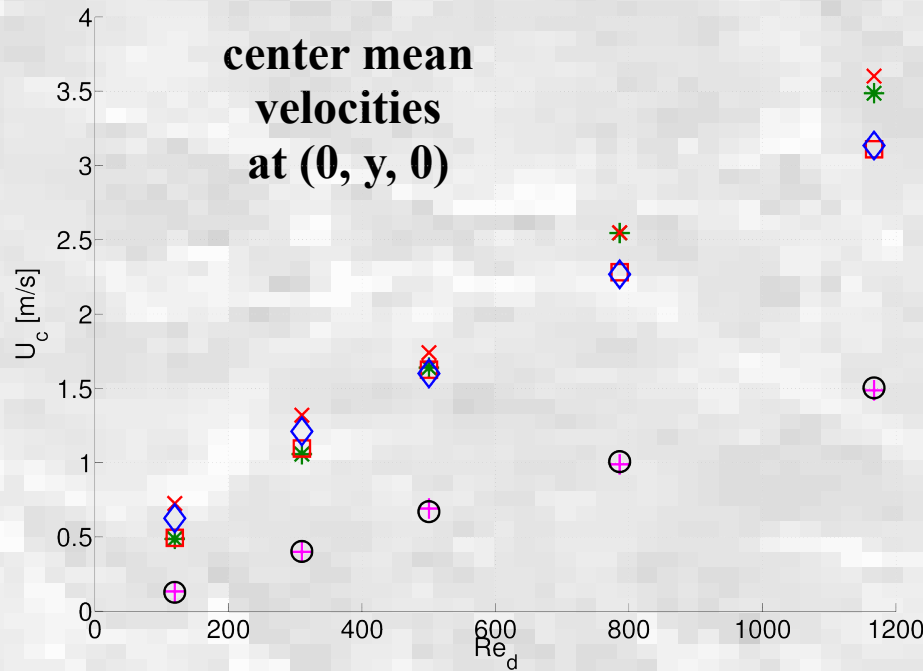
on jet  
development

(A) Upstream  
of obstacle:

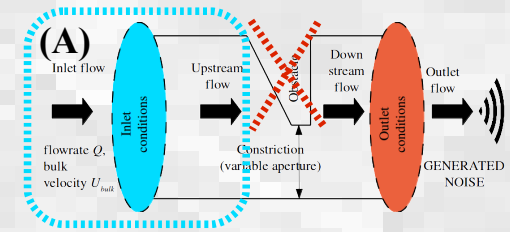
- transverse  
profile  $(0, y, 0)$

(B) Downstream  
of obstacle:

- transverse profile  $(x_{exit}, y, 0)$   
- longitudinal profile  $(x, H_c/2, 0)$   
- horizontal profile  $(0, 0, z)$

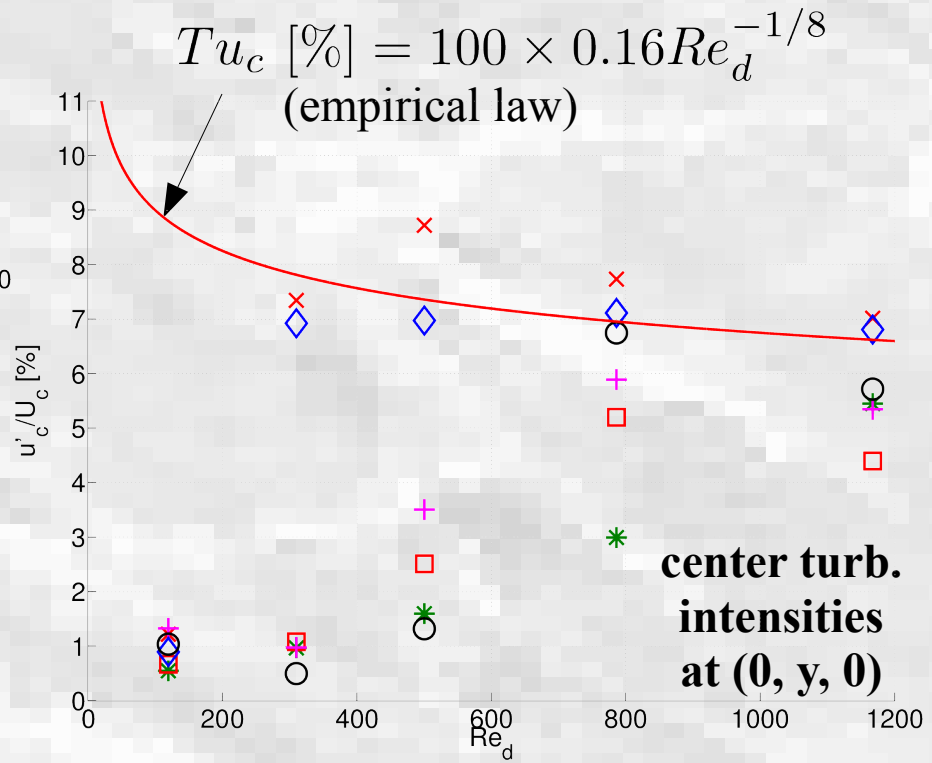


**Effect of IC & Re**

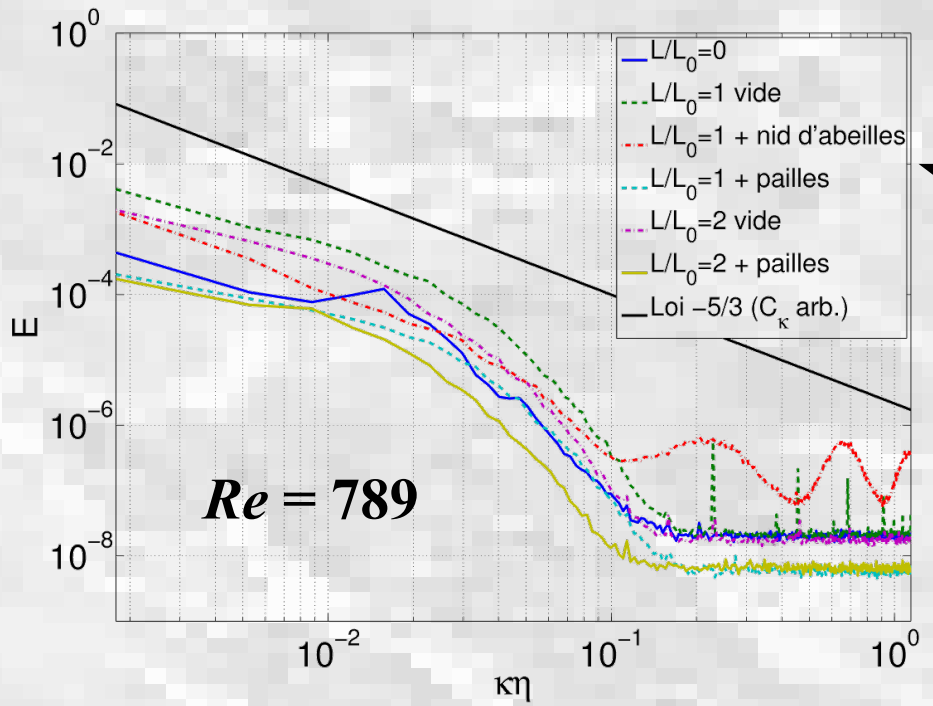


**Comparison of initial conditions:**

- ×: no-duct
- \*: 31cm-duct
- ◇: 31cm-duct + straws
- : 31cm-duct + honeycomb
- +: 62cm-duct
- o: 62cm-duct + straws

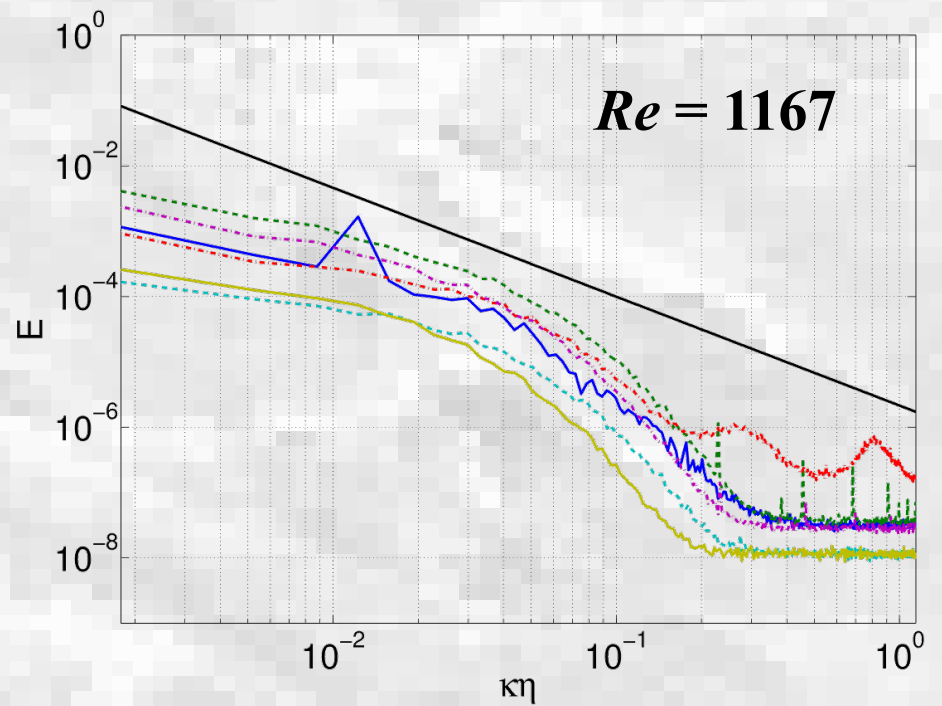
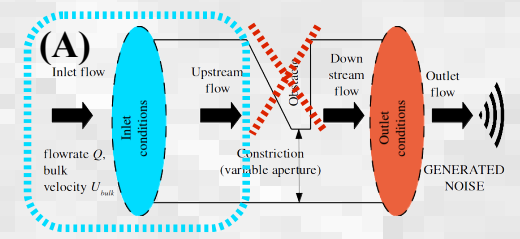


**Kolmogorov spectra**



**Effect of IC & Re**

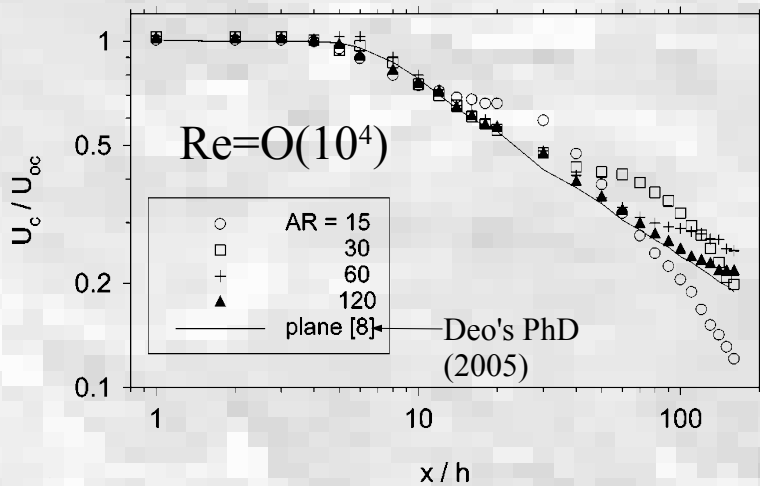
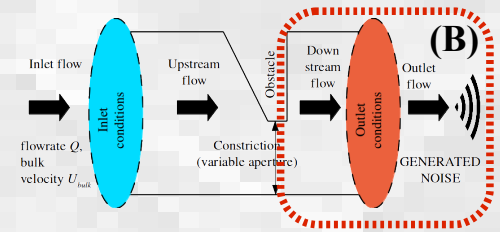
(duct lengths:  
 $L_0 = 31\text{cm}; 2L_0 = 62\text{cm}$ )



**E**: power spectral density of center velocity  
**k**: wave number [ $\text{m}^{-1}$ ]  
 $\eta = H = 25\text{mm}$

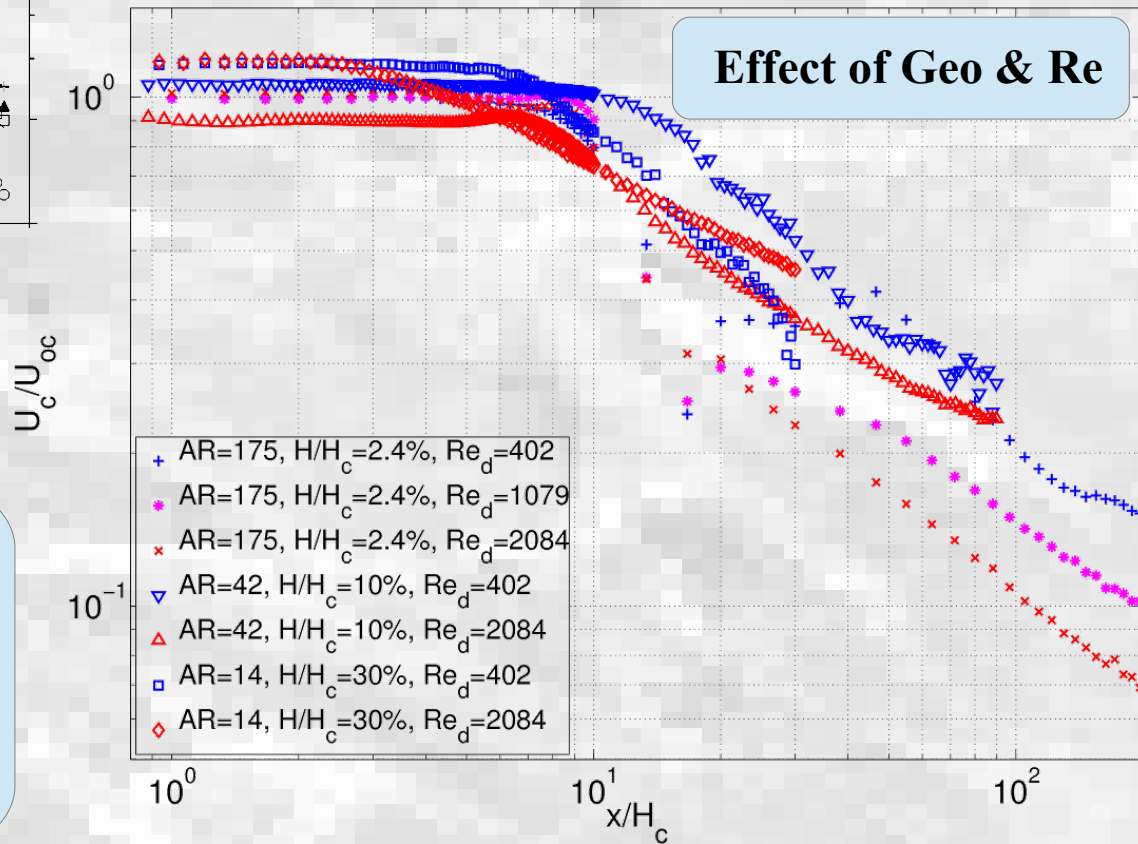


Jet longitudinal decay: comparison with literature

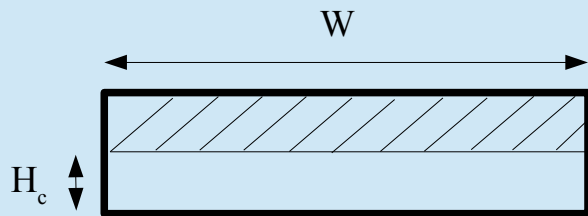


Mi, J., Deo, R. C., & Nathan, G. J. (2005)

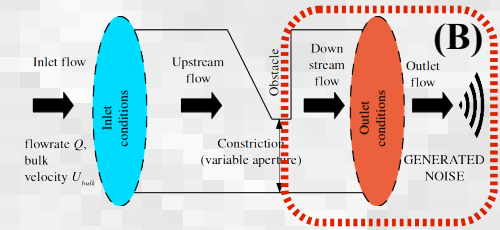
Effect of Geo & Re



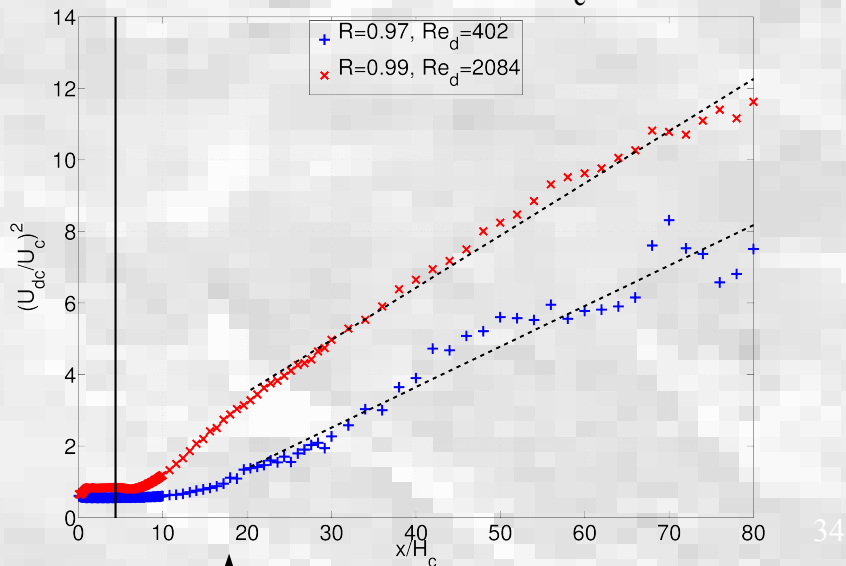
AR = aspect ratio =  $W/H_c$



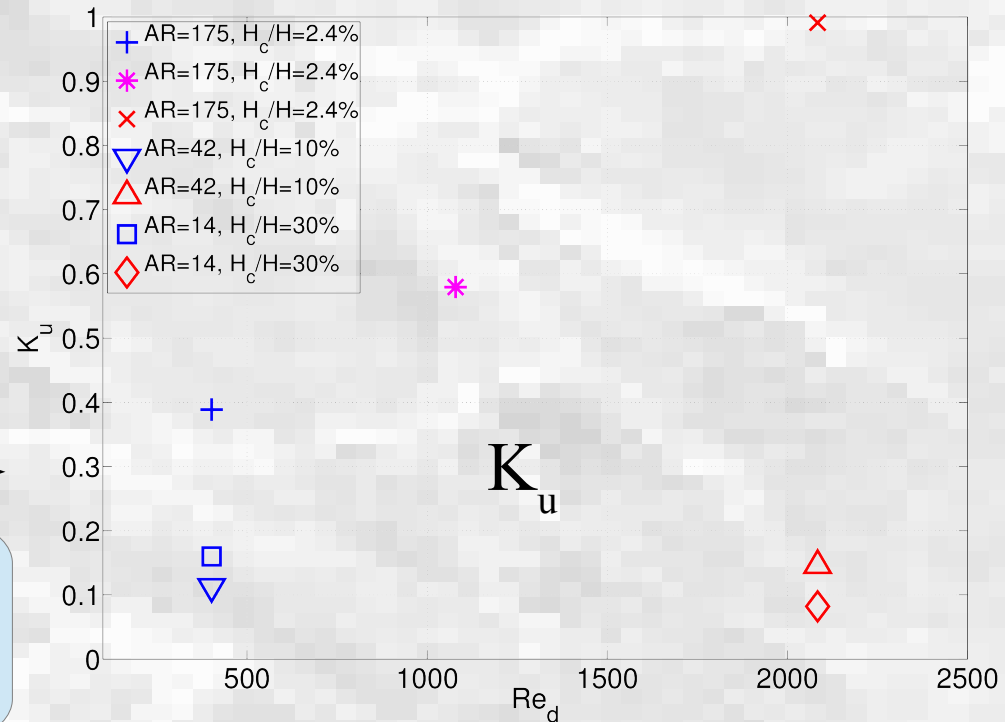
'Square' decay law:  
 $K_u$  = decay rate coef.  
 $x_{01}$  = jet virtual origin



Constriction degree  $H_c/H=10\%$

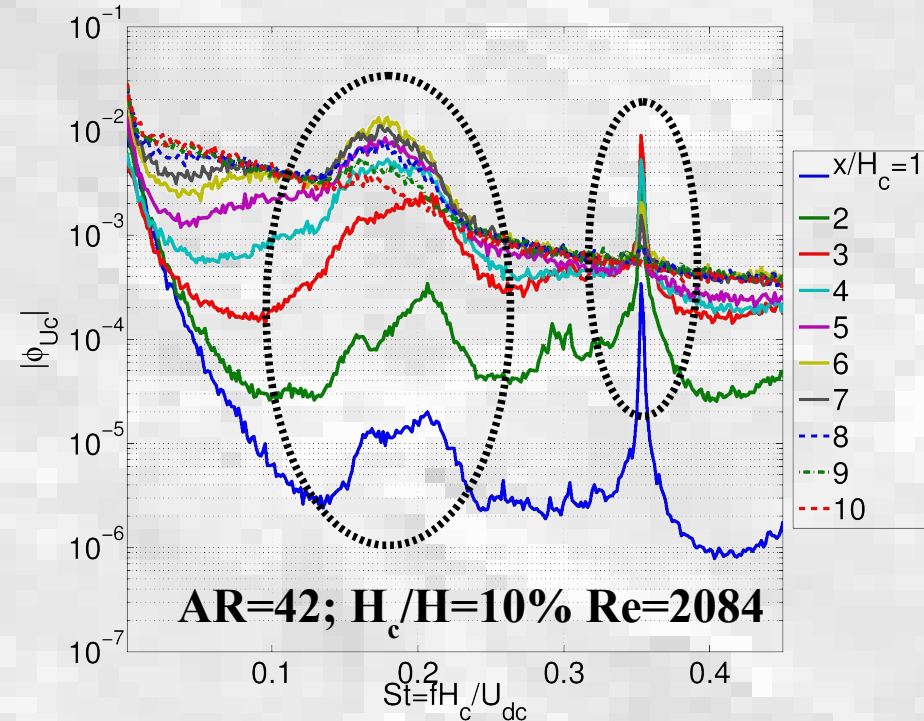
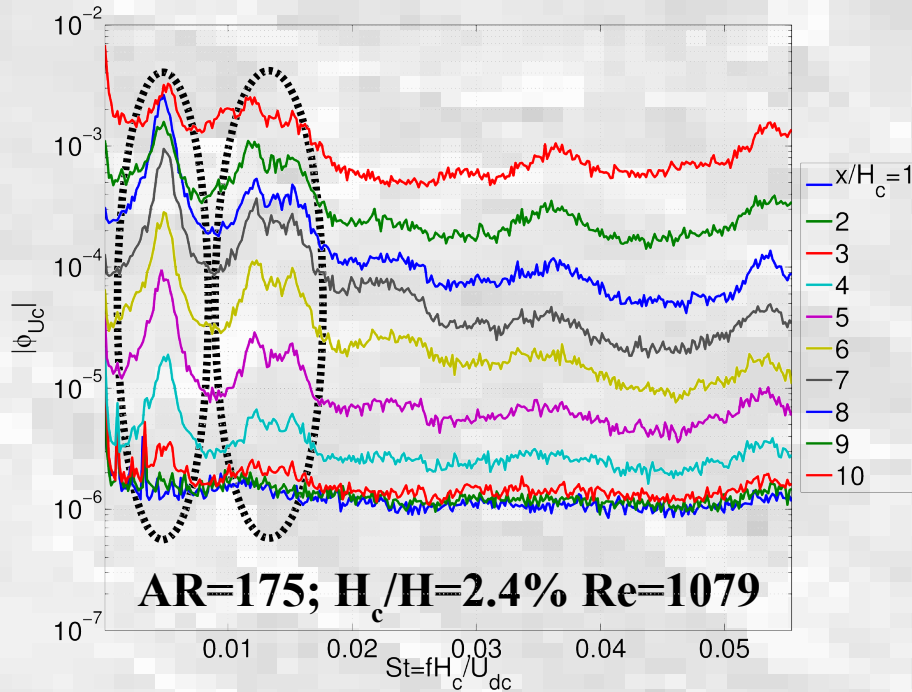


$K_u$ : effect of Geo & Re



$$\left(\frac{U_{dc}}{U_c}\right)^2 = K_u \left(\frac{x}{H_c} + \frac{x_{01}}{H_c}\right)$$

Vortex shedding freq.  $St^*$  (Strouhal numbers)

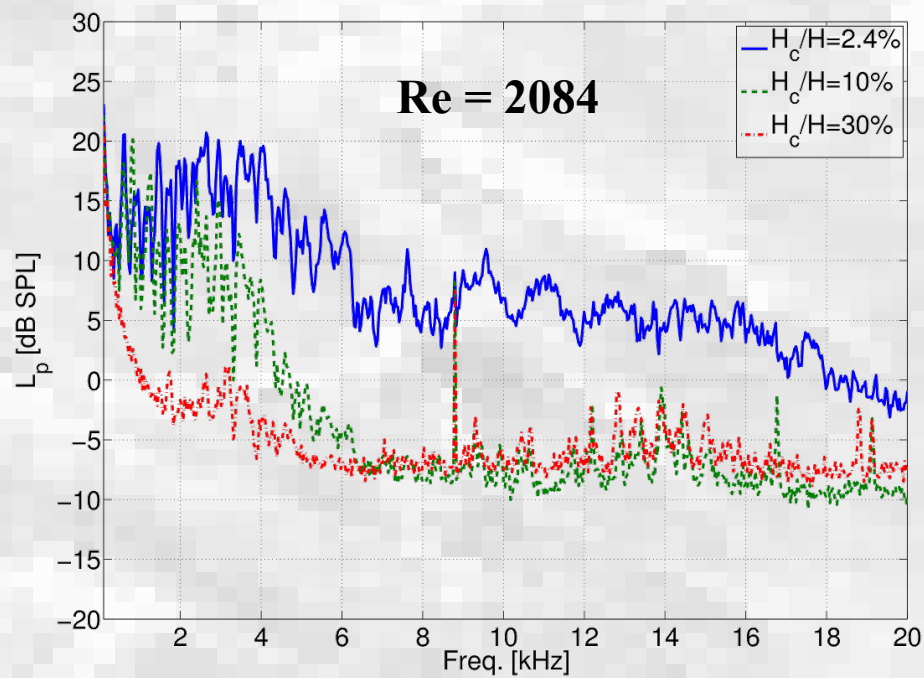
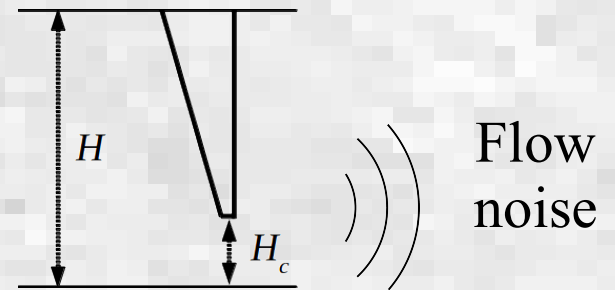
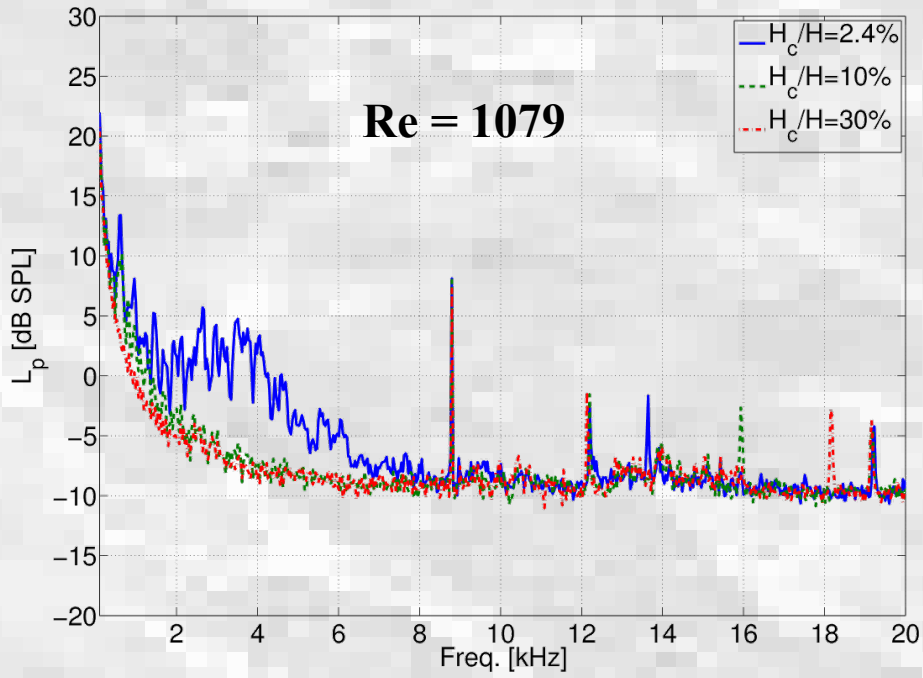


literature →

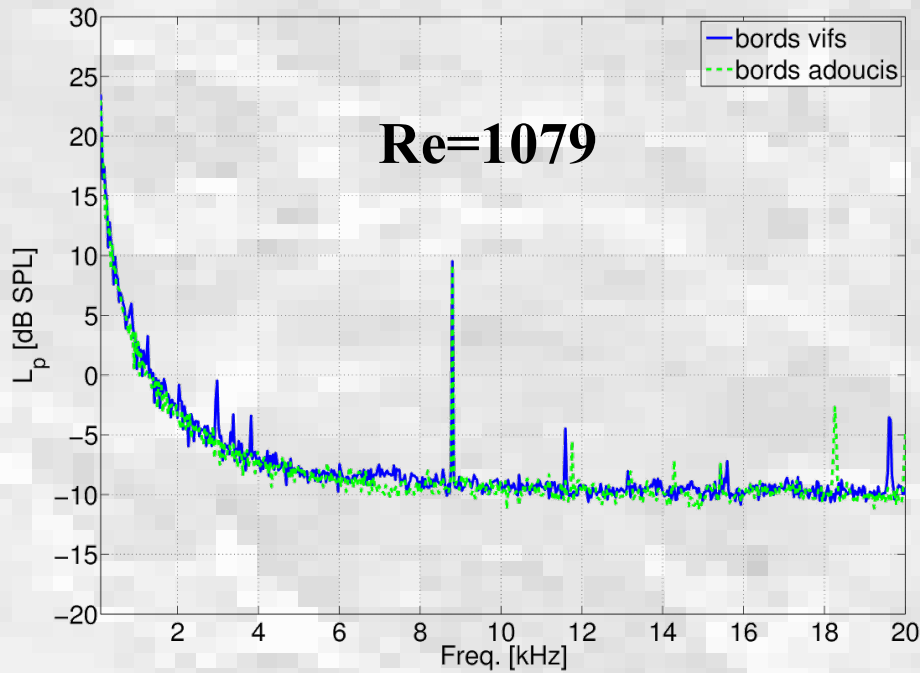
Étude	Géométrie	$Re$	$AR$	$St^*$
Beavers et Wilson [BW70]	plane	500–3000	–	0.43
Tsuchiya et al. [THTS89]	rectangulaire	3500	5	0.40
Sato [Sat60]	plane	1500–8000	10 à 67	0.23
Namer et Ötügen [NÖ88]	rectangulaire	1000–7000	56	0.27
Deo et al. [DMN07b]	plane	18000	–	0.24

**Effect of  
Geo & Re**

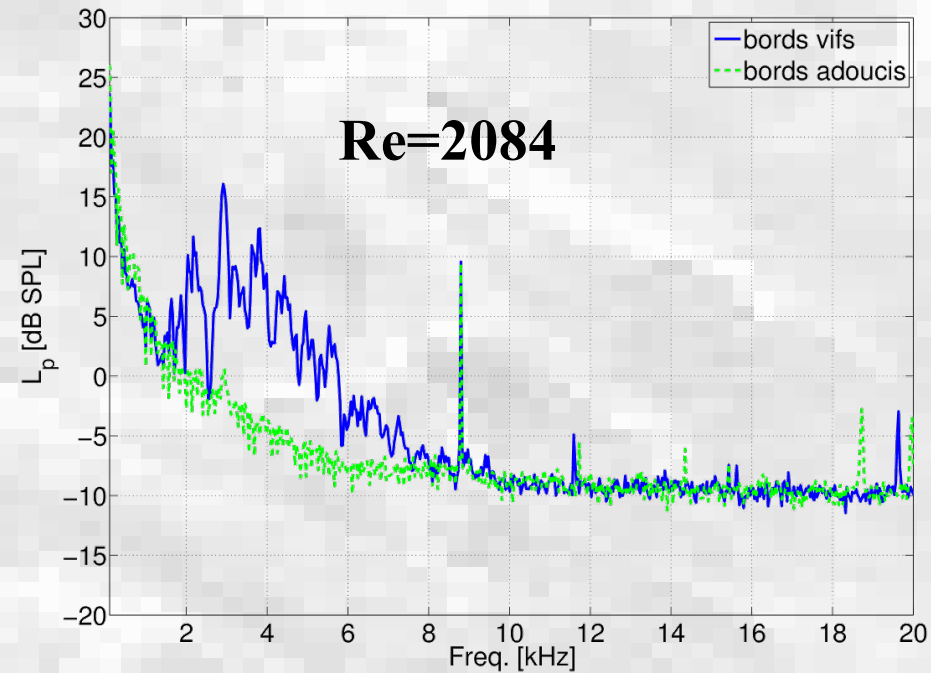
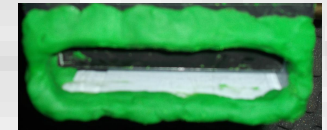
**Influence of Geo & Re**



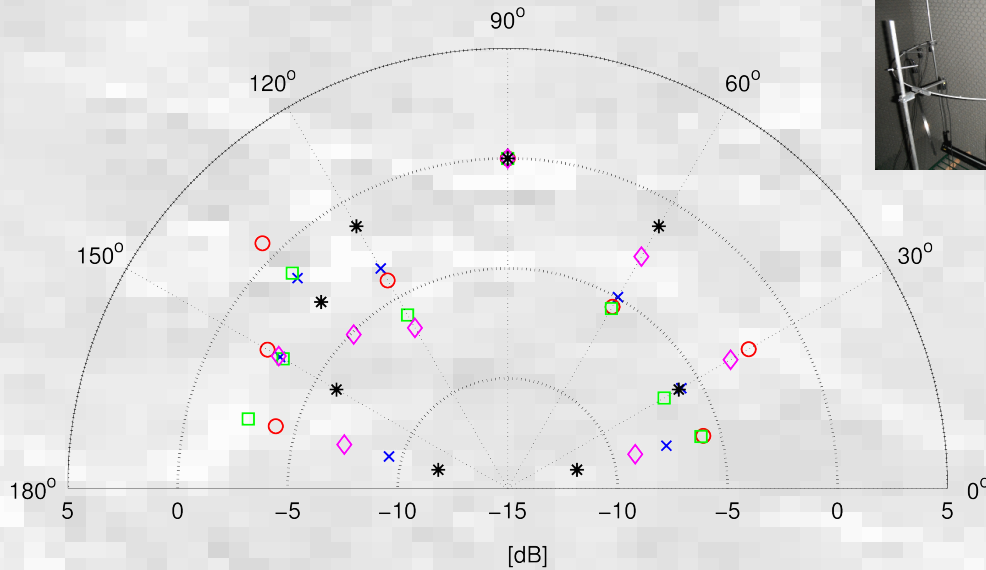
**Constriction degree**  
 $H_c/H = 2.4; 10; 30\%$



**Outlet section edges:  
sharp vs soft**



**Constriction degree:  
 $H_c/H = 2.4\%$**

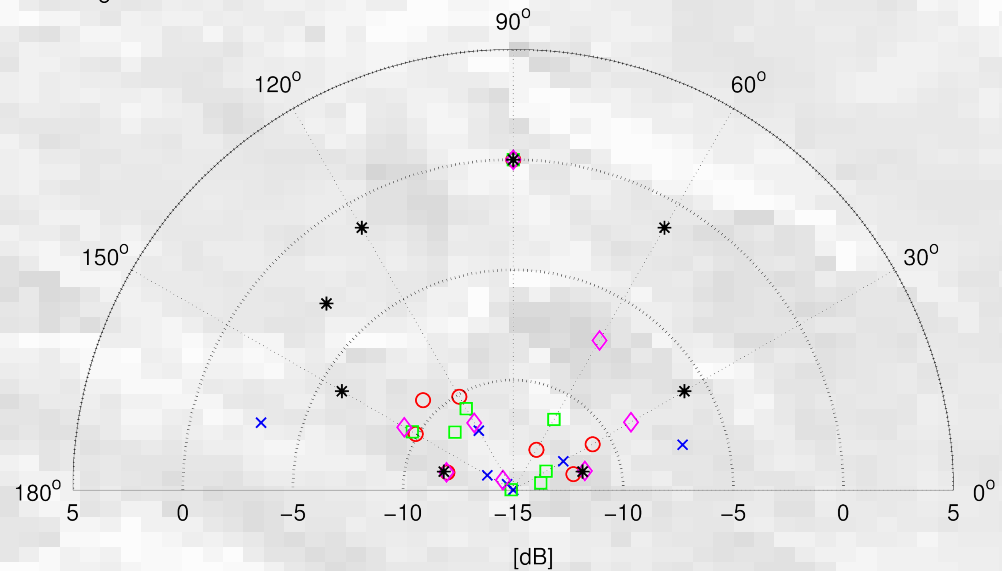


**$Re = 402$**



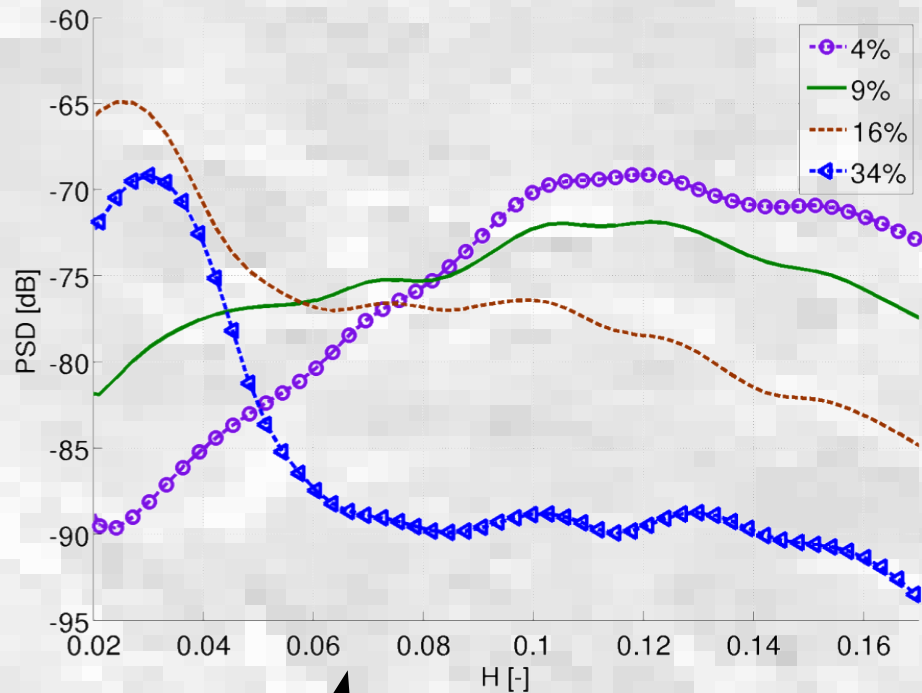
**Noise directivity**  
 $H_c/H = 2.4\%$

**$Re = 2084$**



$ka = 0.3$  ( $\times$ );  $ka = 0.35$  ( $o$ );  
 $ka = 0.40$  ( $\square$ );  $ka = 0.45$  ( $\diamond$ );  
 (corresp. freq. 1622; 1893; 2163;  
 2433 Hz)

**theoretical dipole directivity added  
 for comparison (\*)**

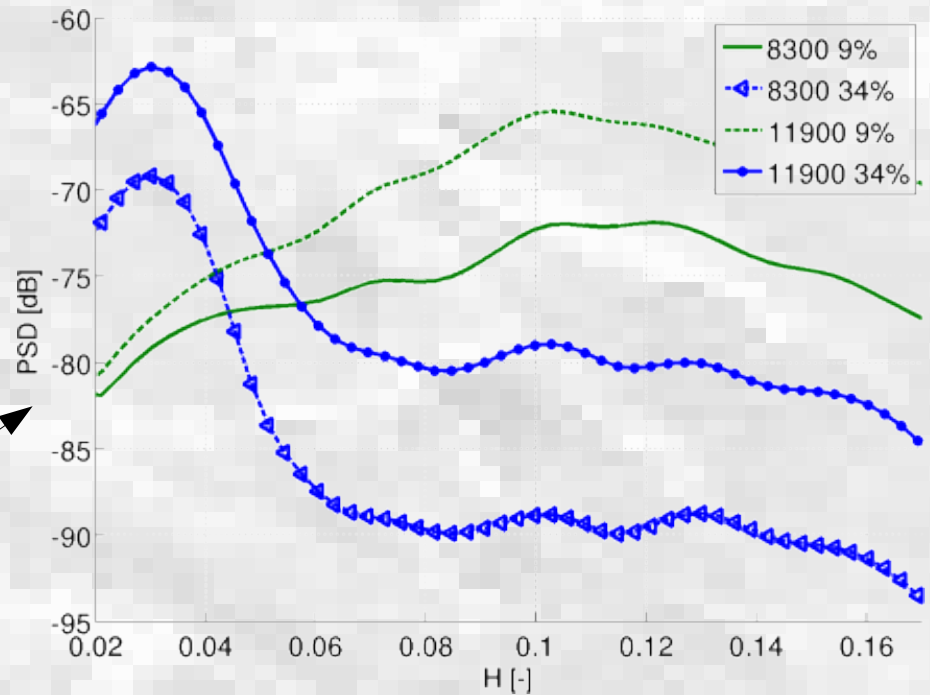
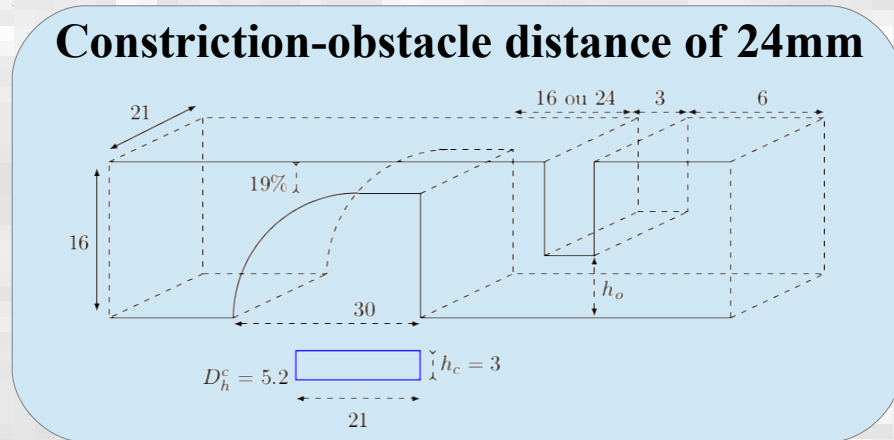


**Re = 8300 & constriction degrees 4; 9; 16; 34%**

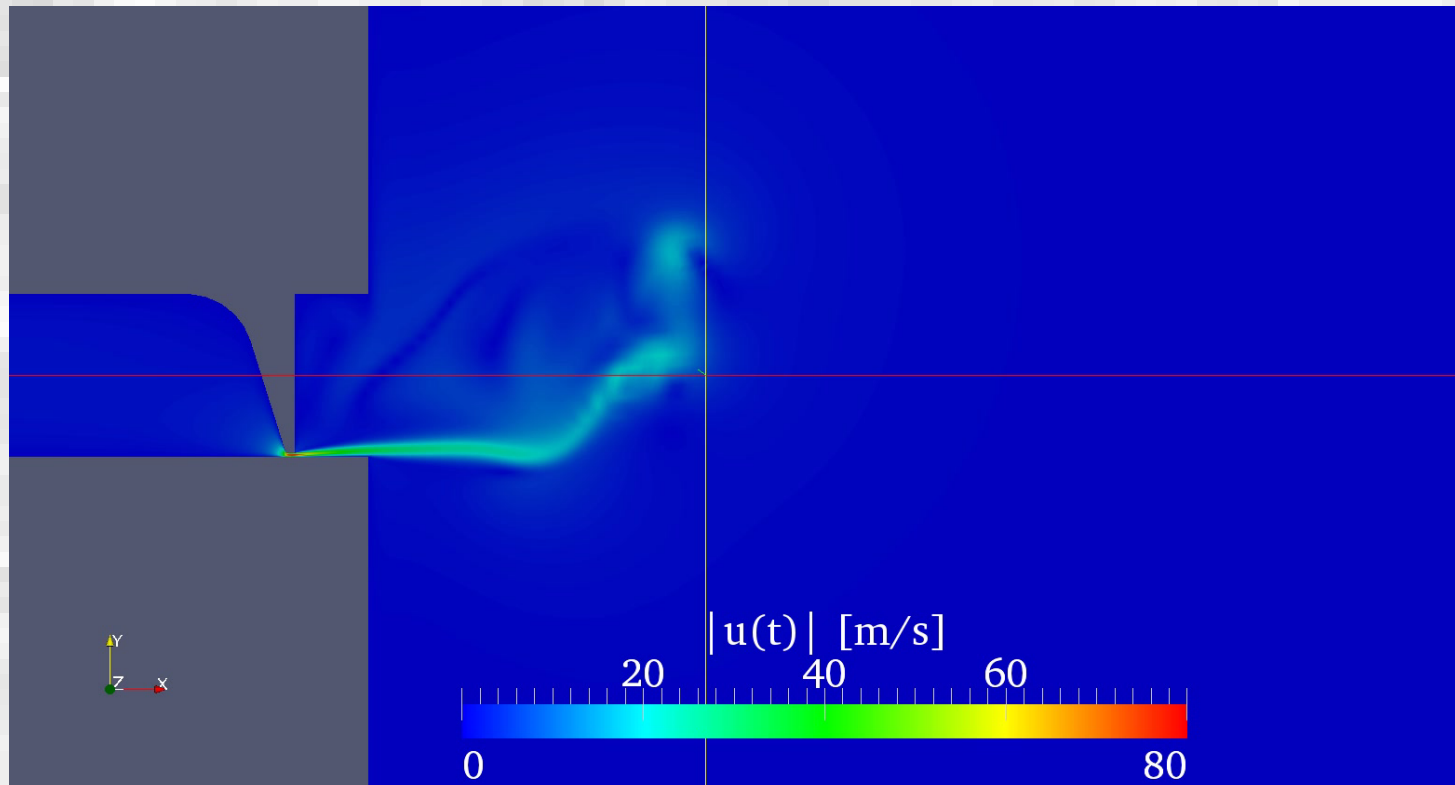
Helmholtz number

$$H = \frac{f D_h^c}{c}$$

**Re = 8300; 11900 & constriction degrees 9; 34%**



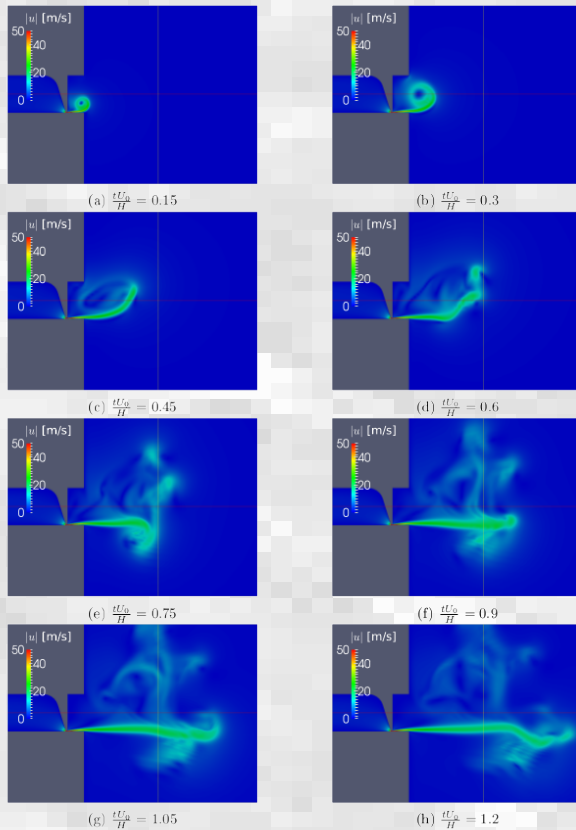
**Example:  $H_c/H = 2.4\%$  &  $Re = 2084$**





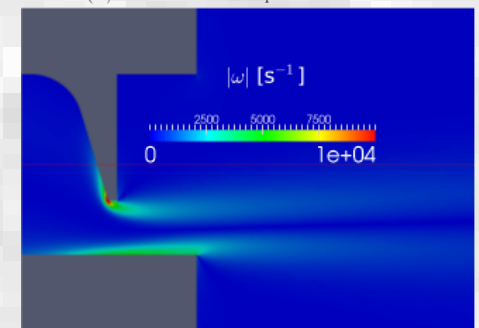
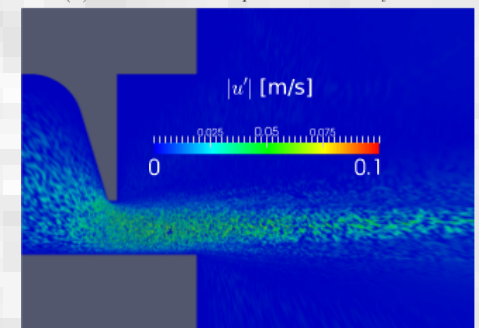
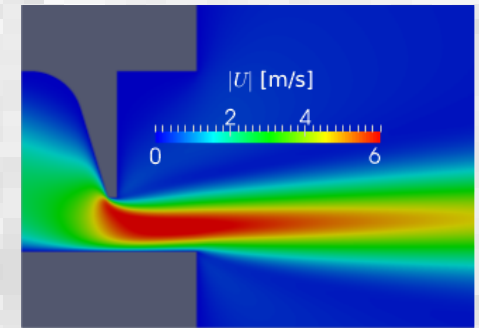
## Example case:

- \*  $Re = 2084$
- \*  $H_c/H = 2.4\%$
- \* Uniform inlet vel. Profile
- \* Mean velocity field

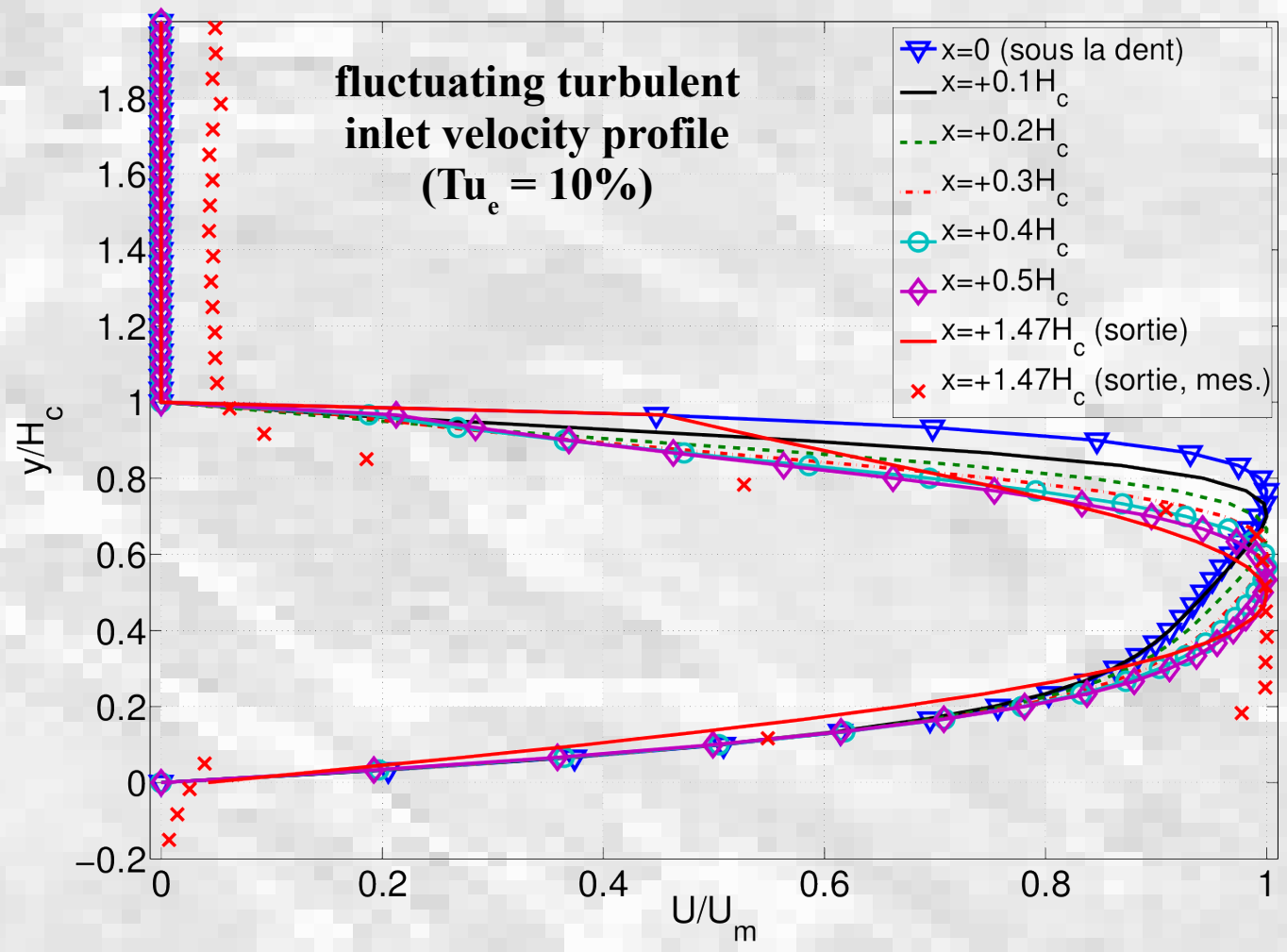


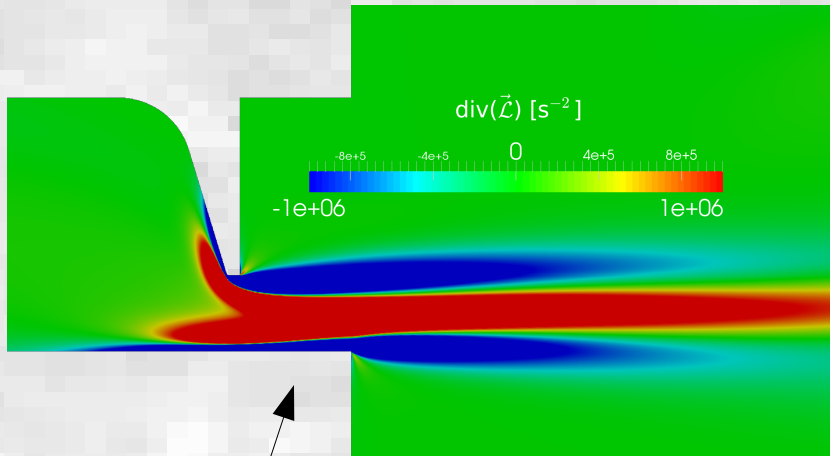
## Other example:

- \*  $Re = 2084$
- \*  $H_c/H = 30\%$
- \* Uniform inlet vel. Profile
- \* TOP: mean vel.
- \* MID: rms vel.
- \* BOT: vorticity



**Comparison of transverse mean velocity profiles simulated at several longitudinal positions downstream from the obstacle ( $H_c/H = 30\%$ ;  $Re = 2084$ )**



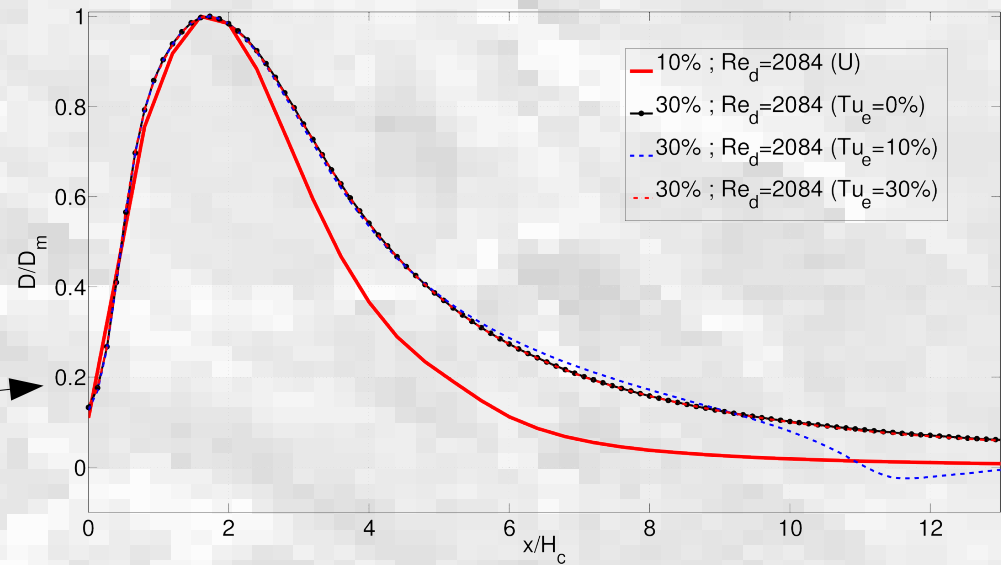


Longitudinal visualization of Lamb vector divergence field ( $H_c/H = 30\%$ ;  $Re = 2084$ )

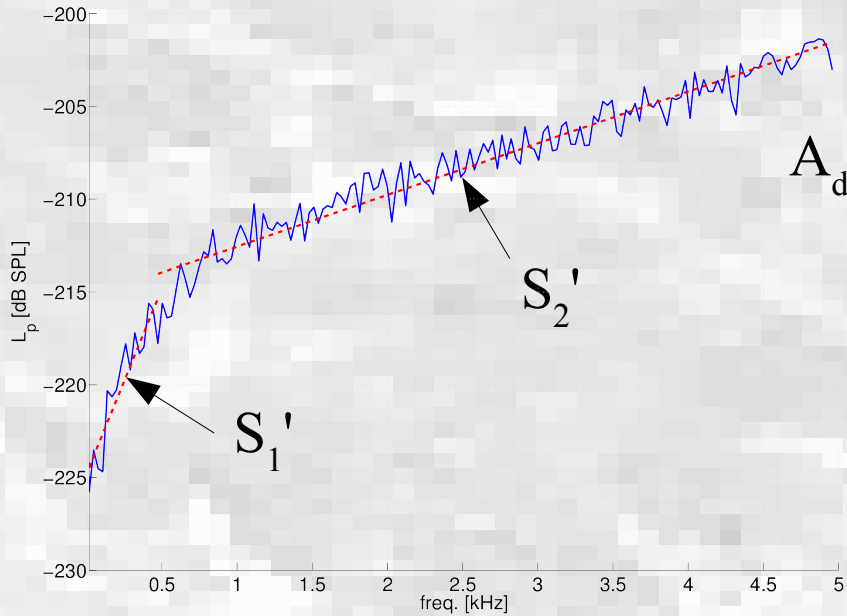
Lamb vector  $\rightarrow \vec{\mathcal{L}} = \vec{u} \times \vec{\omega}$

velocity  $\rightarrow \vec{u}$       vorticity  $\rightarrow \vec{\omega}$

Comparison of normalized Lamb vector divergences for different inlet conditions & Reynolds numbers



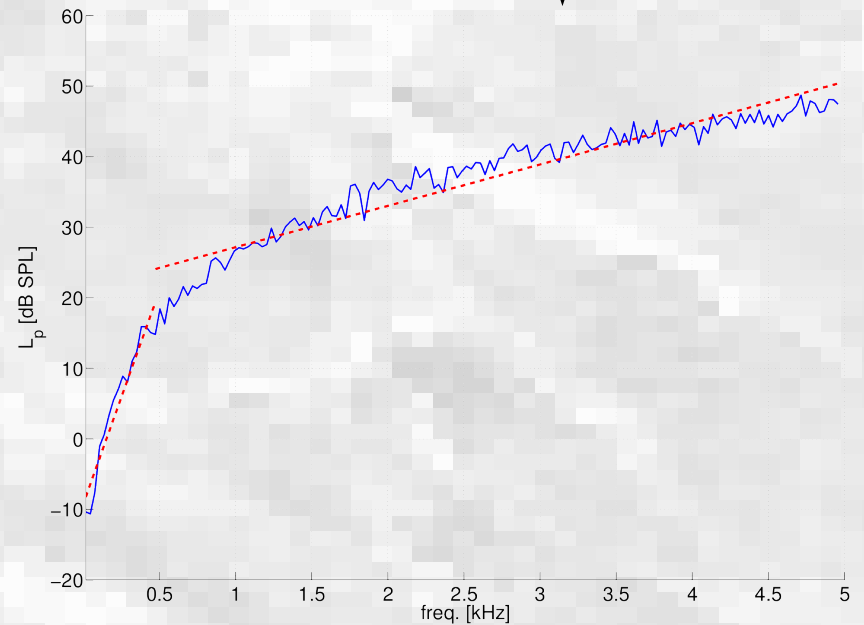
$H_c/H = 10\%$ ;  $Re = 2084$



without

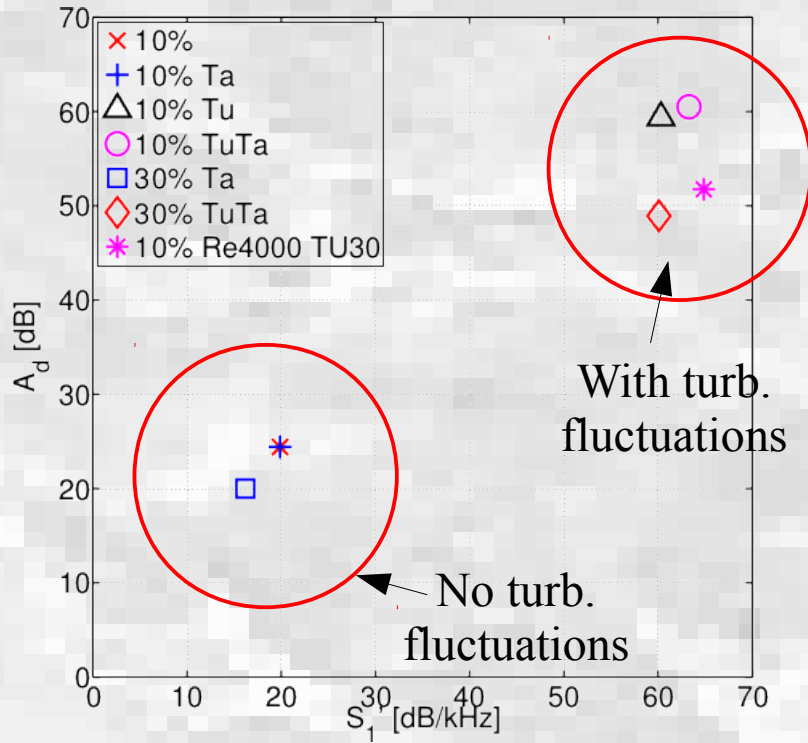
Random Gaussian  
turbulent fluctuations

with



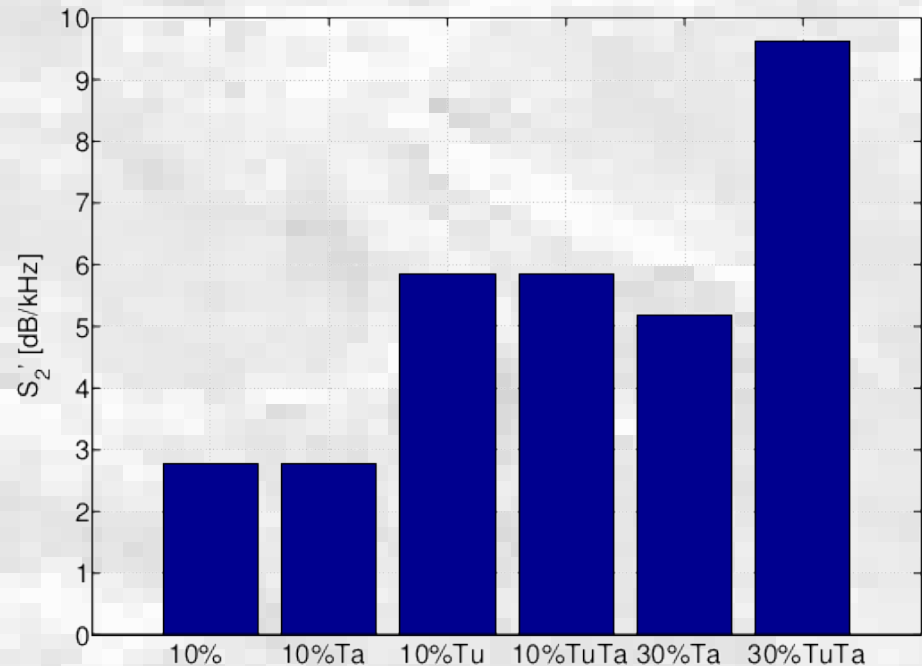
**Spectral parameters:**

- \* dynamic amplitude  $A_d$
- \* spectral slopes  $S_1'$  &  $S_2'$



### Spectral parameters:

- \* dynamic amplitude  $A_d$
- \* spectral slopes  $S_1'$  &  $S_2'$



**P%:** constriction degree  
**Tu:** with Gaussian turbulent fluctuations  
**Ta:** with 'buffer layer'

I. Introduction

II. Theory

III. Method

IV. Results

V. Conclusion

## Previous studies:

- \* Reynolds number  $Re = 4000$  (exp.+sim.)
- \* Constriction degree (exp.+sim.)
- \* Uniform inlet velocity profile (sim.)

## This thesis

**Unvoiced  
fricative  
production**

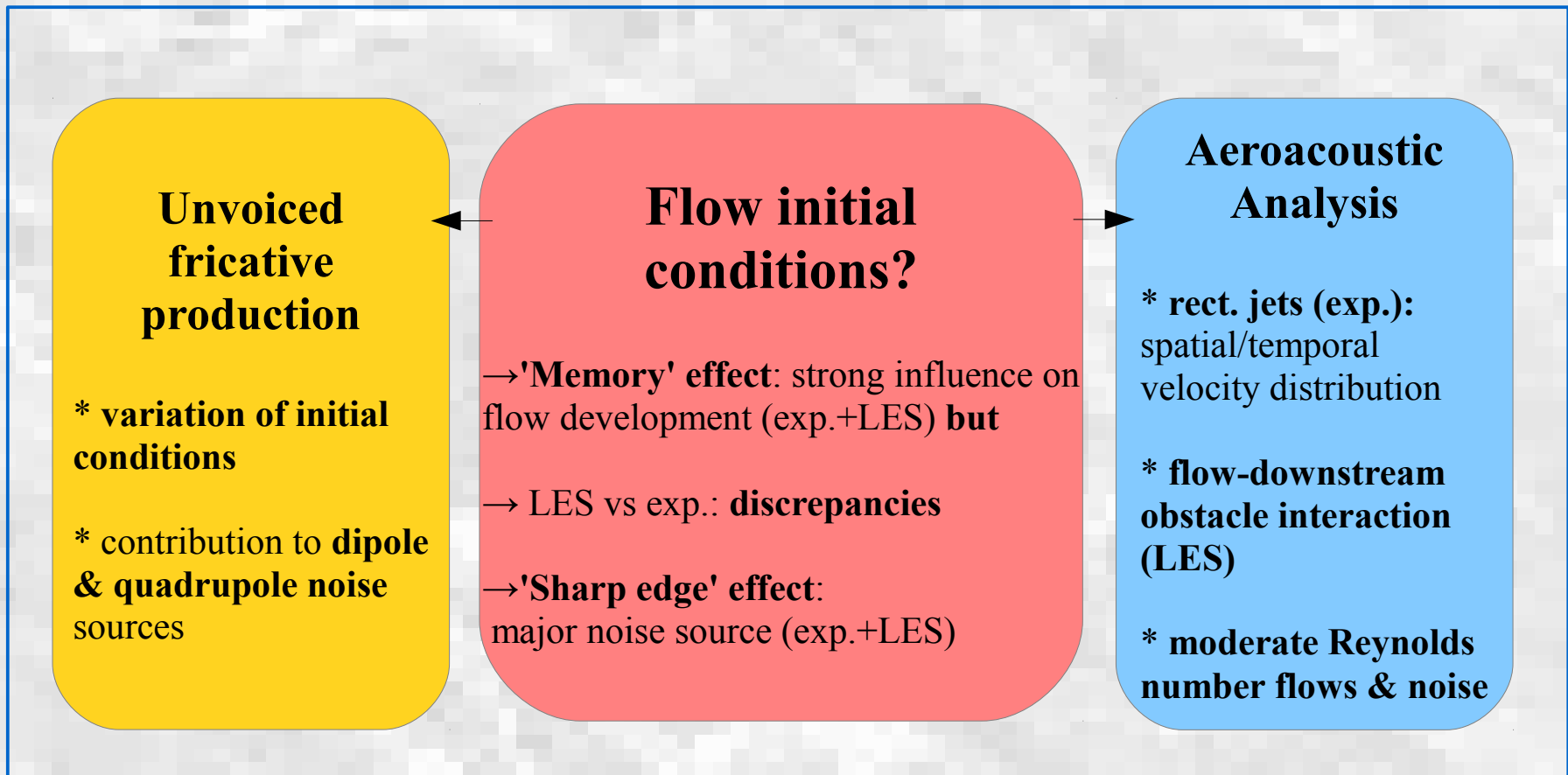
Flow initial  
conditions?

Reynolds  
numbers  $Re$ ?

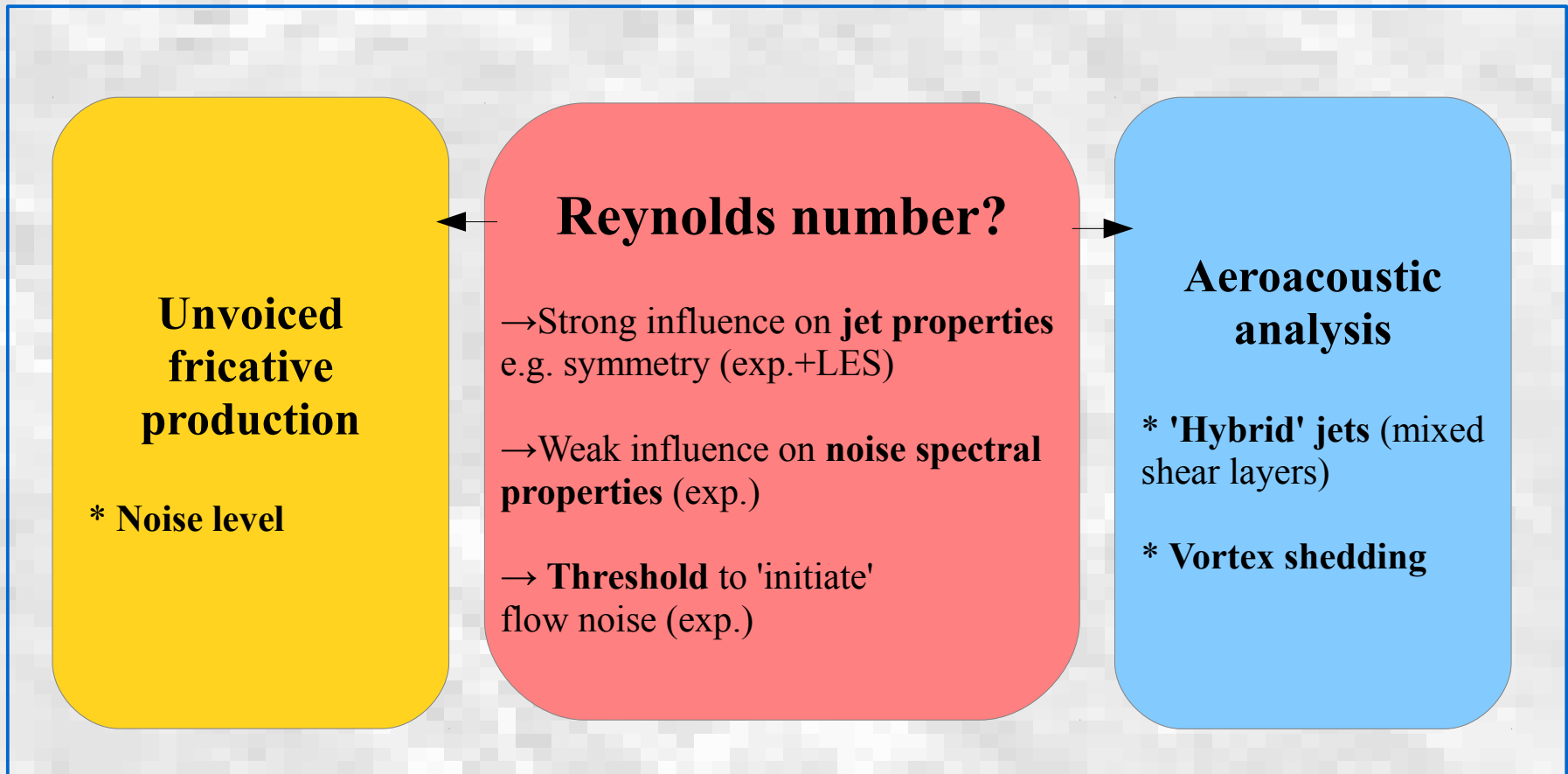
Obstacle(s)  
geometry?

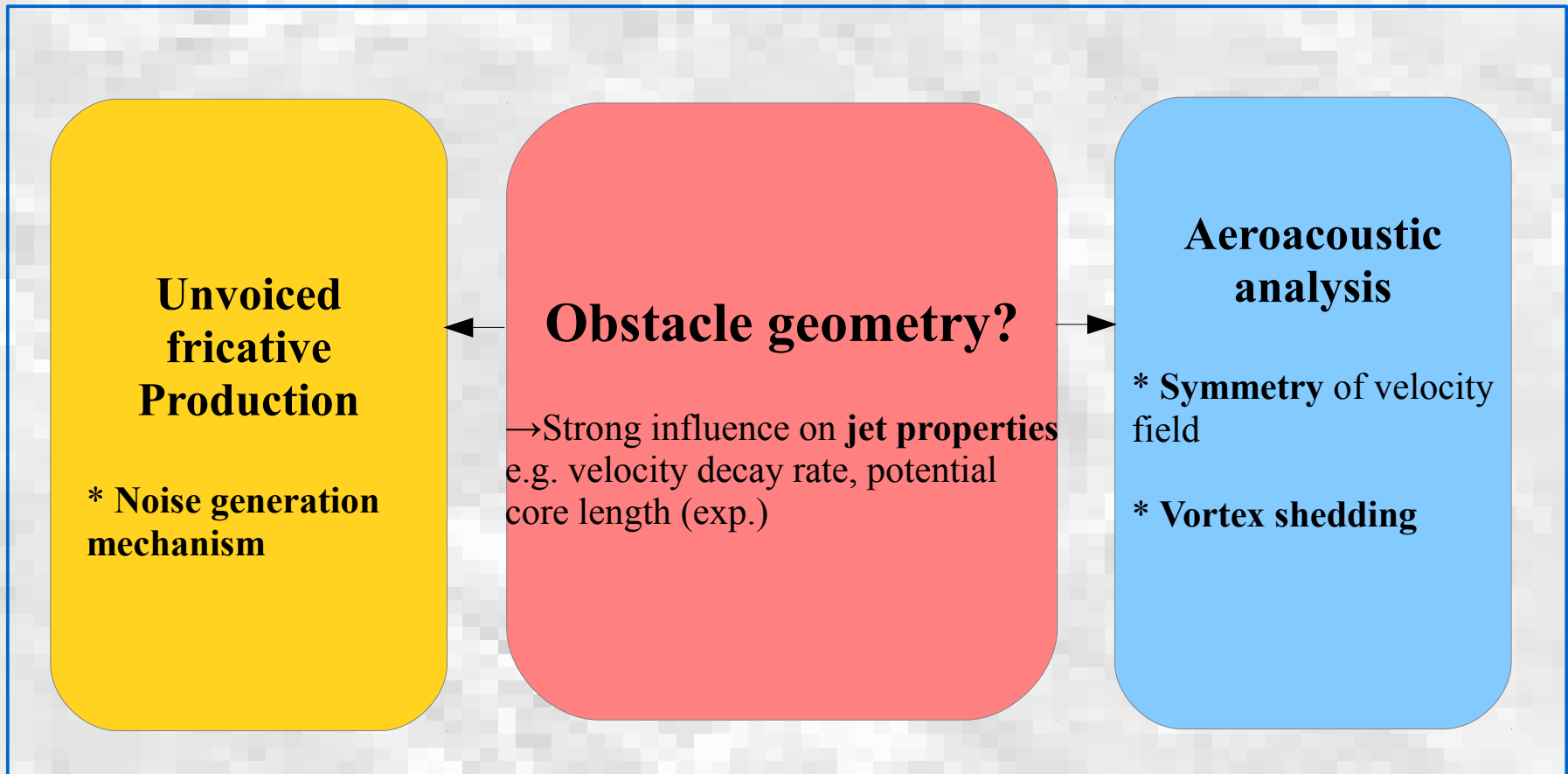
**Aeroacoustic  
analysis**

- \* Experiments
- \* Simulations









- \* **Study of jet stability...**
- \* Further development of **turbulence simulation method**, e.g. taking into account large coherent structures...
- \* Further development of **aeroacoustic prediction methods** (e.g. Ffowcs Williams & Hawkings analogy taking into account solid boundaries)...
- \* **Transverse modes...**
- \* **Other (potential) applications:**
  - Oral/dental health care...

## JOURNAL PUBLICATIONS

Steady laminar axisymmetrical nozzle flow at moderate Reynolds numbers: modelling and experiment

Grandchamp, Xavier and **Fujiso, Yo** and Wu, Bo and Van hirtum, Annemie. Journal of Fluids Engineering - T ASME 134 2012 011203

Insulation room for aero-acoustic experiments at moderate Reynolds and low Mach numbers.

Van Hirtum, Annemie and **Fujiso, Yo**. Applied Acoustics 73 1 2012 72-77

## CONFERENCES

Experimental and numerical characterization of aerodynamic noise applied to moderate Reynolds number airflow

**Fujiso, Yo** and Van Hirtum, Annemie and Kazunori, Nozaki and Wada, Shigeo. ICA 2013 proceedings - Volume 19 of POMA (Proceedings of Meetings on Acoustics) - 21st International Congress on Acoustics (ICA 2013) - 165th Meeting of the Acoustical Society of America

Study of unvoiced fricative speech production: Influence of initial conditions on flow development.

**Fujiso, Yo** and Van Hirtum, Annemie and Nozaki, Kazunori and Wada, Shigeo. ICA 2013 proceedings - Volume 19 of POMA (Proceedings of Meetings on Acoustics) - 21st International Congress on Acoustics (ICA 2013) - 165th Meeting of the Acoustical Society of America

Aeroacoustic characterisation of single and dual tooth-shaped obstacle replicas in relation to the study of unvoiced fricative speech production.

**Fujiso, Yo** and Van Hirtum, Annemie. Acoustics 2012 Nantes - Acoustics 2012

Ecoulement laminaire axisymétrique stationnaire dans un convergent : modélisation et validation expérimentale

**Fujiso, Yo** and Wu, Bo and Grandchamp, Xavier and Van Hirtum, Annemie. Actes du CFM 2011 - 20ème Congrès Français de Mécanique (CFM 2011)

Jet rond en aval d'une contraction brusque.

Grandchamp, Xavier and **Fujiso, Yo** and Van Hirtum, Annemie. Actes du CFM 2011 - 20ème Congrès Français de Mécanique (CFM 2011)

Caractérisation d'un convergent axisymétrique destiné à la validation expérimentale de production de parole

**Fujiso, Yo** and Wu, Bo and Grandchamp, Xavier and Van Hirtum, Annemie. Actes des 9ème RJCP 2011 - 9ème Rencontres des Jeunes Chercheurs en Parole 2011 (RJCP 2011)

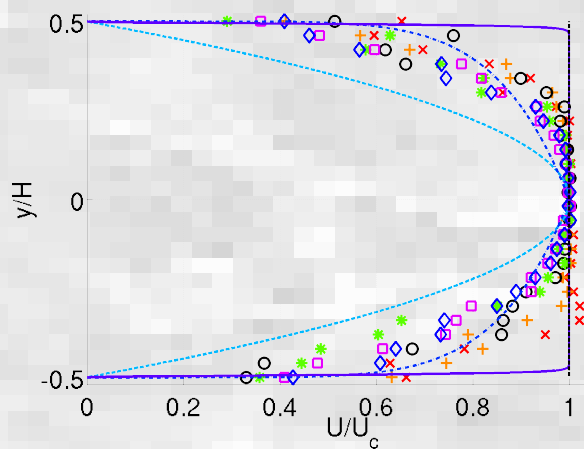
# Thank you for your attention!

## **Acknowledgements:**

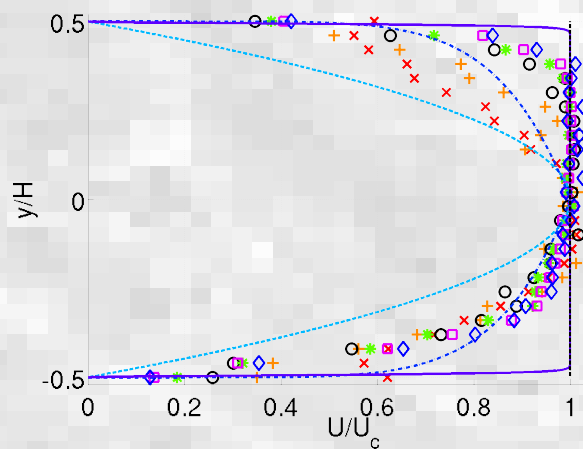
ANR Petaflow ANR-09-BLAN-0376-01  
Rhône-Alpes region (CMIRA 2011)  
K. Nozaki & S. Wada  
Osaka Univ. / Cybermedia Center



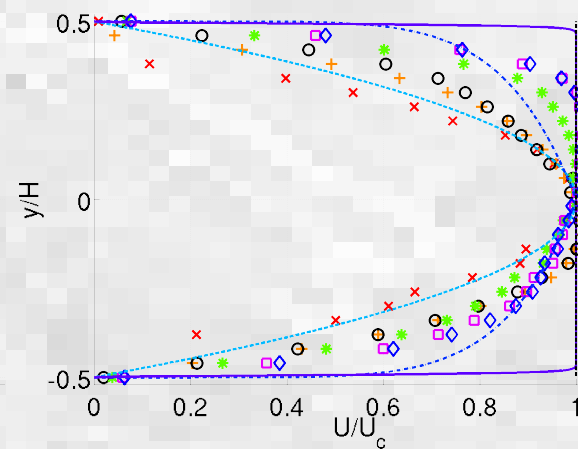




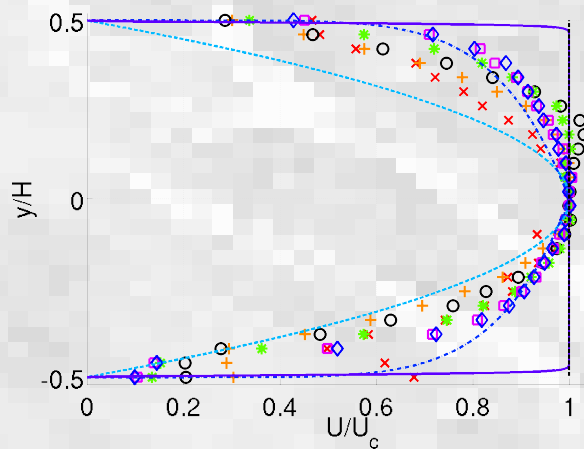
L=0cm



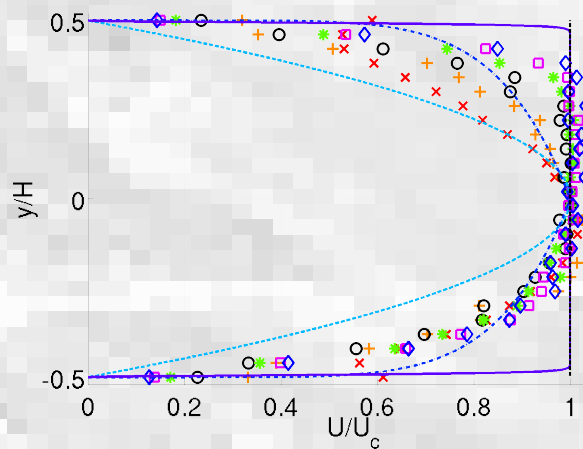
L=31cm



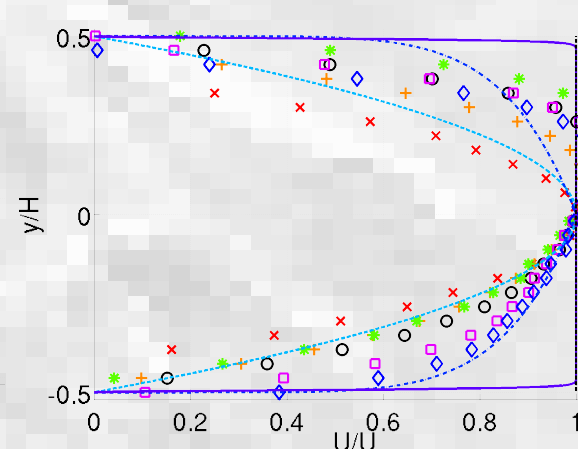
L=31cm + nid  
d'abeille



L=31cm +  
pailles



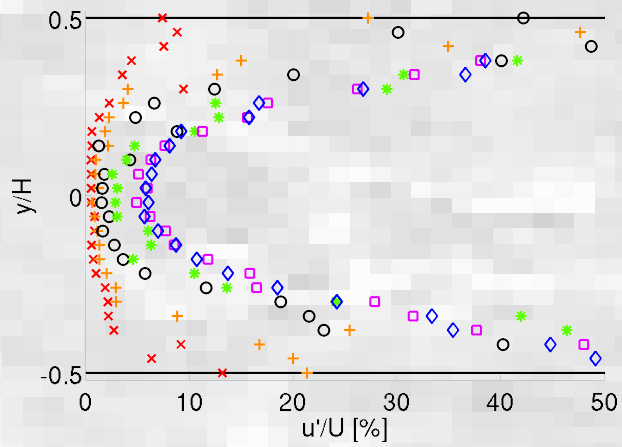
L=62cm



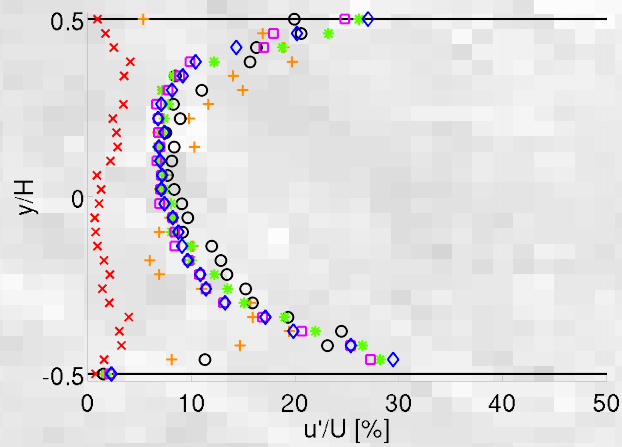
L=62cm +  
pailles



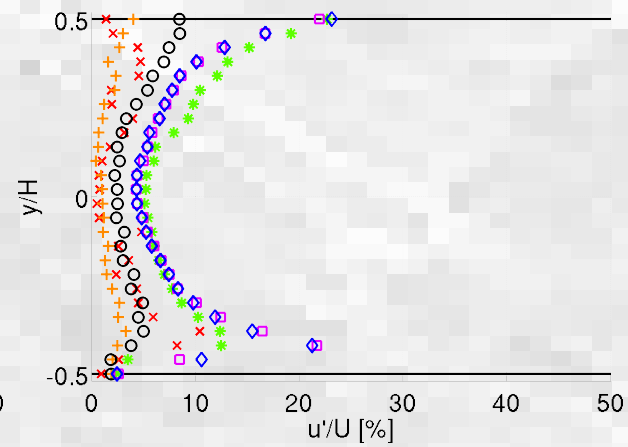
# Ducts with obstacle(s): *in-vitro* exp. Inlet flow data: turbulence intensity profiles



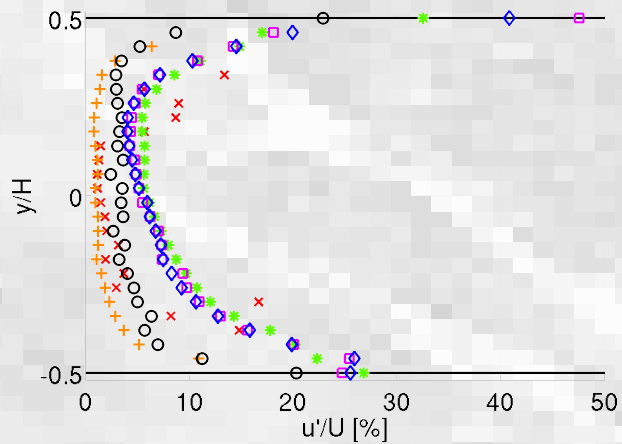
$L=0\text{cm}$



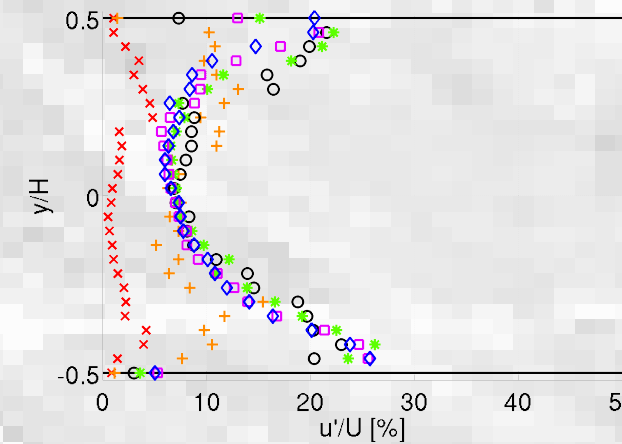
$L=31\text{cm}$



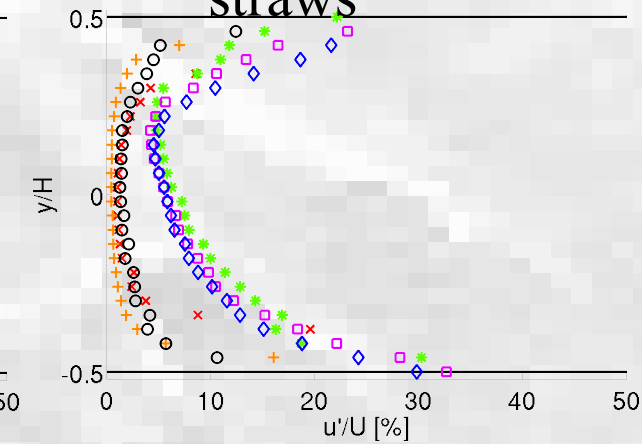
$L=31\text{cm} +$   
straws



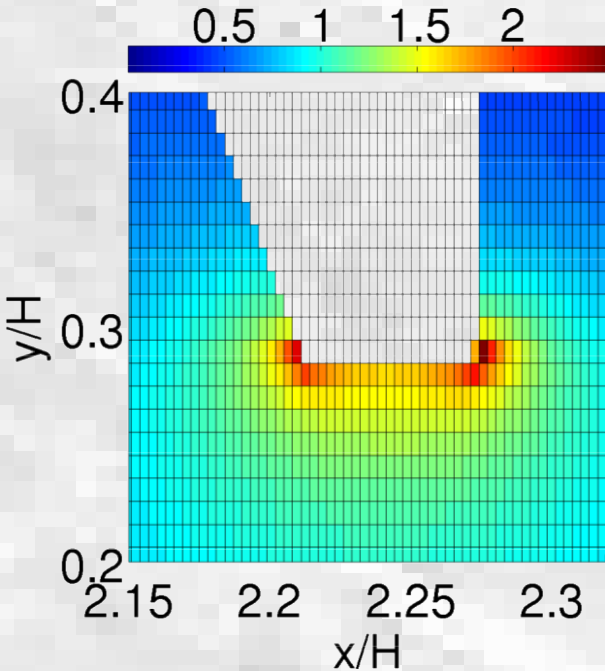
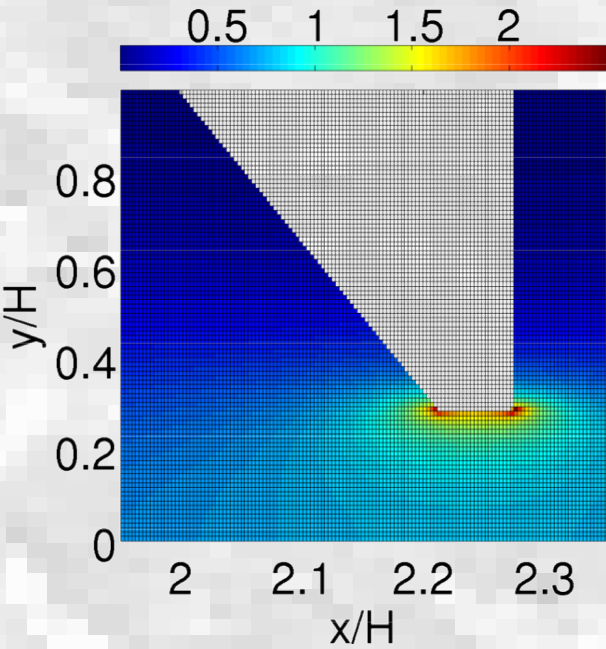
$L=31\text{cm} +$   
honeycomb

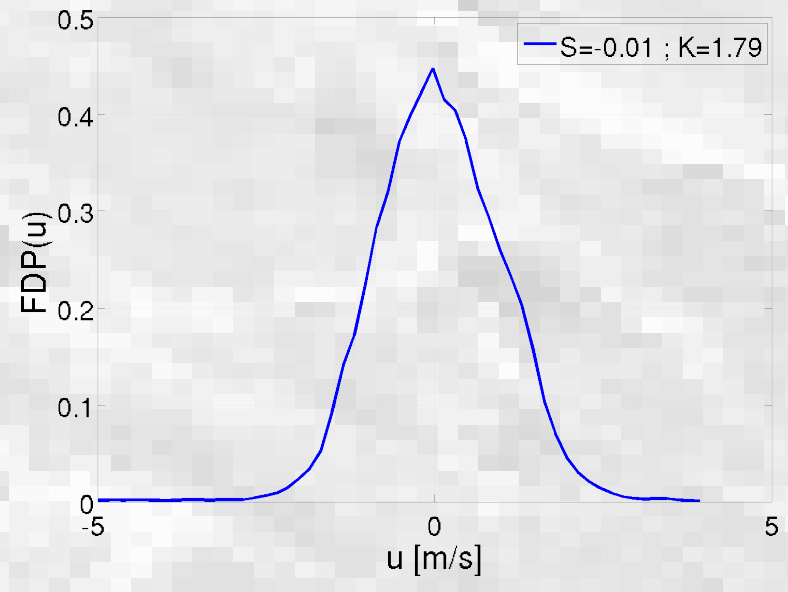
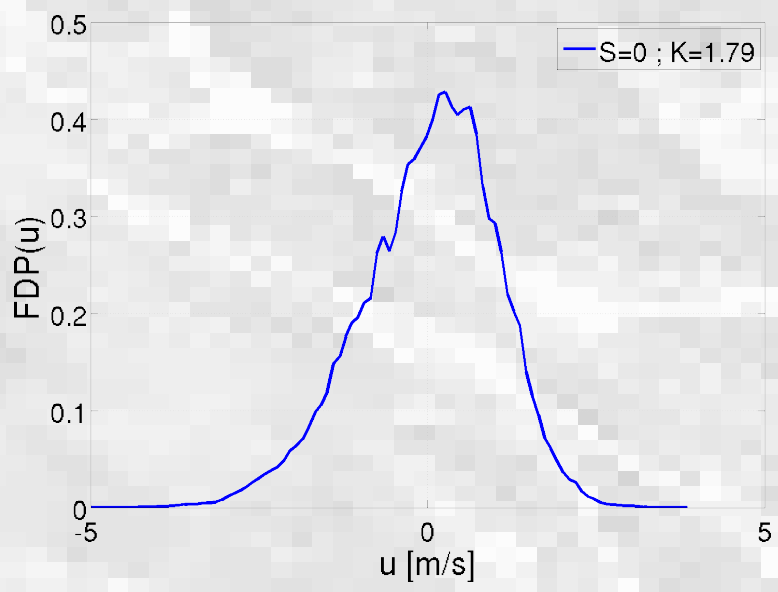
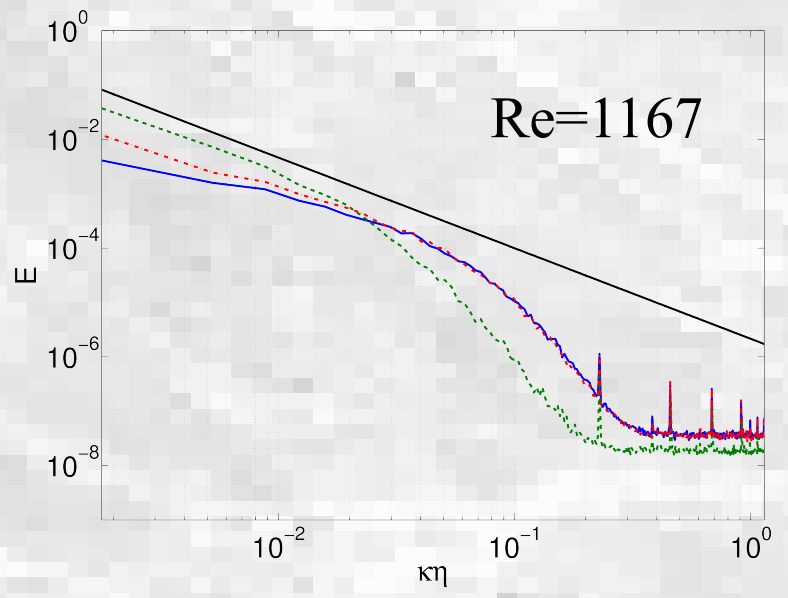
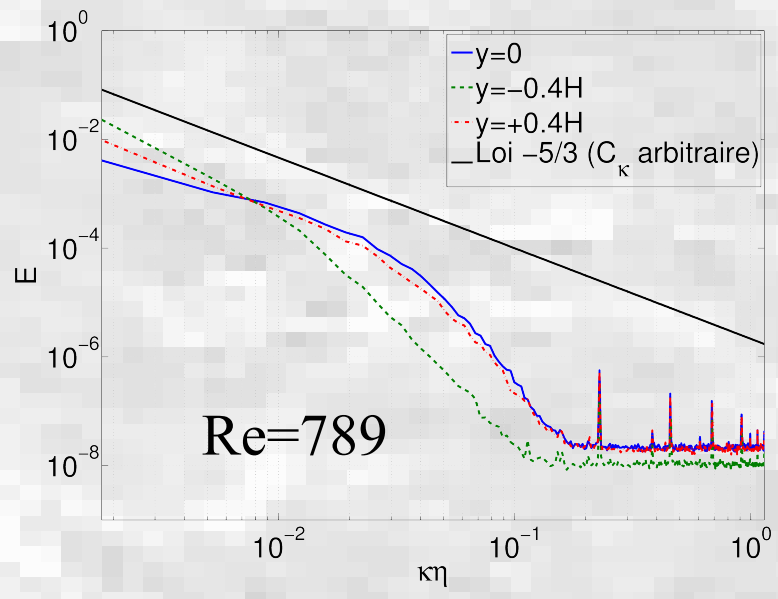


$L=62\text{cm}$

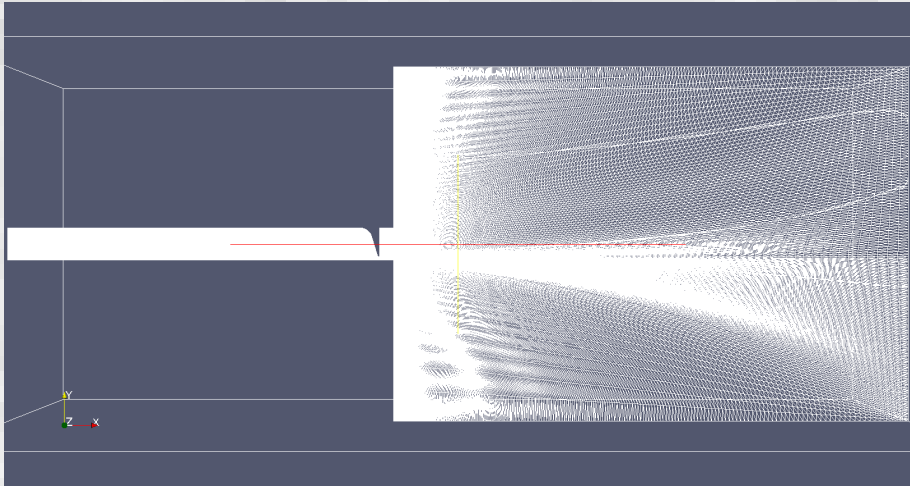


$L=62\text{cm} +$   
straws

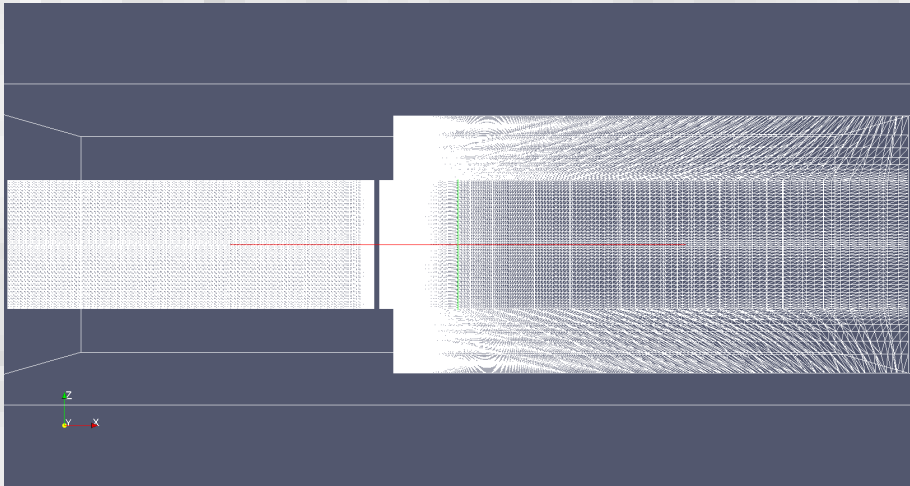
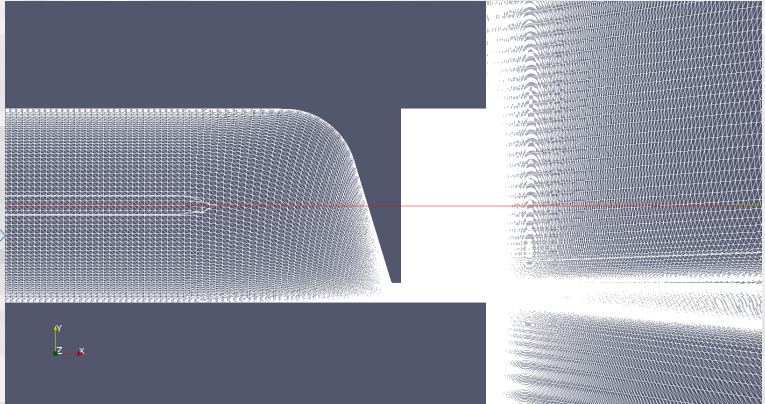




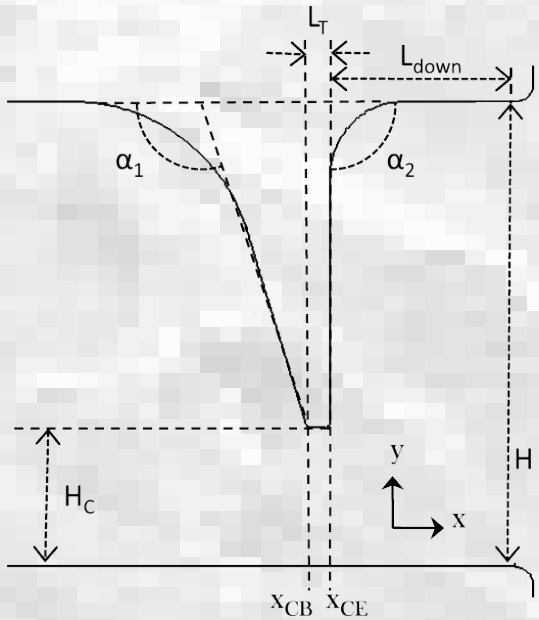
Ducts with obstacle(s): num. simul. 3D simul. (LES): geometry

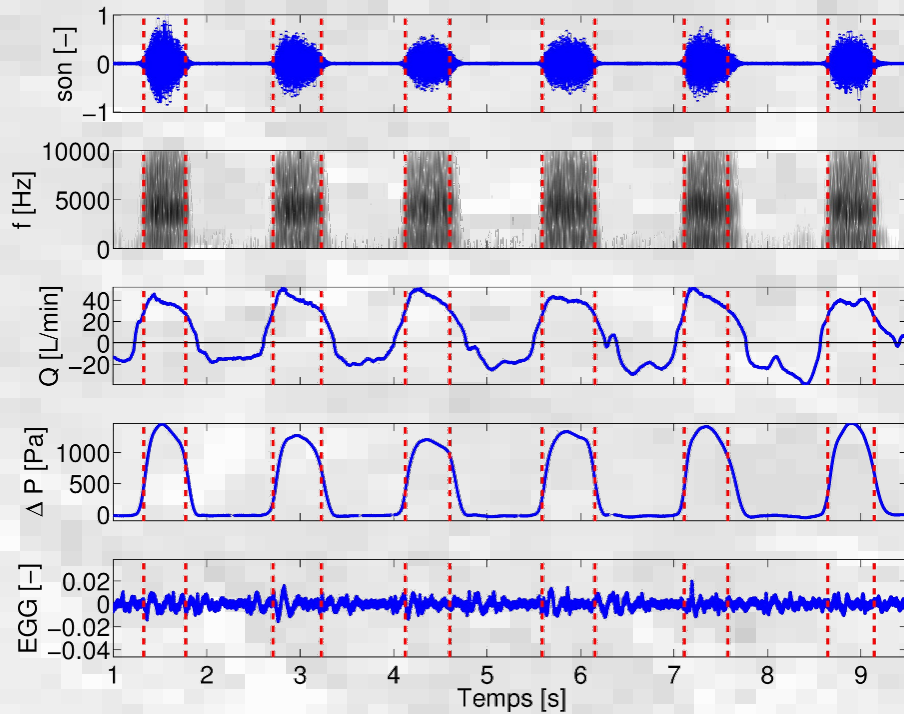


(xy) plane



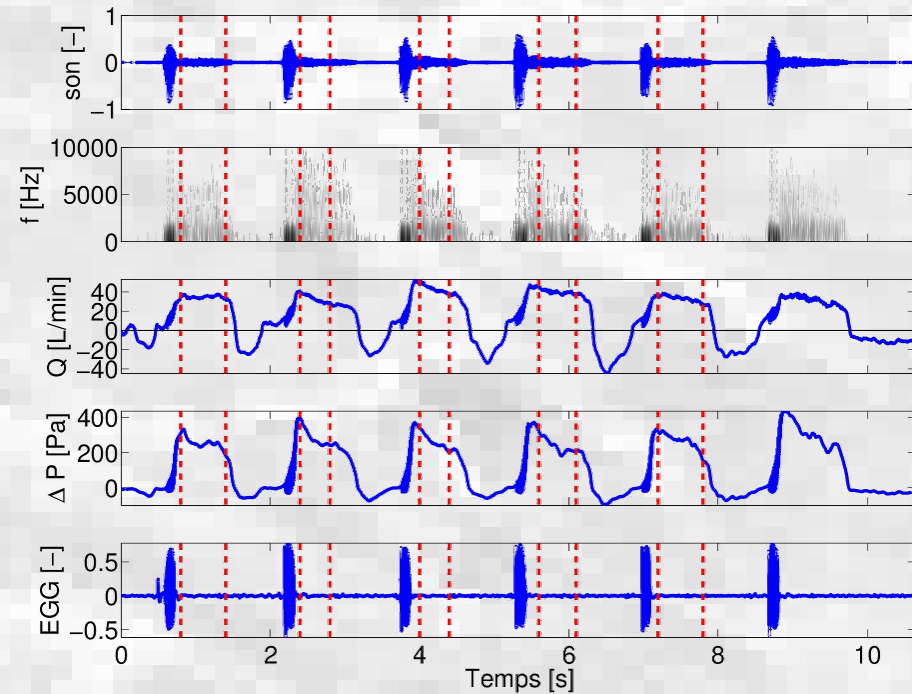
(xz) plane





/s/ subject 'KN'  
'medium' level

/f/ subject 'YF'  
'medium' level



→ Production of sibilant /s/ severely affected by teeth!

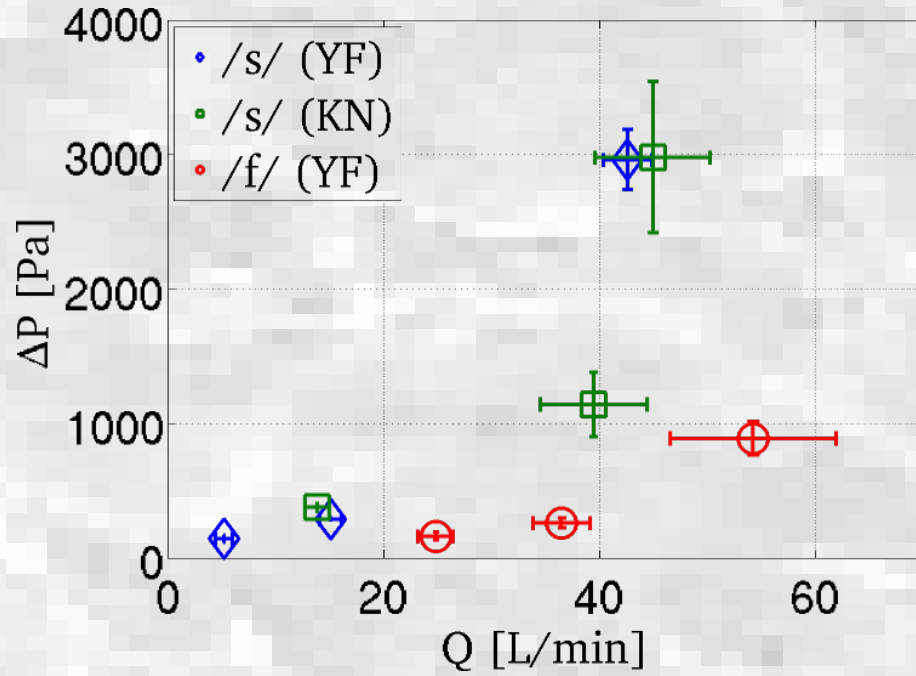


→ How to quantitatively assess this?

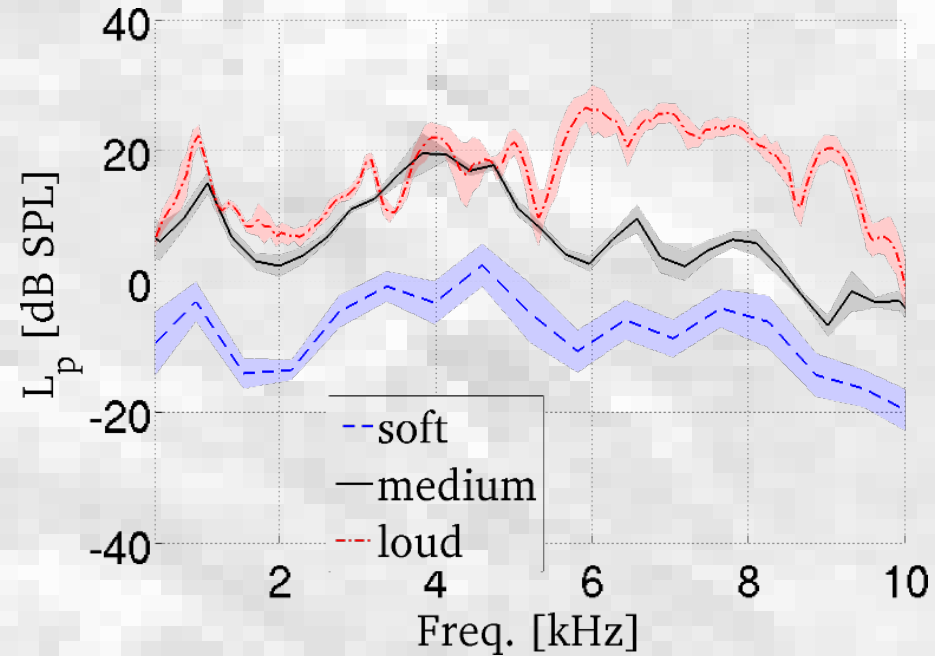
→ *In-vitro* reconstruction of *in-vivo* geometry?

→ Relevance of a dual approach? (*in-vivo* & *in-vitro* exp. data)

→ A potential biomarker for dental/oral medical care?



$$L_p(f) = 10 \times \log_{10} \left( \frac{|P(f)|}{p_{ref}^2} \right)$$



$$\Delta P = \frac{\rho Q^2}{2c_s^2} \left( \frac{1}{A_c^2} - \frac{1}{A_0^2} \right)$$

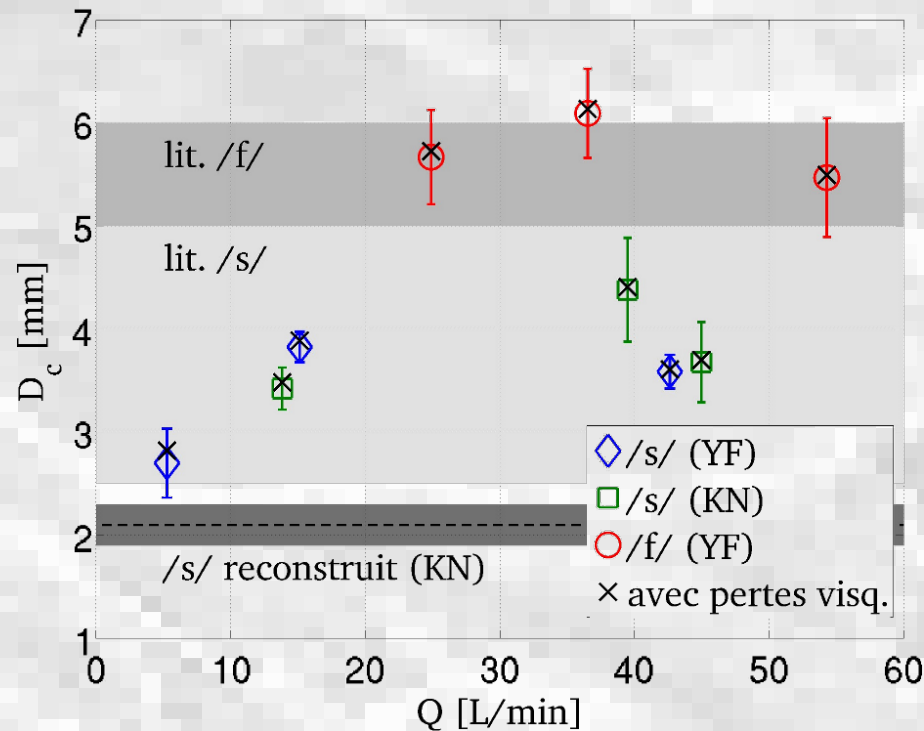
Without viscous losses

$$A_c = \frac{Q}{\sqrt{\frac{2\Delta P}{\rho}}}$$

With viscous losses

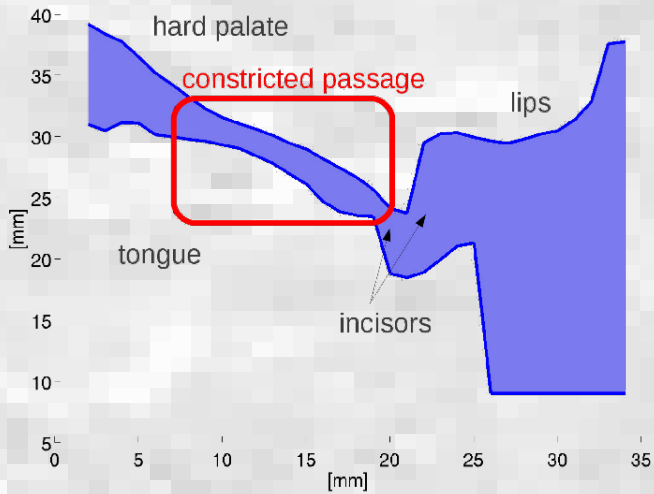
$$A_c = \sqrt{\frac{Q^2 + 16\pi\nu QL}{\frac{2\Delta P}{\rho}}}$$

$$D_C = 2\sqrt{A_c/\pi}$$



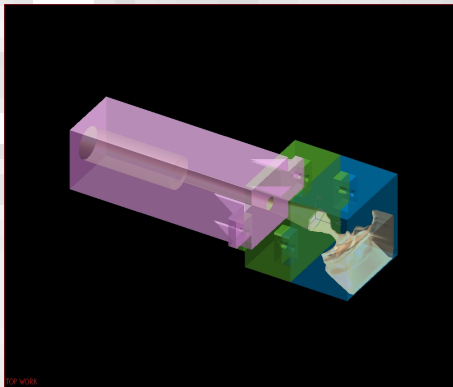
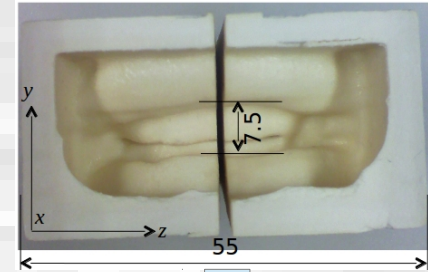
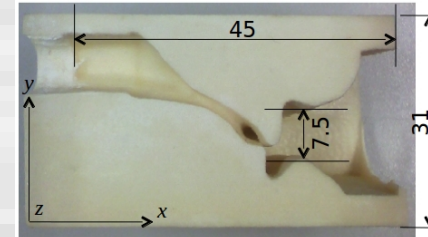


CT\* scan during a 30s sustained sibilant /s/

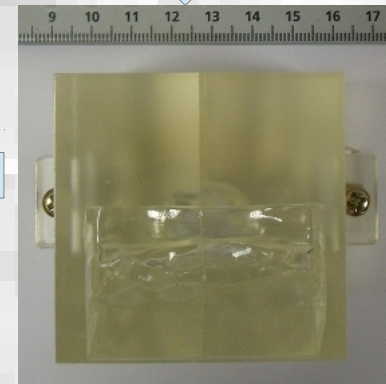


\*CT Computerized Tomography

Plaster cast



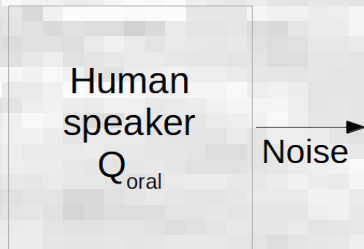
Mechanical replica (upstr. duct + reconstr. oral cavity)



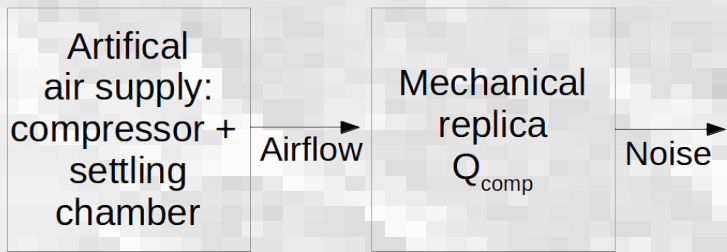
Reconstructed oral cavity

**Acoustic experiment: comparison of human & reconstructed sibilant /s/ noises**

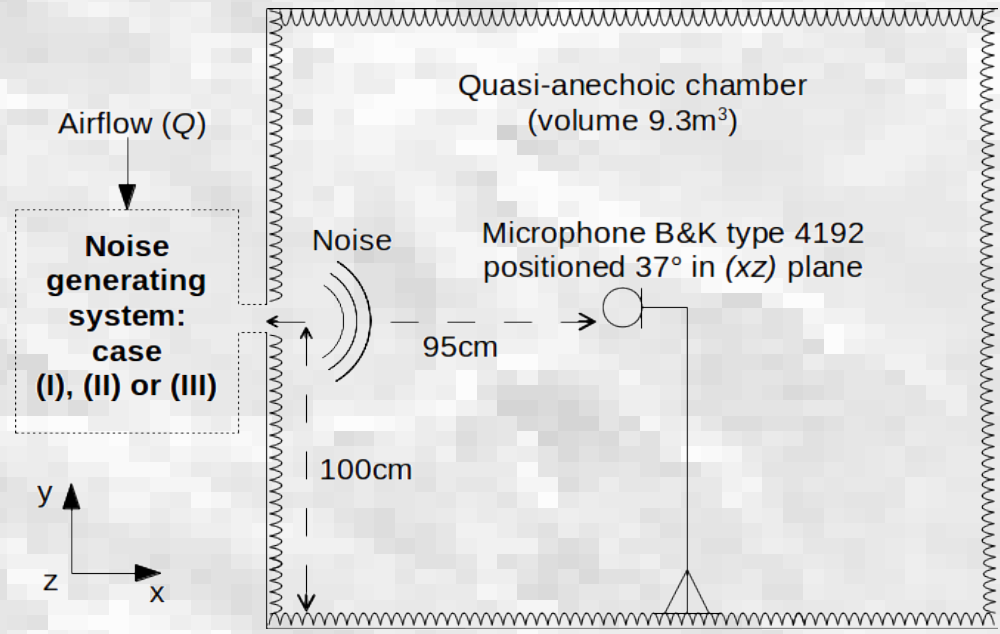
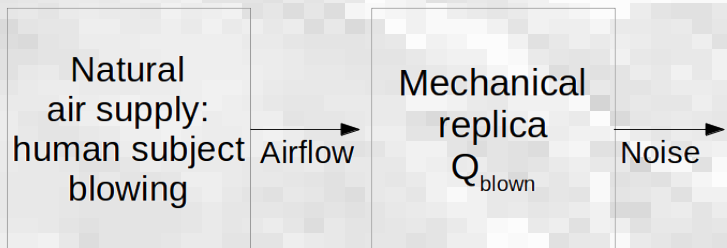
- **Case (I):  $Q_{oral}$  a priori measured**  
('soft', 'medium', 'loud')

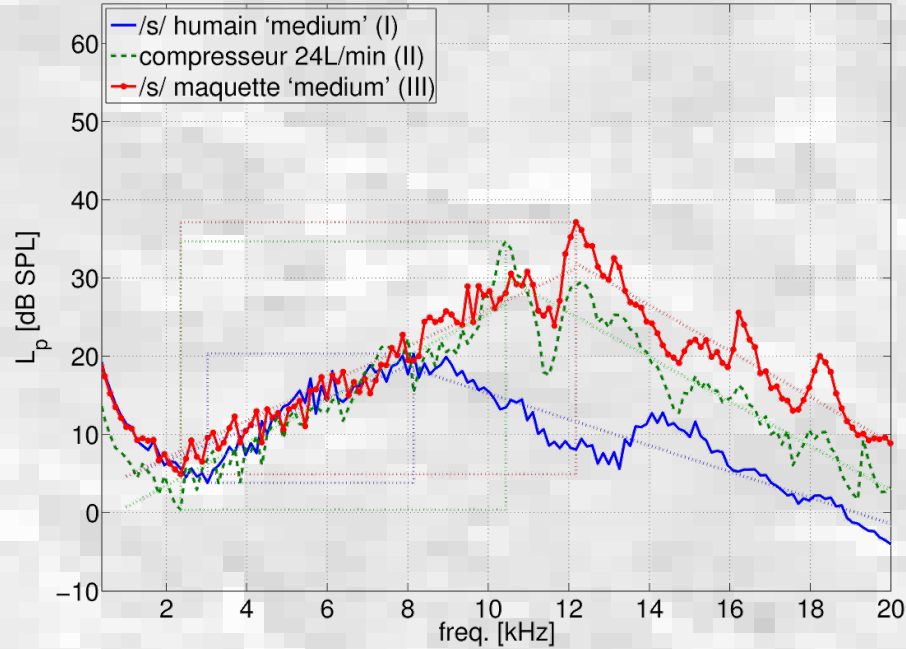


- **Case (II):  $Q_{comp}$  measured by volume flow meter**

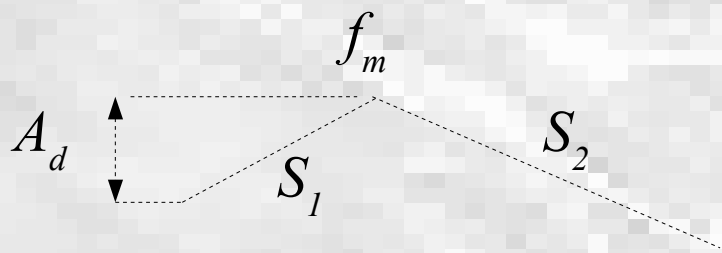


- **Case (III):  $Q_{blown}$  a priori measured**  
('soft', 'medium', 'loud')





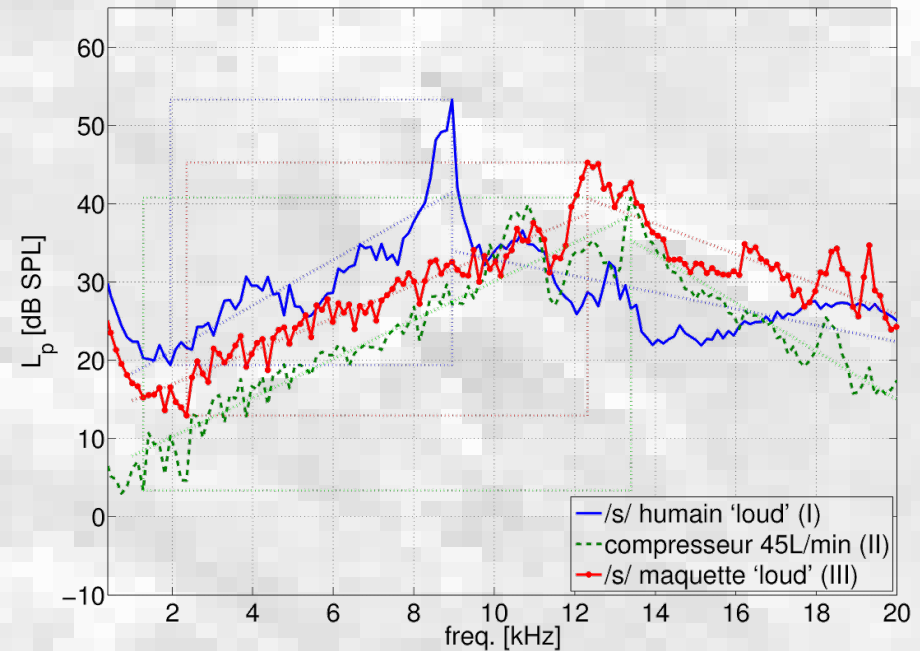
medium

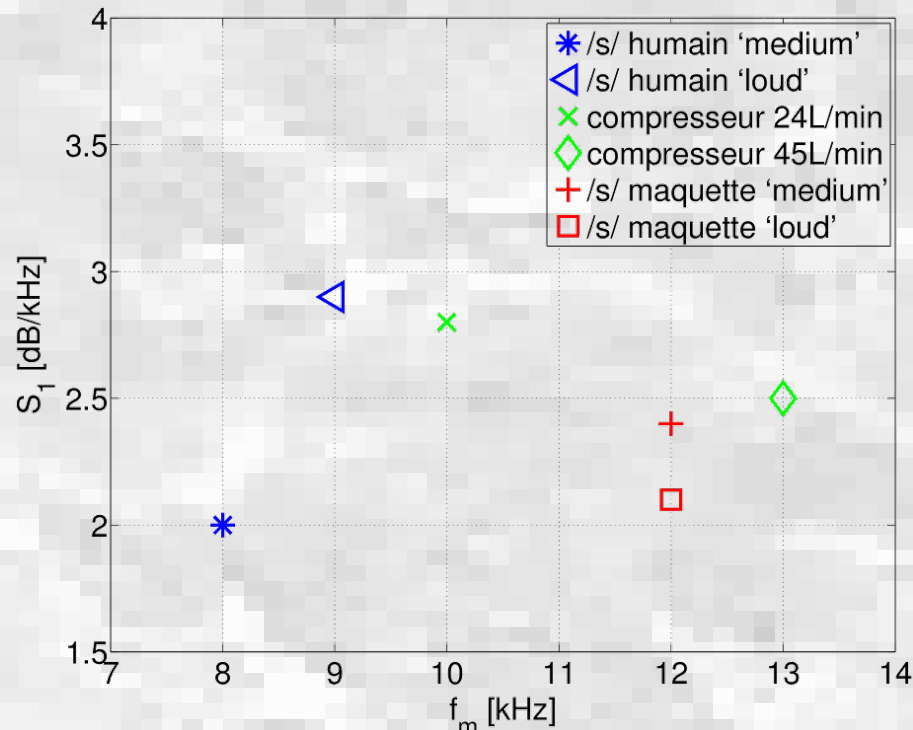


**Spectral parameters:**

- \* spectral peak  $f_m$
- \* spectral slopes  $S_1$  &  $S_2$
- \* dynamic amplitude  $A_d$

loud

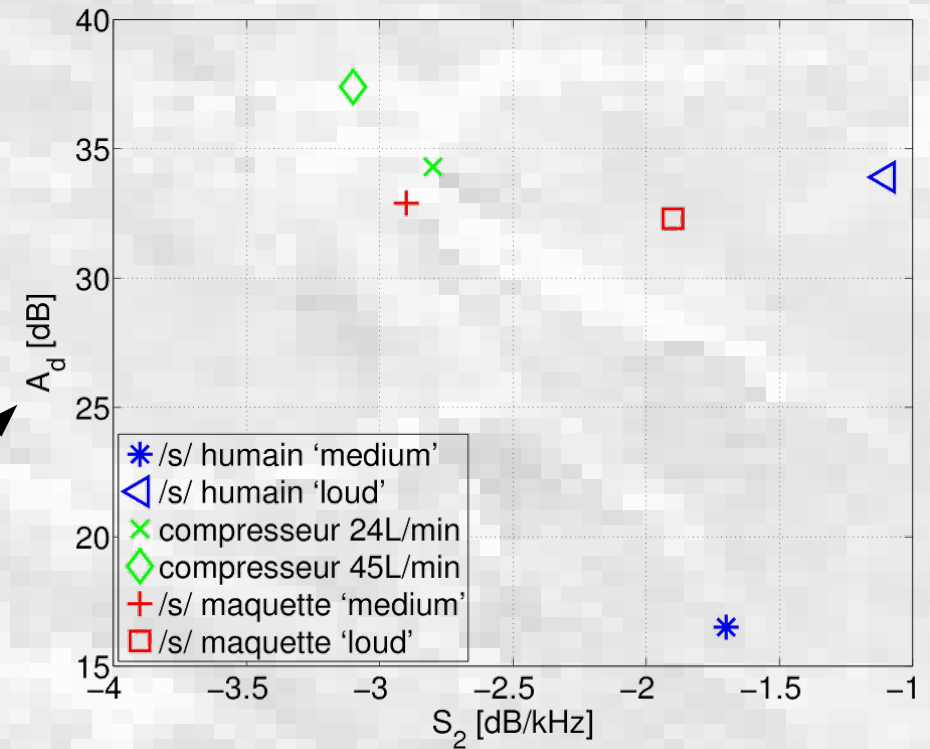


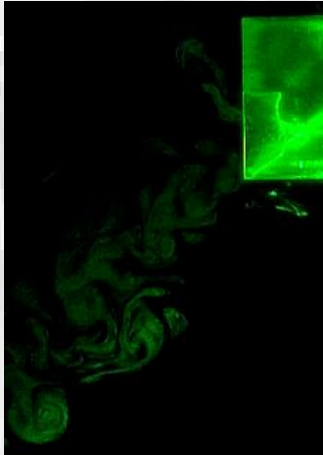


spectral peak

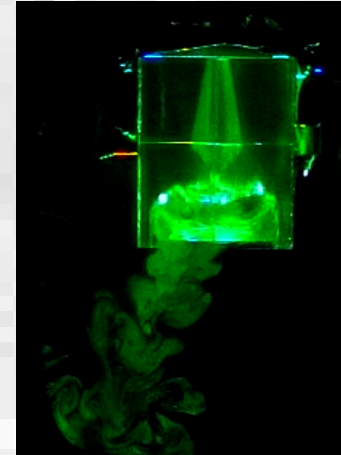
dynamic amplitude

S<sub>1</sub> & S<sub>2</sub>: spectral slopes



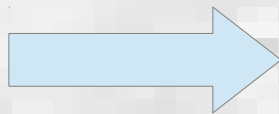


Transverse views [rajouter débits]

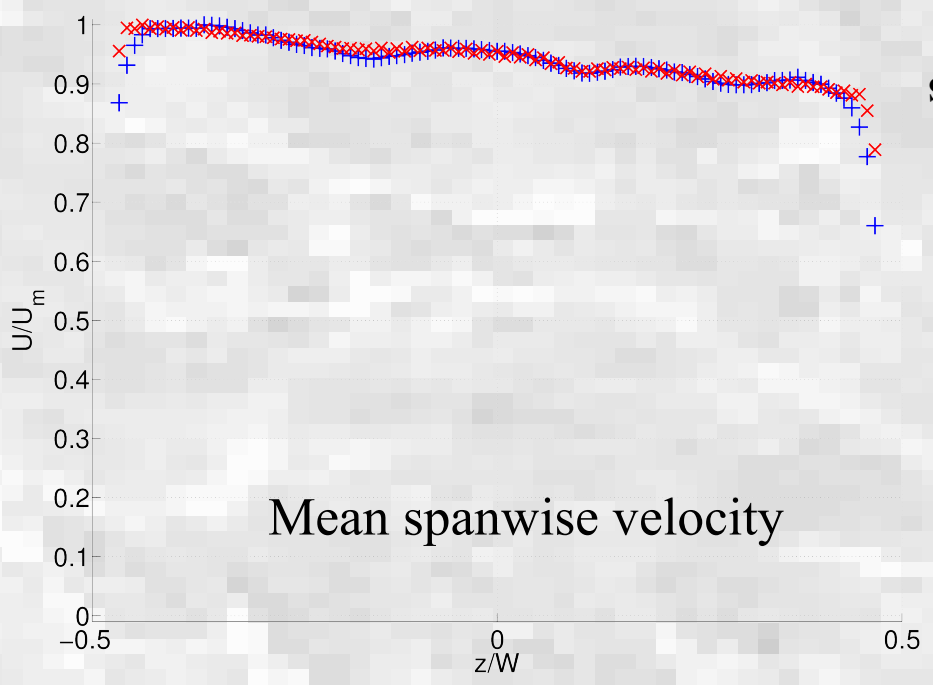


Longitudinal view  
[36L/min]

→ Complicated flow (bifurcating...)!

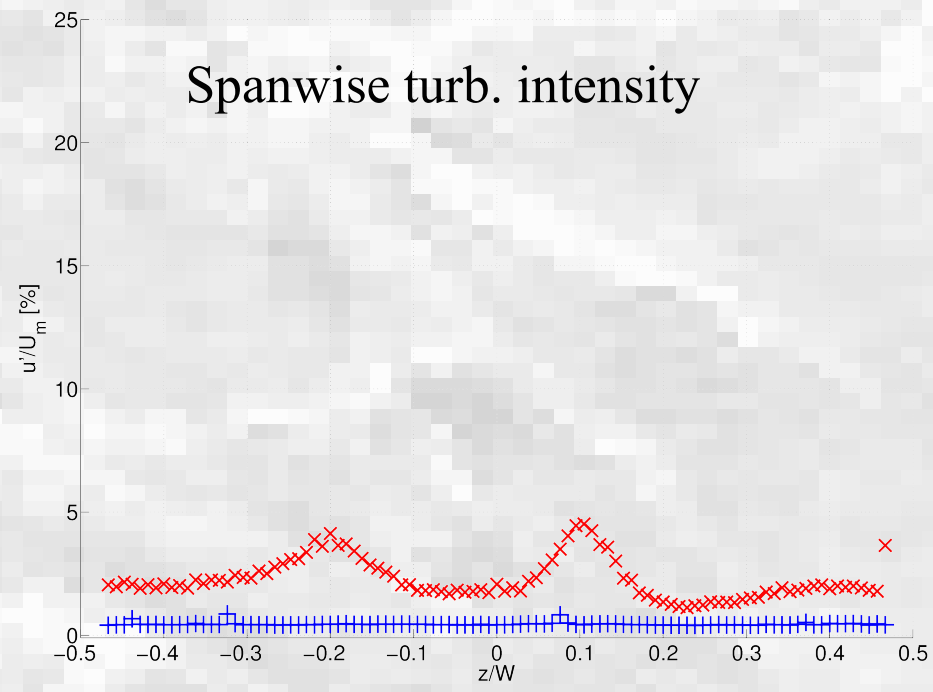
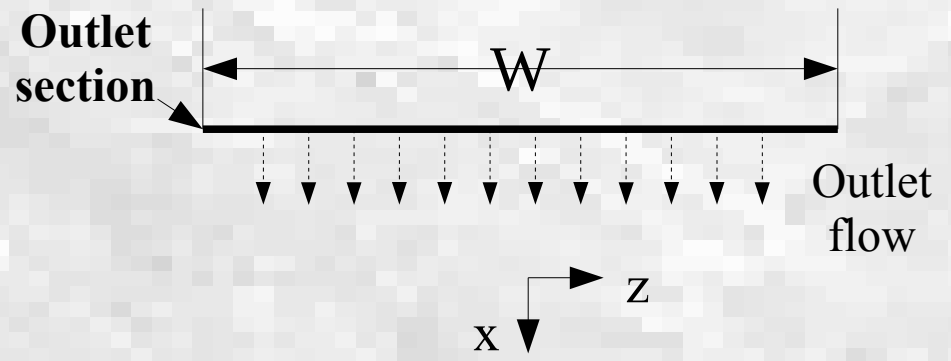


**Focus on simplified duct +  
obstacle(s) geometries...**

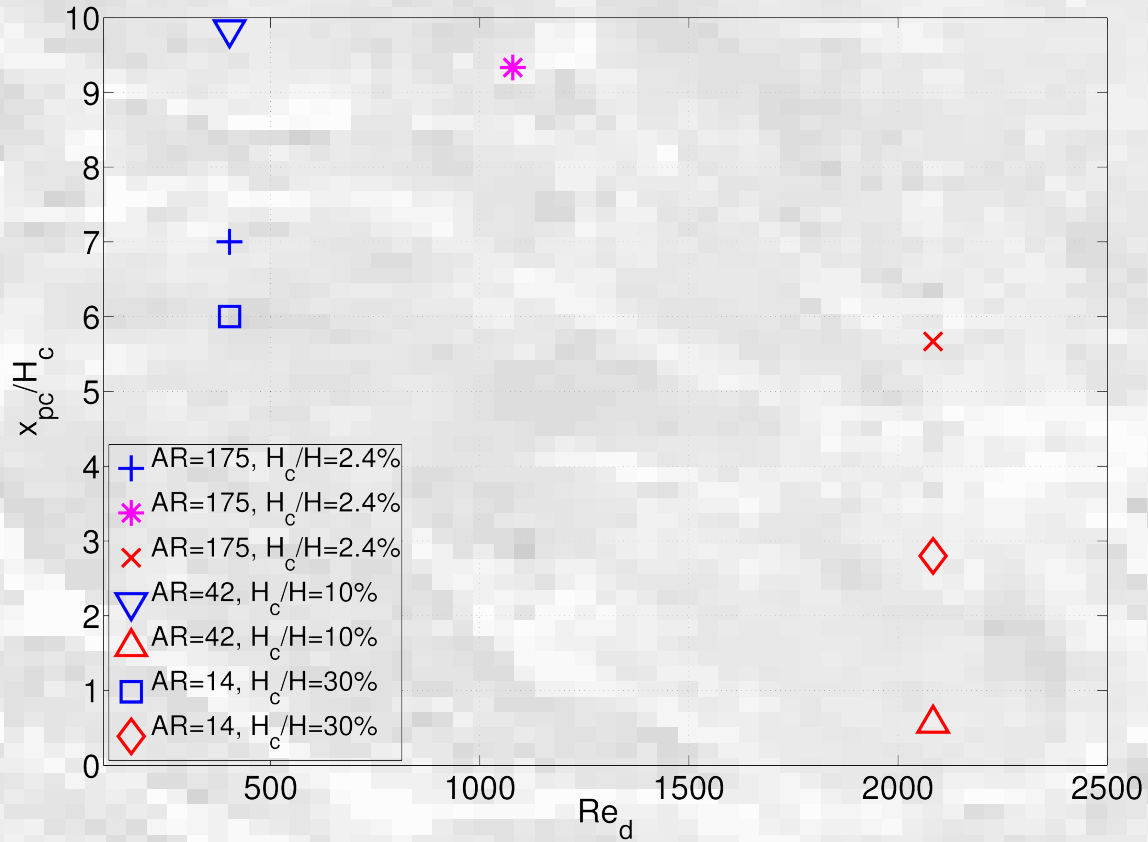


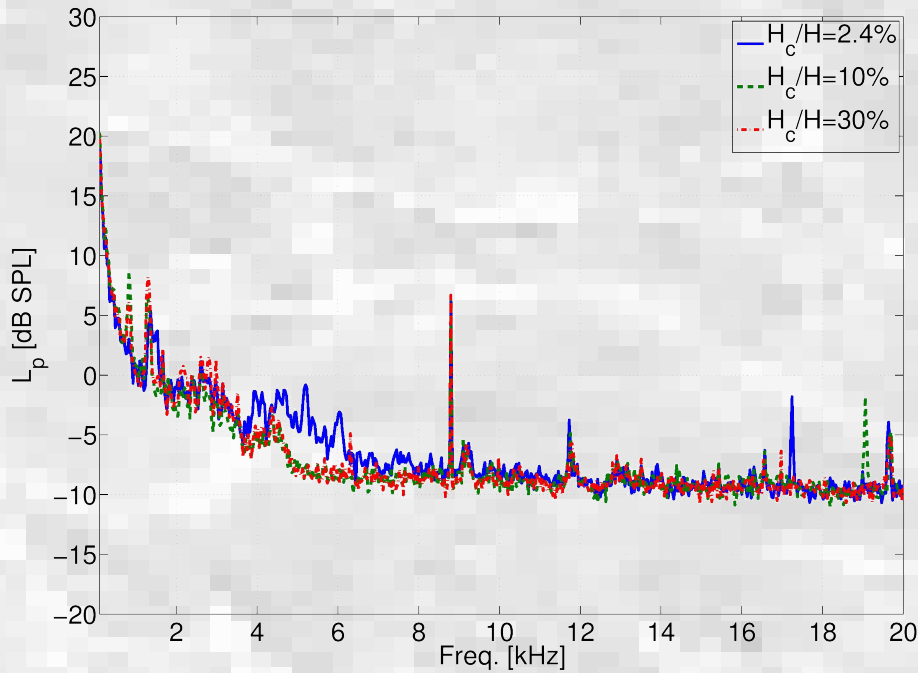
Mean spanwise velocity

→ **2D flow hypothesis admitted!**

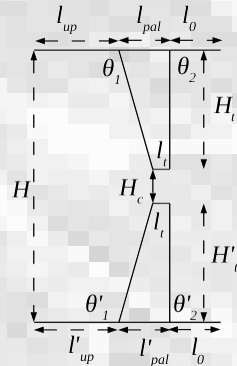


Spanwise turb. intensity



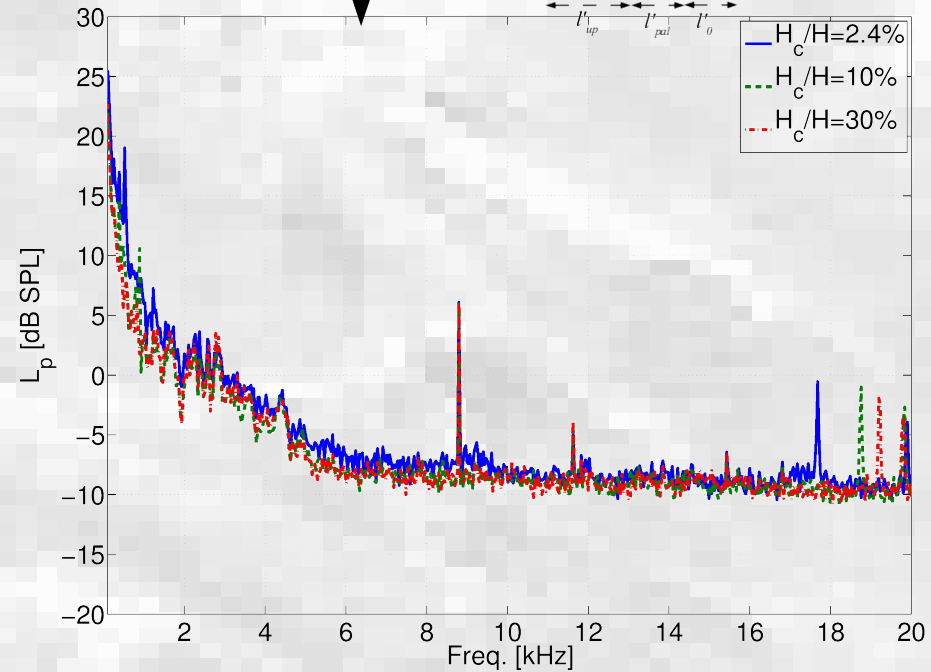
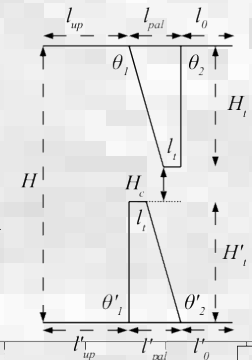


Symmetric configuration

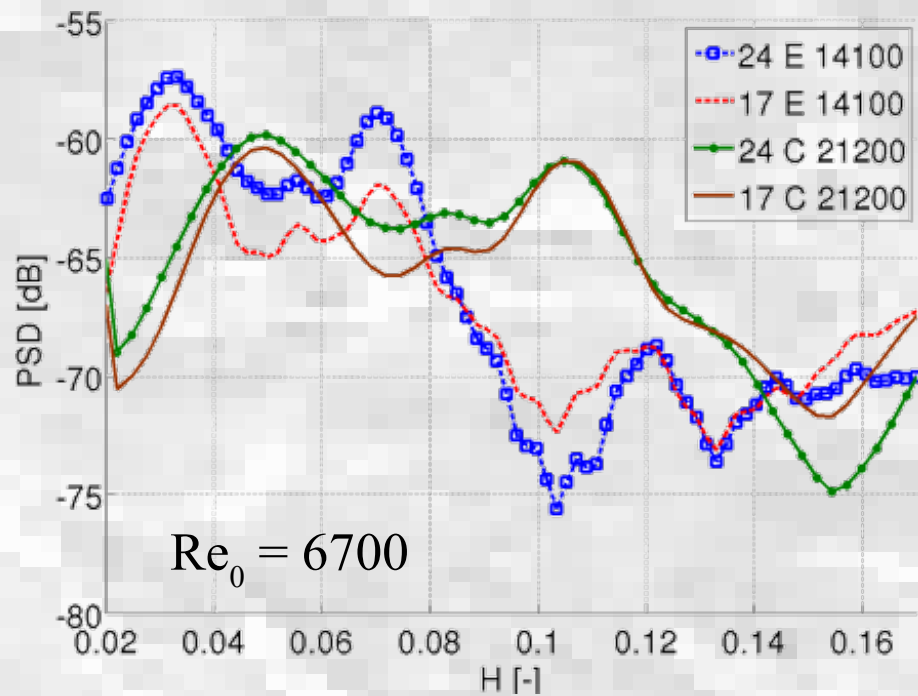


Influence of obstacle configuration & aperture degree  $H_c/H$ ;  $Re = 2084$

Asymmetric configuration

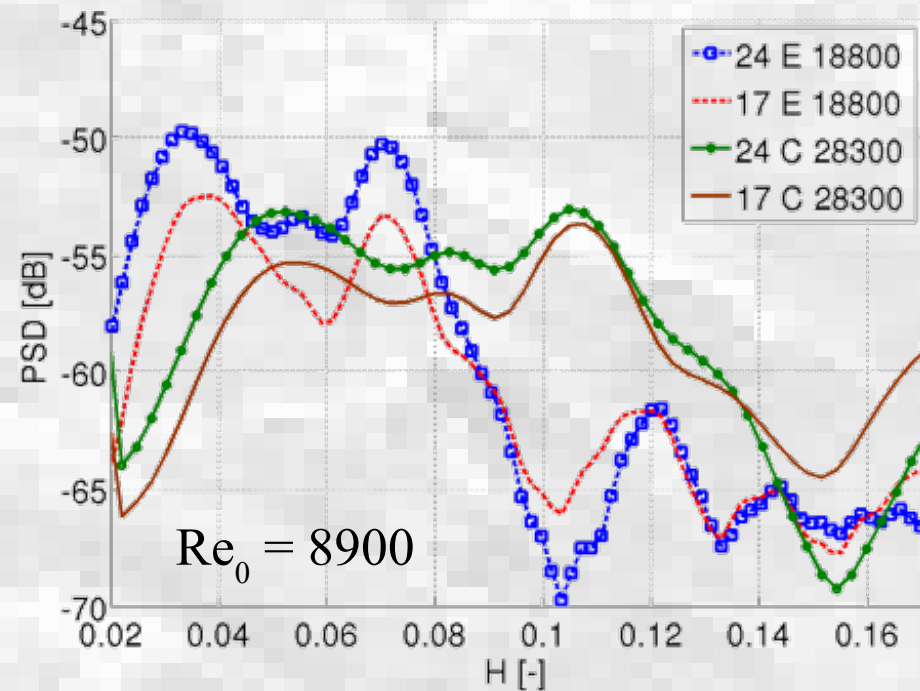
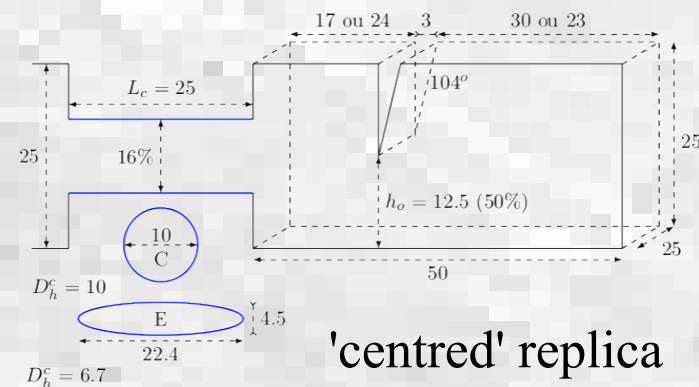


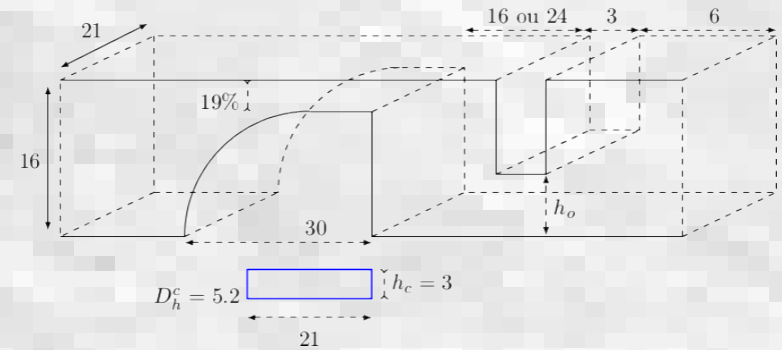
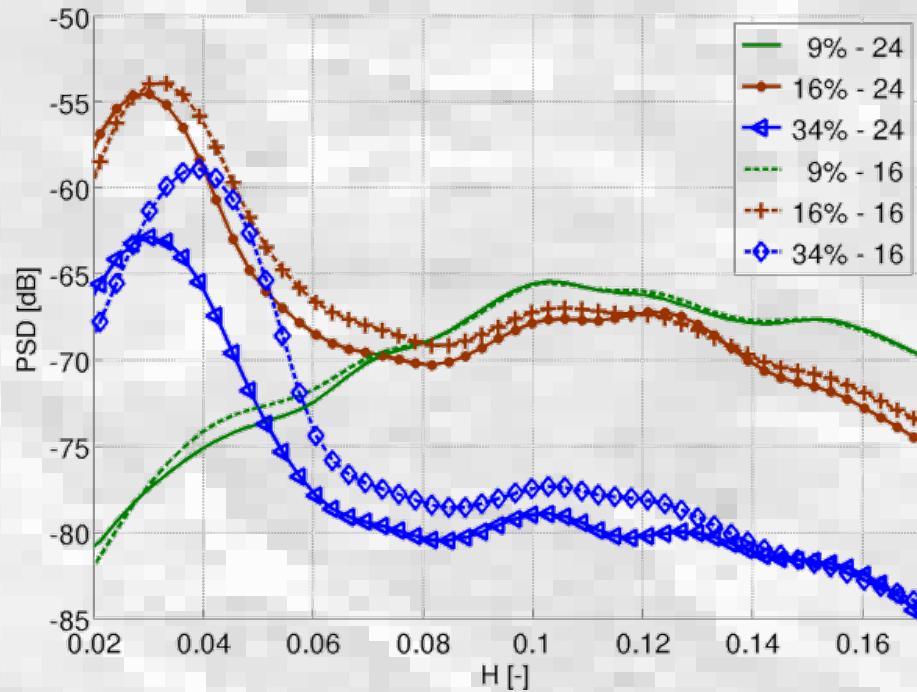




→ Measured spectra as function of **constriction-obstacle distance** (17 or 24mm); **cross-section shape** (E or C); **cross-section Reynolds number**  $Re_c$  (14100; 21200; 18800; 28300)

Helmholtz number: 
$$H = \frac{f D_h^c}{c}$$





'offset' replica

- \*  $Re_c = 11900$
- \* aperture degrees 9; 16; 34%
- \* constriction-obstacle distance 16 or 24mm



Wind turbine:  
 $Re=O(10^7)$ ,  $M<0.2$



Boeing 787:  $Re=O(10^8)$ ,  
 $M<0.9$



TGV:  $Re=O(10^7)$ ,  
 $M<0.4$



Volvo V60:  
 $Re=O(10^6)$ ,  $M<0.2$



Hurricane:  $Re=O(10^9)$ ,  
 $M<0.3$

- Various applications...
- Various Reynolds & Mach numbers...

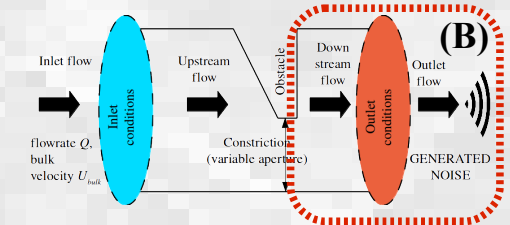
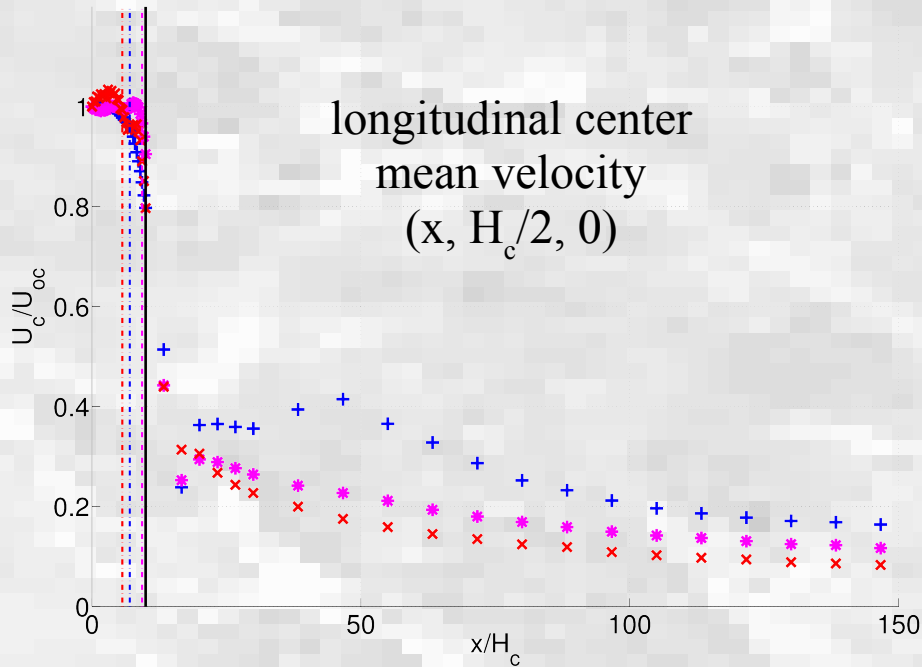
$$Re = \frac{UH}{\nu}$$

$$M = \frac{U}{c}$$

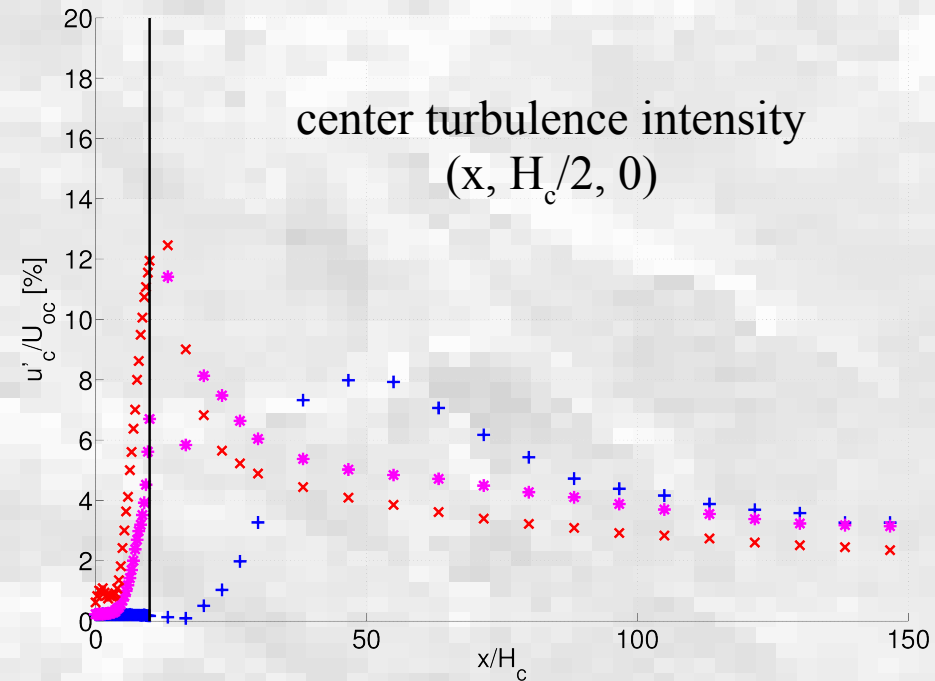
- \*  $U$ : characteristic velocity [m/s]
- \*  $H$ : characteristic length [m]
- \*  $c$ : speed of sound in air [ $\approx 343$ m/s at 293K]
- \*  $\nu$ : air kinematic viscosity [ $\approx 15 \cdot 10^{-6}$ m<sup>2</sup>/s at 293K]

→ What about moderate Reynolds & low Mach numbers flows? i.e.  $Re=O(10^4)$  &  $M<0.3$

Jet longitudinal decay:  $H_c/H = 2.4\%$



Effect of  $Re$

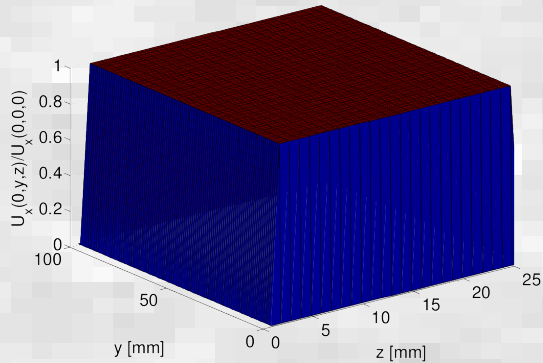


Reynolds numbers:

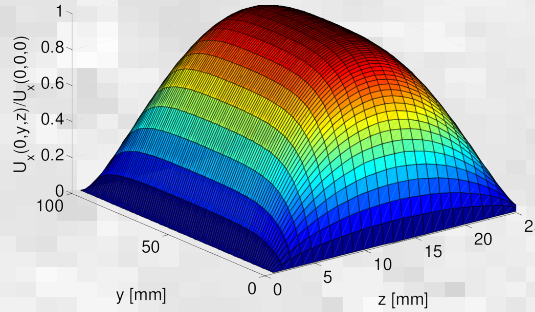
+ : 402

x : 1079

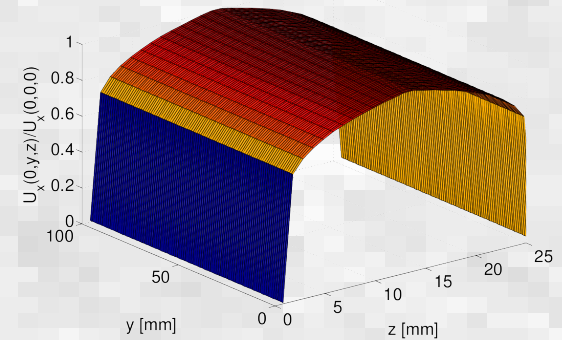
\* : 2084



Uniform inlet vel. profile

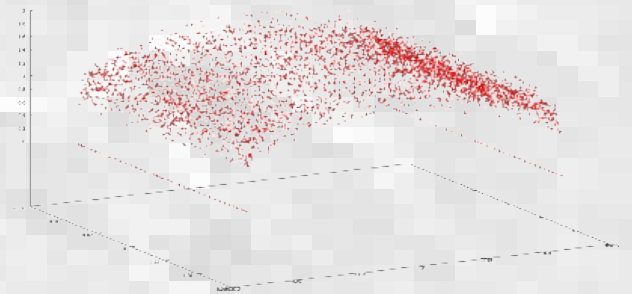


3D-parabolic inlet vel. profile

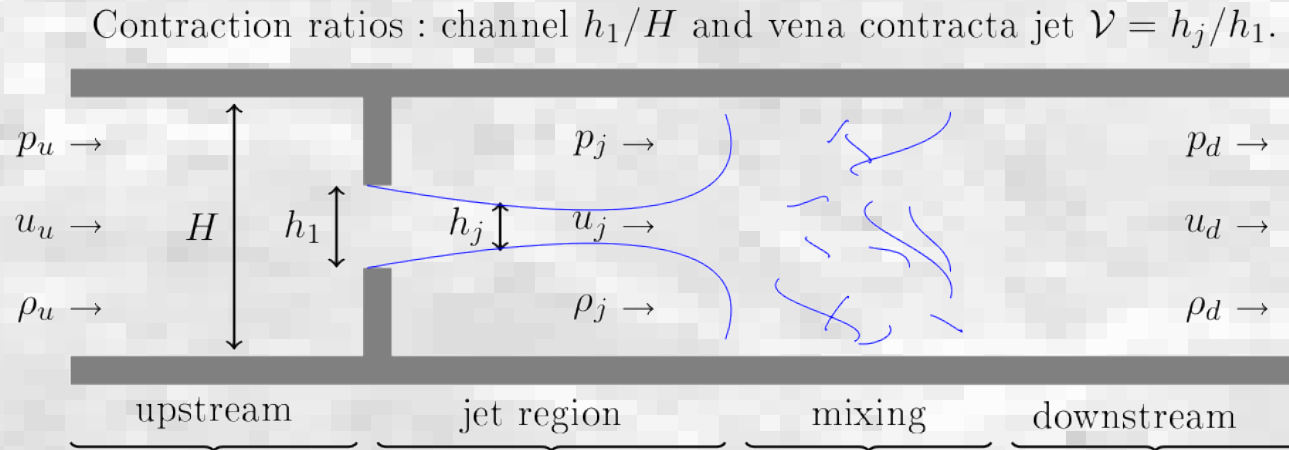


Static turbulent inlet vel. profile

Dynamic turbulent inlet vel. profile:  
\* **gaussian fluctuations**  
\* **injected inlet turbulence intensity levels:  $Tu_e = 0; 10; 30\%$**



**(In)comp. quasi-steady 1D mean flow through a semi-infinite pipe**



**Scattering matrix**

$$\begin{pmatrix} p_d^+ \\ p_u^- \end{pmatrix} = \begin{pmatrix} T^+ & R^- \\ R^+ & T^- \end{pmatrix} \begin{pmatrix} p_u^+ \\ p_d^- \end{pmatrix},$$

$$\begin{pmatrix} p_d^+ \\ p_u^- \end{pmatrix} = \frac{1}{2 + M_u \beta} \begin{pmatrix} 2 & M_u \beta \\ M_u \beta & 2 \end{pmatrix} \begin{pmatrix} p_u^+ \\ p_d^- \end{pmatrix},$$

$M_u$ : Mach number of pipe steady flow

$$\beta = \left( \frac{H}{h_j} - 1 \right)^2$$

(1)

## Potential (irrotational) incomp. 2D flow model

$$\vec{u} = (u, v)$$

**Continuity & irrotational flow:**

$$u = \frac{\partial \psi}{\partial y}, \quad v = -\frac{\partial \psi}{\partial x},$$

$$u = \frac{\partial \phi}{\partial x}, \quad v = \frac{\partial \phi}{\partial y},$$

**Laplace's equation:**

$$\nabla^2 \psi = \frac{\partial^2 \psi}{\partial x^2} + \frac{\partial^2 \psi}{\partial y^2} = 0$$

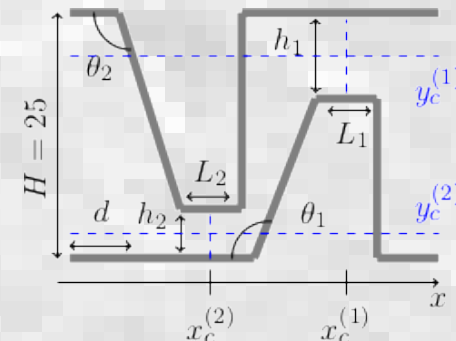
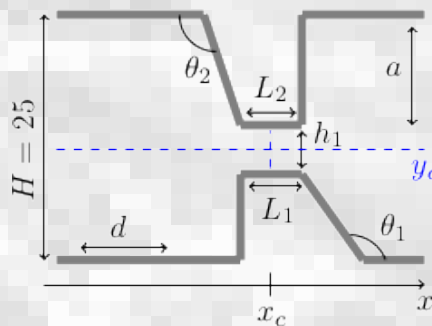
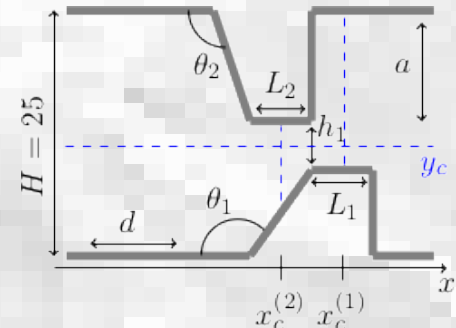
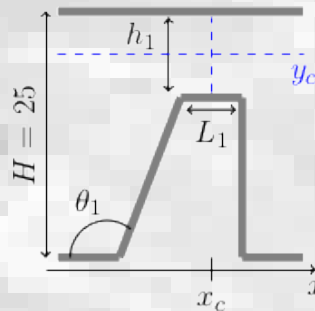
$\Psi$ : stream function

$\Phi$ : velocity potential

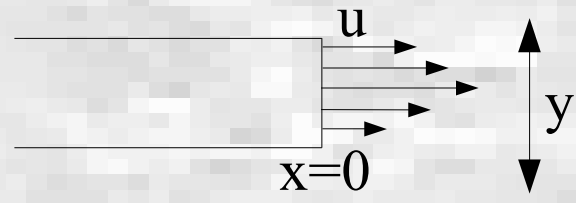
**Cauchy-Riemann conditions:**

$$\frac{\partial \phi}{\partial x} = \frac{\partial \psi}{\partial y}, \quad \frac{\partial \phi}{\partial y} = -\frac{\partial \psi}{\partial x}$$

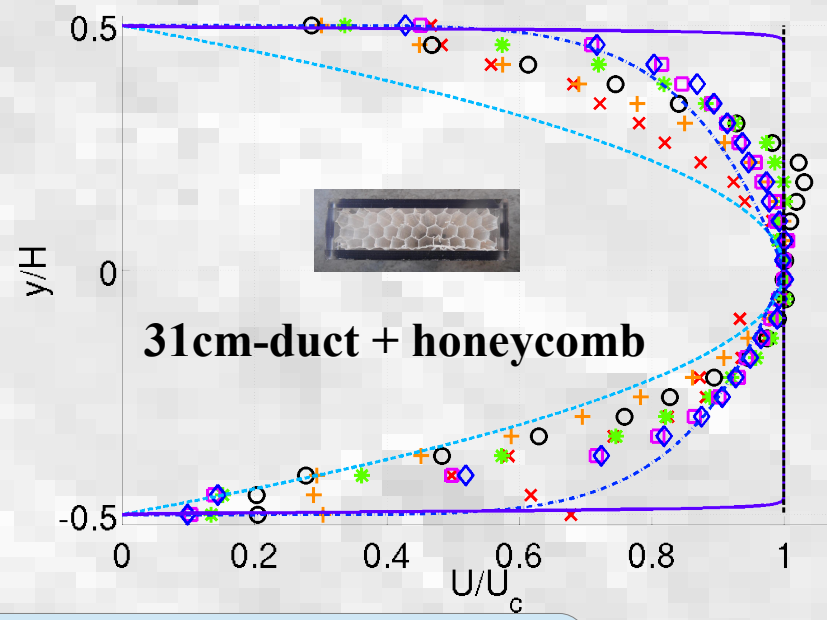
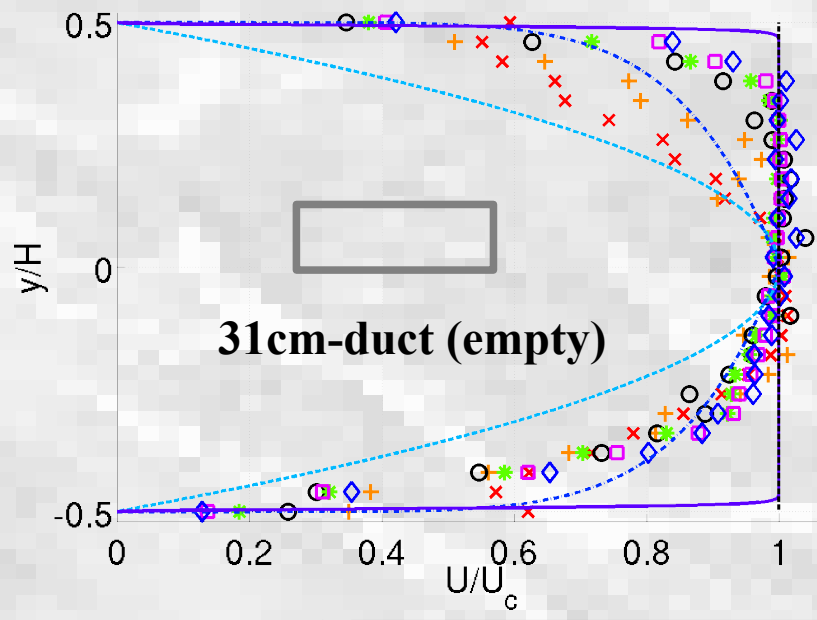
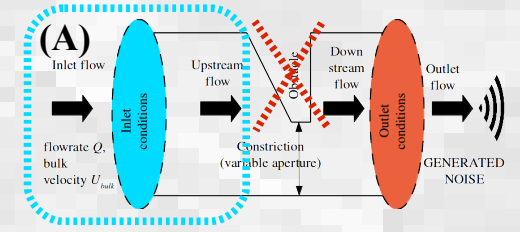
**Geometries:**



Transverse mean velocity profiles at (0, y, 0)



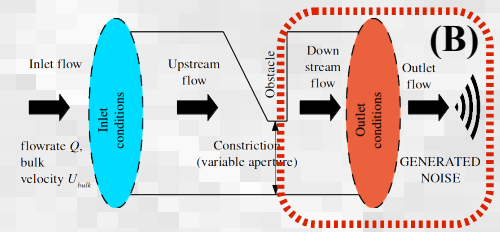
Effect of IC & Re



Reynolds numbers:  
 120 (×); 310 (+); 501 (o); 789 (\*); 1167 (□); 1350 (◇)

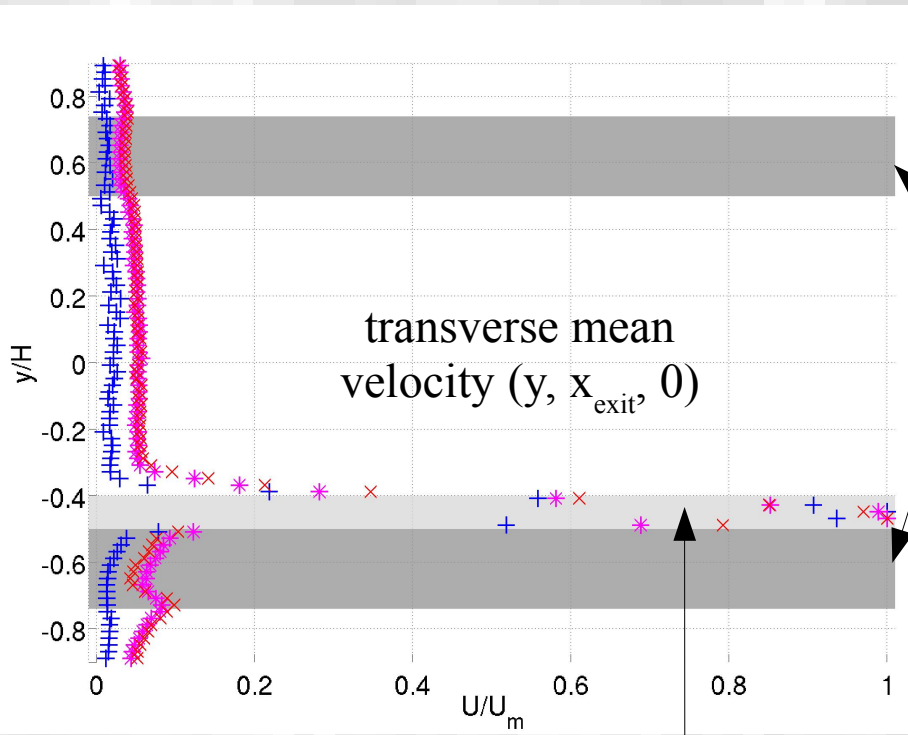


Jet transverse profiles:  $H_c/H = 10\%$  + honeycomb



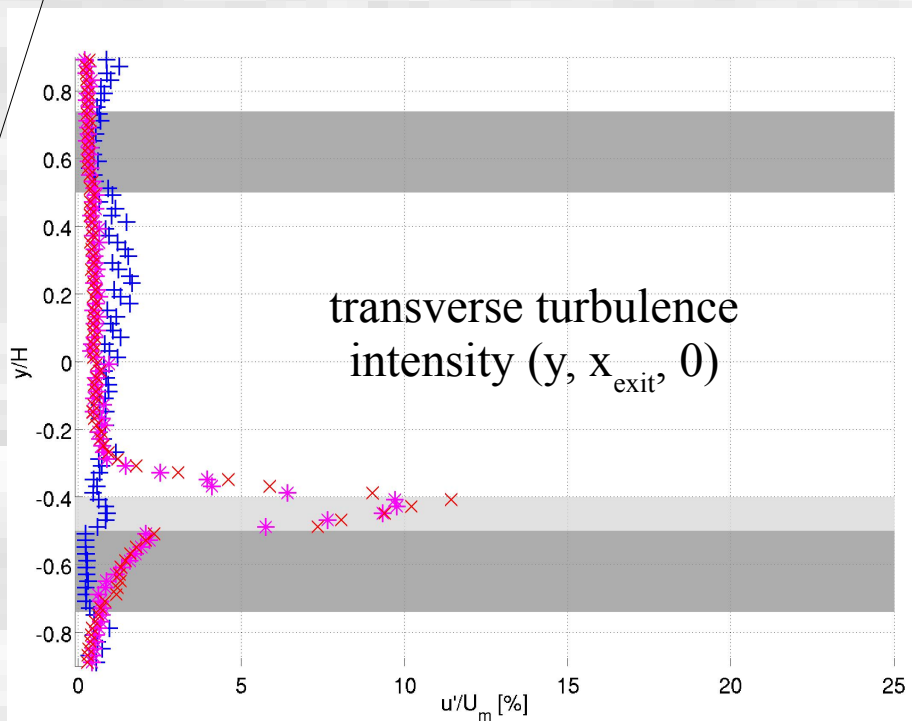
Effect of  $Re$

duct walls transverse regions

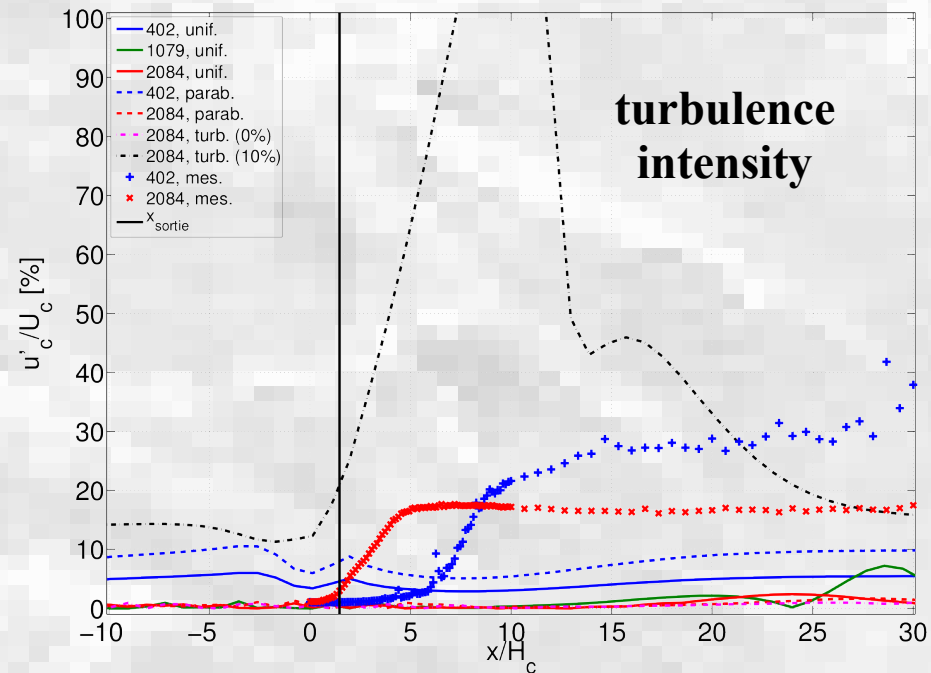
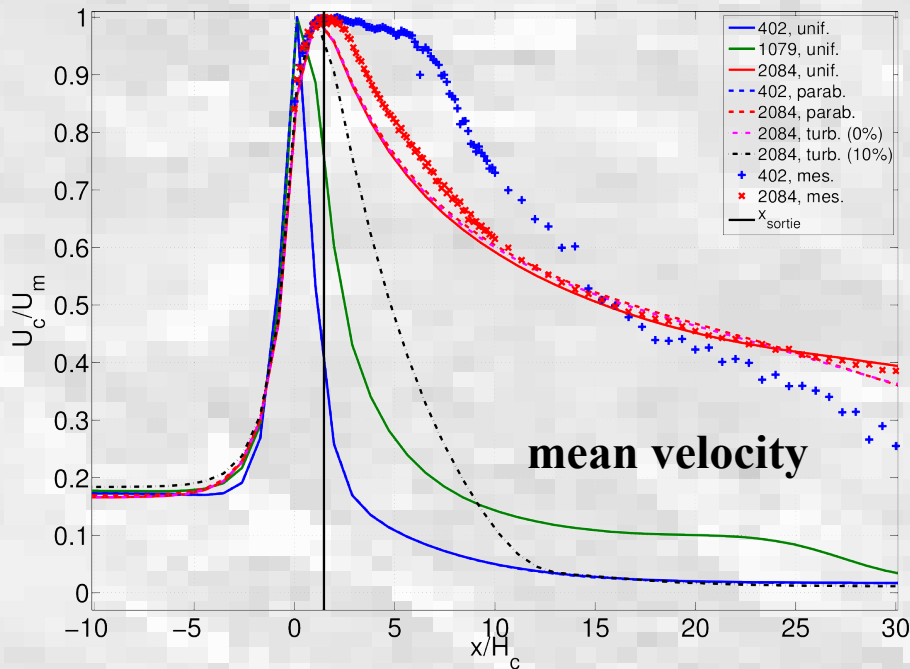


Reynolds numbers:  
 +: 402  
 x: 1079  
 \*: 2084

constriction transverse region (below obstacle)



## Comparison of longitudinal mean center velocity profiles for several inlet conditions & Reynolds numbers (aperture degree $H_c/H = 30\%$ )



× & +: measured data